The chemical response of deep, leached and weathered soils of the Mpumalanga Highveld, South Africa, to irrigation with saline mine water

Ross Campbell
BSc.(Hons.) Geology (UCT)

A dissertation submitted in partial fulfilment of the requirements for the degree of Master of Science in Environmental Geochemistry
Department of Geological Sciences
Faculty of Science
University of Cape Town
January 2001

Abstract

Coal mining in the Highveld region of Mpumalanga Province, South Africa generates between 14 and 30 million litres of waste water per day. Much of the water is saline (TDS > 2500 mg/l) and has high concentrations of dissolved SO_4^{2-}, Ca^{2+} and Mg^{2+}. Crop irrigation has been proposed as a useful way to dispose of saline mine water and enhance agricultural productivity in this low rainfall (<800 mm/year) region. In order to avoid undesirable salinization of the regional groundwater, it is necessary that soils immobilize, at least partially, the dissolved salt load of irrigation water. For example, the build-up of gypsum in the soil would immobilise Ca^{2+} and SO_4^{2-}.

Since the end of 1997, the cultivation of crops under centre-pivot irrigation with saline mine water has been subject to field trials on 70 ha of land at Kleinkopje Colliery in Mpumalanga. The natural soils (comprising 2 out of 3 of the irrigated fields) are deep, sandy, dystrophic and acidic. The other irrigated field is situated on a rehabilitated mining area, and consists of a 600 mm layer of sandy soil capping mine waste rock. A study of soil profiles to 3 m depth in both irrigated and non-irrigated fields has been carried out to assess the impact of irrigation with saline mine water. The results indicate mechanisms and patterns of solute movement and retention in the soil which may have implications for groundwater quality.

While irrigation has caused marked salinization of the soil solution, the presence of gypsum in the soils could not be confirmed. The saturation index for gypsum calculated from the ionic composition of saturated paste extracts (SPE) indicates undersaturation with respect to gypsum. Well-equilibrated, increasingly dilute aqueous soil extracts were used to confirm that the observed undersaturation in SPE was not the result of incomplete equilibration with gypsum in the soils. The conclusion drawn is that cation and anion adsorption sites are favoured over gypsum as sinks for Ca^{2+} and SO_4^{2-}. It is deduced that gypsum does not precipitate in these soils until the adsorption sites reach equilibrium with a soil solution which is oversaturated with respect to gypsum. Even then, seasonal flushing by rain probably dissolves accumulated gypsum.

The solubility of the major ions in the soil appears to be controlled by adsorption and exchange rather than dissolution and precipitation. Ca^{2+} strongly displaces Mg^{2+} from exchange sites, leading to a decrease in the exchangeable Ca^{2+}/ Mg^{2+} ratio with depth in the soil. This process is likely to accelerate the movement of Mg^{2+} into groundwater. Sulphate is adsorbed on positively charged surfaces, probably kaolinite edge sites and sesquioxide surfaces. Association of maximum concentrations of soluble and adsorbed SO_4^{2-} with water table depths suggests that SO_4^{2-} is susceptible to leaching during the wet season. The reduction in exchangeable acidity in irrigated soils may be linked to sulphate sorption.

If gypsum accumulates in the soil it will limit the transfer of Ca^{2+} and SO_4^{2-} into the groundwater, but not the movement of Mg^{2+} and other ions into the groundwater. If gypsum does not precipitate and accumulate in the soil profile and the capacity of the soils to retain adsorbed ions is exceeded, then the irrigation water's dissolved salts will eventually move into the groundwater.

Acknowledgements

I'd like to thank the following people for their contributions to this research:

Mr. Azah Peter Abanda and Ms. Meris Smith, my classmates this year, for their friendship and the examples of persistence and excellence which they both set.

Dr. John Annandale of the Department of Plant production and Soil Science at the University of Pretoria, for his hospitality and for making the sampling for this study possible.

Ms. Bernadette Azzie, for her helpfulness and generosity with her knowledge and books.

Dr. John Compton, for his willingness to delve into soil chemistry, his own broad knowledge of geochemistry, his organizational skills, assistance with experimental work, proof-reading of the manuscript, patience and sense of humour, without which this year would have been much harder.

Prof. Martin Fey, for his guidance, inspiring knowledge of soil chemistry, fine teaching ability and enthusiasm.

Mr. Matt Gordon, for his assistance during my use of the laboratories at the Department of Soil Science at Stellenbosch University.

Mr. Vusi Gubevu, whose persistence in adversity has been an inpiration, and whose company and many jokes shared by e-mail were a delight.

Mr. Christo Joubert of Kleinkopje Colliery, for his efficiency and helpfulness in supplying water quality and rainfall data from Kleinkopje.

Dr. Nebo Jovanovic of the Department of Plant production and Soil Science at the University of Pretoria, for his valuable assistance during sampling and his efficient and friendly co-operation.

Dr. Simon Lorentz of the School of Bioresources Engineering and Environmental Hydrology at the University of Natal, for sharing the results of his work on soil hydrology at Kleinkopje.

Ms. Sarah Miller for running an impeccable laboratory during her short stay in the Department of Geological Sciences at UCT.

Mr. Giovanni Narciso of the ARC-ISCW Remote Sensing Centre, for supplying the geographical co-ordinates of the centre-pivot fields.

Dr. Jim Oster, of the U.S. Salinity Laboratory and the University of California, Riverside, for his valuable insight and interest in this work.

TABLE OF CONTENTS

LIST OF FIGURES

LIST OF TABLES

1 Introduction

Coal mining in the Highveld region of Mpumalanga, South Africa generates an estimated 14 to 30 million litres of waste water each day (Barnard et al., 1998). The acidity and salinity of mine waste water makes it unsuitable for release into natural water courses, and its disposal poses a major problem to the coal mining industry. The Highveld region is also of agricultural importance, much of the region considered to be arable land of high potential (Barnard et al., 1998). Agricultural productivity is limited by the sub-humid climate (average annual rainfall of between 600 and 700 mm and average annual evaporation between 1600 and 1800 mm - DWAF, 1986). Du Plessis (1983) suggested that lime-treated acid mine water could be used to irrigate crops, thus simultaneously exploiting the region's agricultural potential and disposing of mine waste water. Subsequent research by Barnard et al. (1998), Annandale et al. (1999) and Pretorius et al. (1999) has investigated this possibility, with particular emphasis on the selection of crop plant species tolerant to so-called gypsiferous mine water (in reference to its high concentrations of calcium and sulphate), using numerical models to predict salt accumulation and transport in soils under irrigation with mine water, and large-scale field trials at Kleinkopje Colliery in Mpumalanga.

1.1 Objectives

The research presented here aims to complement the ongoing research into irrigation with mine water. In particular, this study is an investigation of the impact that irrigation with mine water at the field trial site has had on the chemistry of the irrigated soils, with an emphasis on solute retention and transport in the soils. It is hoped that a clearer understanding of salt retention and movement will improve predictions of the impact that mine water irrigation would have on groundwater quality.

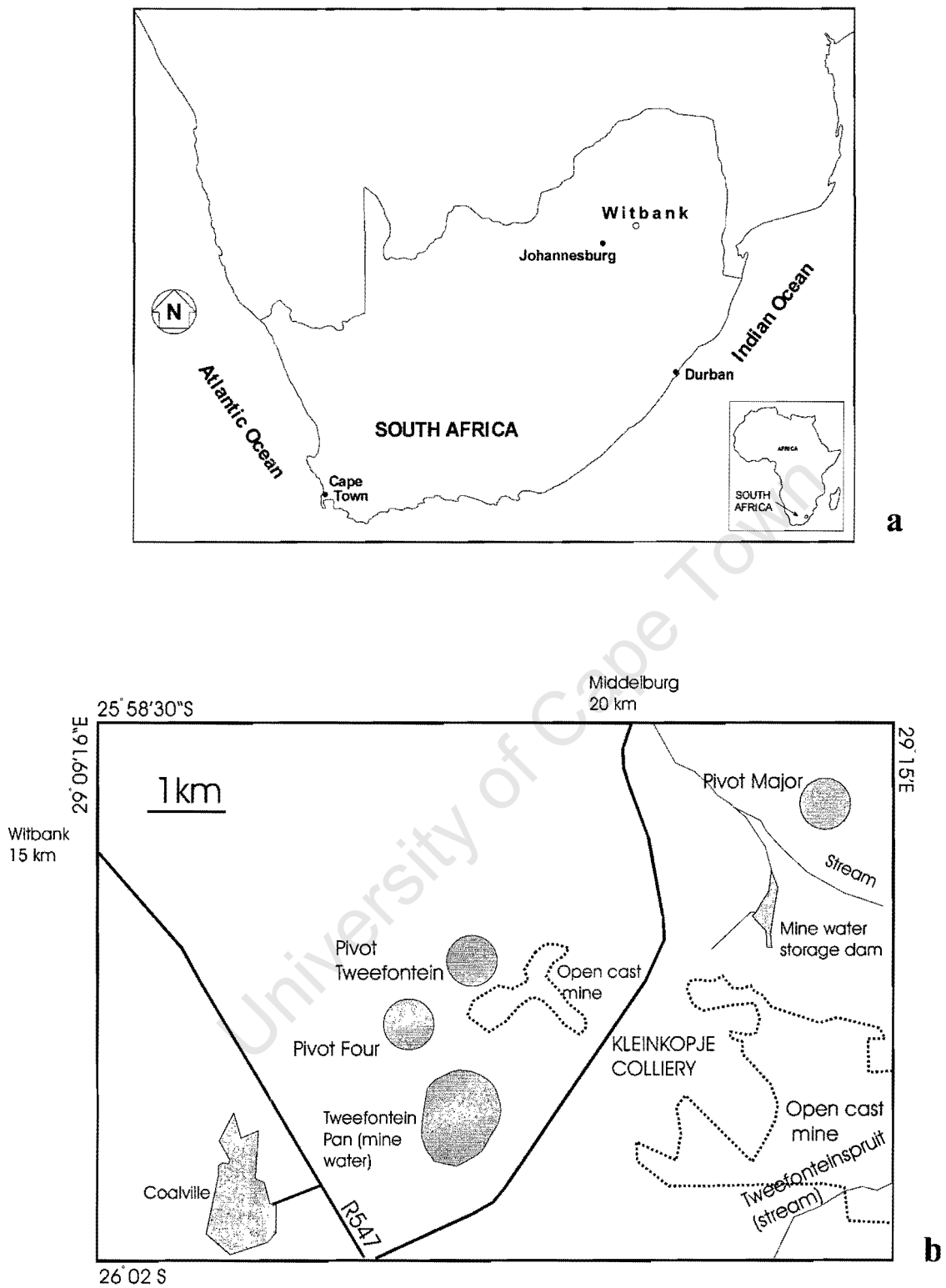

Figure 1.1: (a) The location of Witbank and (b) a map of the area around Kleinkopje Colliery, indicating the major roads, open cast mine workings, streams and positions of the centre pivot fields Major, Tweefontein and Four.

1.2 The field trial site: Kleinkopje Colliery

Situated at 1500 m to 1600 m above sea level, some 15 km south of the industrial town of Witbank, Kleinkopje is an open-cast coal mine owned by Amcoal (Figure 1.1). Coal mining in the Witbank area began in 1889 and exploits the No.1 and No.2 seams of the Vryheid Formation, part of the Permian Ecca Group in the Karoo Supergroup (Paul, 1995). The Ecca Group sandstones and shales are the dominant lithologies (Department of Mines and Geological Survey, 1978), and the terrain is relatively flat, sloping gently toward the north-east.

1.2.1 Hydrology

The mine lies within the catchment of the Olifants River, which flows into the Loskop Dam, an important source of water for domestic, agricultural and industrial use in the Mpumalanga Highveld (Halbich, 1997). Aquifers in the Karoo rocks tend to be confined to zones of fracturing or weakness, such as those associated with dolerite intrusions, faults and coal seams. Shallow perched aquifers in the weathered zone also occur (DWAF, 1995). Rainfall figures for the period of the irrigation field trials are presented in Figure 1.2.

1.2.2 Soils

The soils are predominantly red and dystrophic (highly leached, especially of basic cations) to mesotrophic (moderately leached), and plinthic (Soil and Irrigation Research Institute, 1979). More specifically, using the South African soil classification terminology (Soil Classification Working Group, 1991), the soils under irrigation with gypsiferous mine water include the Bainsvlei form (Redhill family) (Annandale et al., 1999), and the Hutton form (Dr. N. Jovanovic, Department of Plant Production and Soil Science, University of Pretoria, pers. comm., 2000).

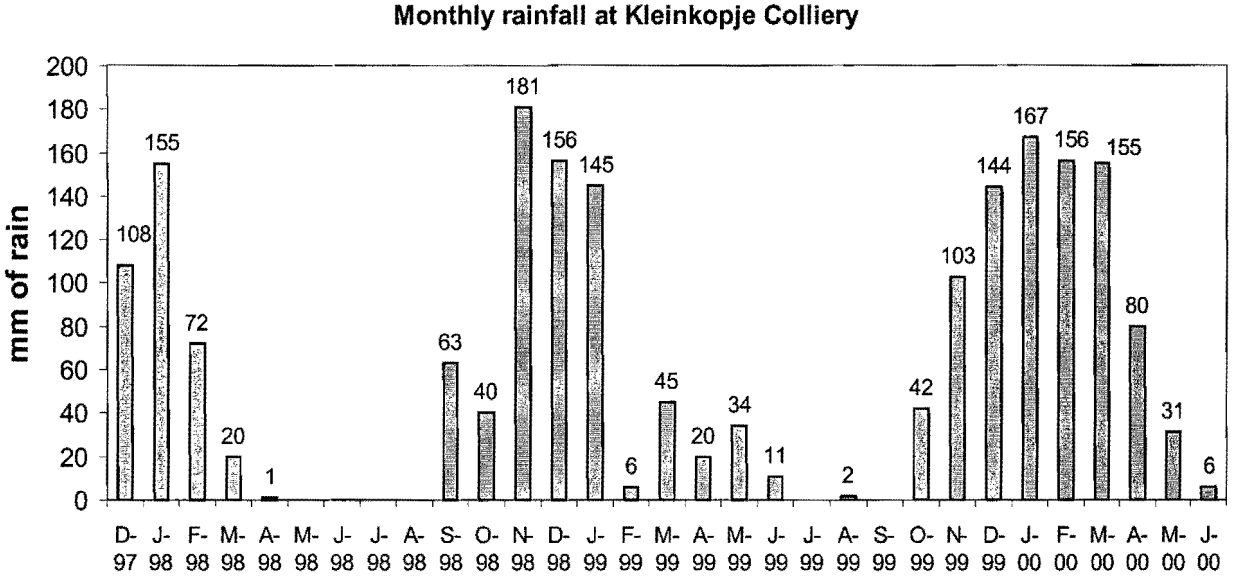

Figure 1.2: Monthly recorded rainfall at Kleinkopje Colliery, since the inception of the irrigation experiment in December 1997, to June 2000, the month in which the sampling for this study was carried out (C. Joubert, Senior Hydrologist, Kleinkopje Colliery, pers. comm., 2000).

1.2.3 The mine water irrigation trials and numerical modeling of solute transport in the irrigated soils

Various cultivars of maize and winter wheat have been cultivated under centre-pivot irrigation on 70 ha of land on the mine's property (Annandale et al., 1999). One 20 ha centre-pivot field (pivot Tweefontein) is a rehabilitated mining area which has been filled in with mine spoils and a covering of between 0.5 m and 1.5 m of topsoil. The fields had been irrigated with gypsiferous mine water for between 1 and 2½ years at the time of the samples considered in this study were collected. The two fields on previously cultivated land (pivot Major and pivot Four) are divided into three irrigation treatment sectors, sectors receiving a quantity of water equivalent to the soil's field capacity (i.e, the highest water content at which there is negligible internal drainage, Or & Wraith, 1999), a 20% leaching fraction or a 20% deficit treatment. Irrigation water flux and meteorological conditions are monitored regularly. Monthly irrigation figures for the field capacity treatments are presented in Figure 1.3. Soil water content, soil solution composition (sampled using porous cup lysimeters), soil chemistry (saturated paste extract composition and exchangeable basic cations) and irrigation water quality have been determined periodically (Pretorius et al., 1999).

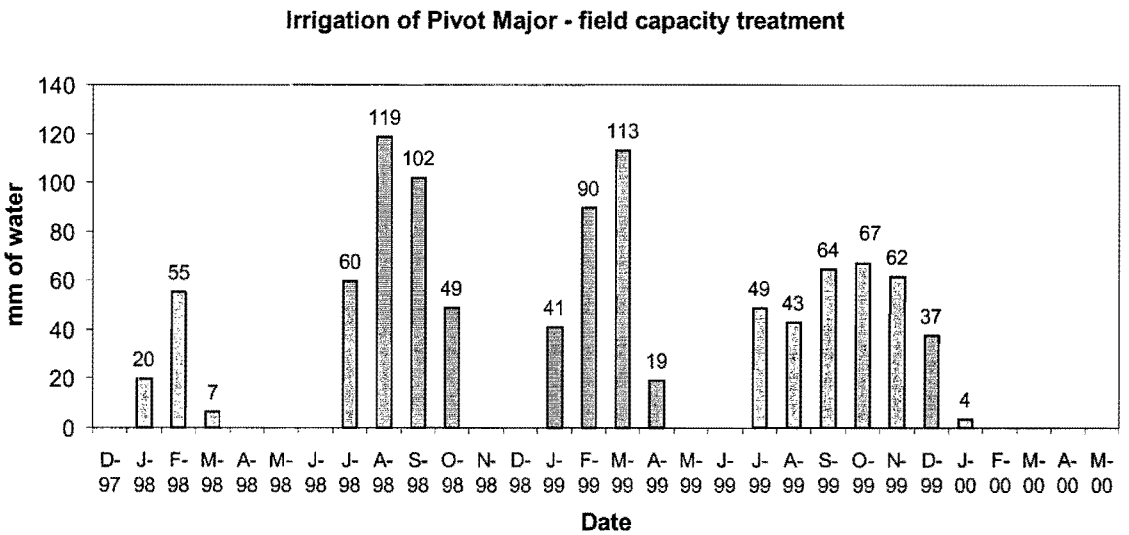

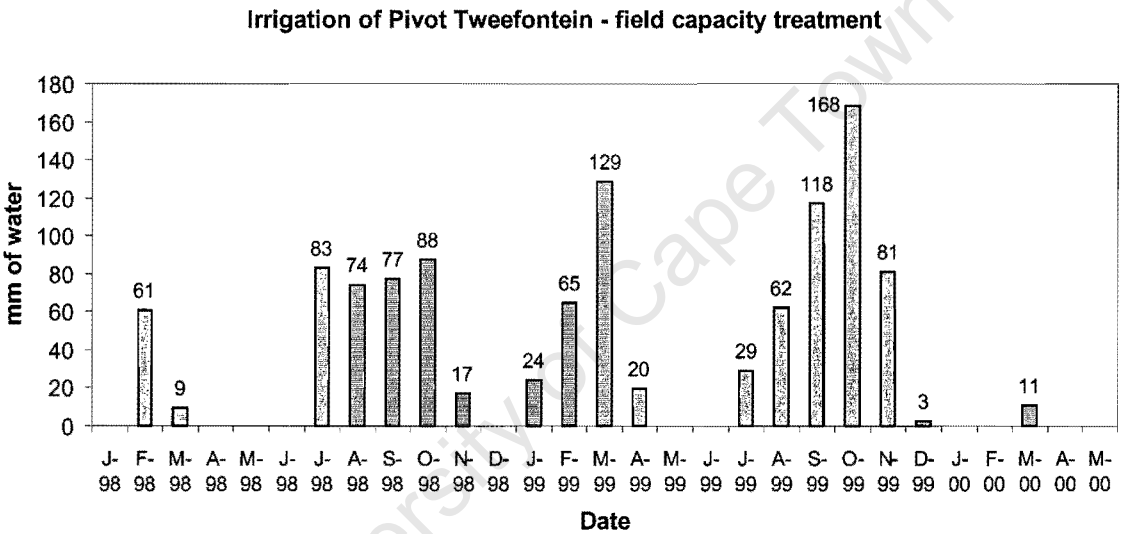

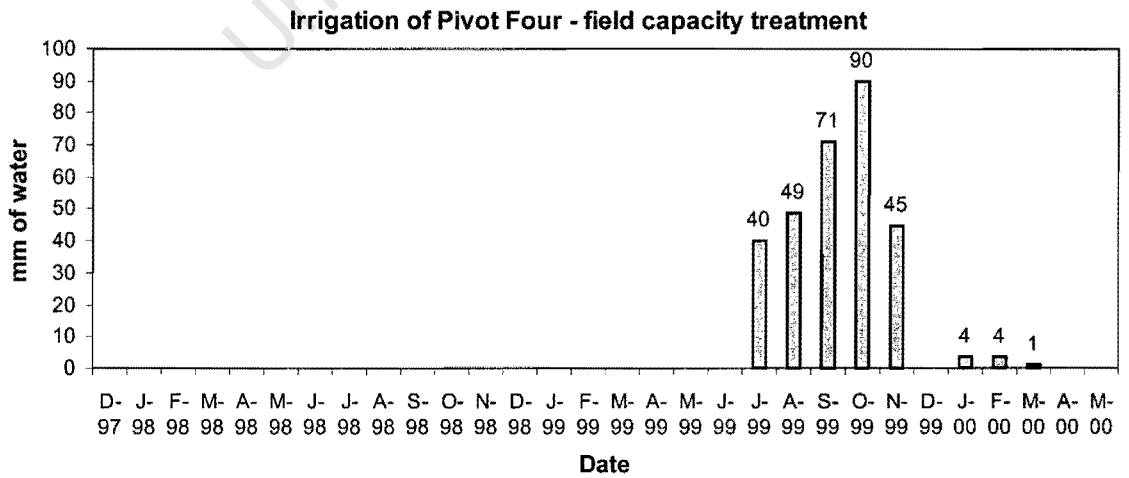

Figure 1.3: Quantities of mine water applied during irrigation field trials to the field capacity treatment sectors of pivots Major, Tweefontein and Four (N. Jovanovic, Department of Plant Production and Soil Science, University of Pretoria, pers. comm., 2000).

Annandale et al. (1999) used the SWB (soil-water balance) model to make long-term projections of salt accumulation and movement in soils irrigated with saline mine water. Barnard et al. (1998) give a detailed description of the SWB model, which is summarised here. The model simulates water movement through the soil profile, the removal of water from the soil by evaporation and transpiration, crop growth, the movement and accumulation of dissolved salts and the precipitation and dissolution of gypsum in the soil.

Water movement is modeled by considering the soil profile as a stack of 0.2 m thick layers, each with a known volumetric water content and a known capacity to hold water (field capacity). If the volume of incoming water exceeds a given layer's field capacity, then the layer below receives the excess water. This process begins at the surface layer with water input from irrigation or rain, and is repeated for each layer.

Evaporation and transpiration are calculated from weather data, factors such as leaf surface area and root density and variables influencing water movement within the plant and from the soil to the roots. Crop growth is modeled as a process which is controlled by water availability and daily sunlight intensity and duration.

The salinity of soil water in each layer is calculated by adding the quantity of ions dissolved in incoming water to the quantity already in each soil layer, and dividing the total by the volume of water previously in the soil plus the volume of incoming water. Water overflowing to the next layer down is modeled as having this new salinity. A number of assumptions are made to support this approach. These include (1) the complete and instantaneous mixing of incoming and soil water, (2) no fertilizers or chemical amendments contribute to soil water salinity and (3) no salts are removed by the crop.

The simulation of gypsum precipitation and dissolution is based on the calculation of the activities of Ca^{2+}, Mg^{2+}, SO_4^{2-} and $CaSO_4^0$, according to Debye-Hückel theory (see sections 1.3.2 and 1.3.3, pages 1-9 to 1-11). Gypsum precipitates when the ion activity product of Ca^{2+} and SO_4^{2-} exceeds the gypsum solubility product (2.63×10^{-5} at 25°C - Drever, 1997). The quantity of gypsum precipitated is calculated by iteratively reducing Ca^{2+} and SO_4^{2-} concentrations by equal increments and recalculating the ion activity product until it becomes equal to the gypsum solubility product. The total reduction in Ca^{2+} and SO_4^{2-} concentrations at equilibrium is equal to the quantity of gypsum which has precipitated from a given volume

of solution. If the ion activity product of Ca^{2+} and SO_4^{2-} is less than the gypsum solubility product, and gypsum has precipitated in the soil layer, then gypsum dissolution is modeled by iteratively increasing Ca^{2+} and SO_4^{2-} concentrations (and reducing the stock of gypsum) until equilibrium is achieved.

There are some shortcomings of this simulation of gypsum solubility. Firstly, the $MgSO_4^0$ ion pair is not taken into account. This species has an association constant of $10^{2.37}$ (Drever, 1997), compared with a value of $10^{2.31}$ for $CaSO_4^0$. In the presence of sufficient Mg in solution, this ion pair will play a quantitatively comparable role to that of $CaSO_4^0$ in reducing the activity of SO_4^{2-} and enhancing gypsum solubility. Secondly, no ion exchange or adsorption phenomena are taken into account. These may be important in controlling the activities of Ca^{2+}, $Mg^{2+}$and SO_4^{2-} in the soil solution, and hence may influence gypsum solubility.

The model was used by Annandale et al. (1999) to simulate 30 years of irrigated cultivation of pearl millet and oats, followed by 20 years of dryland (non-irrigated) cultivation of pearl millet during the summer rainy season on soils of the Bainsvlei form, i.e., the same soil form as is present in Pivot Major. The model predicts that, under irrigation with water of a similar quality to that used at Kleinkopje ((26 $mmol_c/l$ Ca^{2+}, 16 $mmol_c/l$ Mg^{2+} and 42 $mmol_c/l$ SO_4^{2-} - see Table 1.1), at a rate of 1019 mm/year to 1222 mm/year, 14 to 17 x 10^3 kg/ha/year of gypsum would precipitate in the upper 1.1 m of the soil, during the 30 years of irrigation. During the 20 years after irrigation ended, the model predicts the slow dissolution of the accumulated gypsum. The quality of the water draining below 1.1 m depth is expected to stabilize at a TDS of close to 2.6 g/l – the solubility of gypsum at 25°C – in the post-irrigation period.

Although the irrigation water and the soil type used in the model are similar to those in the field trial at Kleinkopje, the real and simulated situations are not strictly comparable. Firstly, maize and wheat are the crops cultivated in the field trial, as opposed to millet and oats. Secondly, the real rate of irrigation is much lower than that simulated. In the 24 months of irrigation since December 1997, pivot Major and pivot Tweefontein have had 1001 mm and 1119 mm of irrigation, respectively, i.e, average values of 500 mm/year and 560 mm/year. Pivot Four, in 14 months of irrigation (January 1999 to March 2000) has had only 304 mm of irrigation (these irrigation values are for the field capacity treatments). Simulations which

incorporate these lower irrigation volumes predict between 5 and 8 x 10^3 kg/ha/year of gypsum accumulation in the upper 1.1 m of soil at Kleinkopje. (Dr. J. Annandale, Department of Plant Production and Soil Science, University of Pretoria, pers. comm., 2000).

1.2.4 Origins and quality of mine water

The composition of the saline mine water used for irrigation is given in Table 1.1. It is likely that this composition reflects initial generation of H_2SO_4 by the oxidation of pyrite, which is often present in association with coal. The chemical process that causes acid mine drainage can be represented as two steps:

1. $4Fe^{2+} + O_2 + H^+ = 4Fe^{3+} + 2H_2O$
2. $FeS_2 + 14Fe^{3+} + 8H_2O = 15Fe^{3+} + 2SO_4^{2-} + 16H^+$ (Drever, 1997).

Table 1.1: The composition of saline mine water (C. Joubert, Senior Hydrologist, Kleinkopje Colliery, pers. comm., 2000).

	Irrigation water applied to pivot Major (mmol$_c$/l)	Irrigation water applied to pivots Tweefontein and Four (mmol$_c$/l)
Ca^{2+}	18-30	13-25
Mg^{2+}	11-18	12-22
Na^+	0.9-1.8	1.7-2.7
K^+	0.2-0.3	0.4-0.6
SO_4^{2-}	28-45	27-45
HCO_3^-	1.2-1.8	1.4-2.0
Cl^-	0.4-0.6	0.9-1.2
pH	6.8-8.0	6.2-8.9

Water percolating through soil and overlying rock to reach the coal seams in which these reactions occur may aquire significant concentrations of alkalinity, contributed by the dissolution of carbonate minerals present in the soil and rock. The alkalinity of the water reaching the coal seam may be sufficient to neutralise the acidity generated by the oxidation of pyrite, in which case the product is a saline mine water with high concentrations of SO_4^{2-} and basic cations.

This is thought to be the process by which the water used to irrigate pivot Major was produced. This water is pumped to surface from disused underground mine workings and is naturally circum-neutral with respect to pH (Table 1.1). The water used to irrigate pivots Tweefontein and Four is collected from the open-cast mining area, and is acidic, but the pH is raised to near neutral by treatment with lime.

1.3 Literature review

The theoretical framework of solute transport and retention in soils is pertinent to the chemical response of soils to irrigation, and is discussed briefly here. In particular, processes influencing solute transport in soils, the theory of ion activities, precipitation and dissolution, and processes of ion adsorption are considered. In addition, irrigation with mine water is effectively the application of a solution of dissolved gypsum and magnesium sulphate, so some of the literature which deals with the agricultural use of gypsum is reviewed here.

1.3.1 Solute transport in soils

The movement of solute ions in a soil is controlled by processes of advection, hydrodynamic dispersion, molecular diffusion and sorption (Leij & Van Genuchten, 1999). Advection is the bulk movement of the solution, and it is modified by hydrodynamic dispersion, the result of variations at soil-pore scale of the velocity of water flow. Molecular diffusion is the tendency of dissolved species to migrate down gradients of chemical potential – e.g. from regions of higher to lower concentration. Sorption processes, including ion exchange and adsorption on surfaces as well as the precipitation of solid phases, influence solute transport by retarding the movement of solute and altering the solution composition (Leij & Van Genuchten, 1999).

1.3.2 Ion activities

The chemical behaviour of species in solutions is often described in terms of the species' activities (Drever, 1997). In particular, the activity coefficients of solute ions are commonly estimated using empirical expressions such as the Debye-Hückel equation:

$$\log \gamma_i = -Az_i^2\sqrt{I}$$

where A is a constant depending on temperature and pressure, z_i is the charge on the particular ion, and I is the ionic strength of the solution, given by

$$I = \tfrac{1}{2}\Sigma m_i z_i^2$$

where m_i is the molar concentration of the mth ion. The activity {i} of an ion i is given by

$$\{i\} = \gamma_i m_i$$

The Debye-Hückel equation takes into account the electrostatic interactions between ions in solution which modify their behaviour from that which might be expected from the ideal case of a point charge in an infinitely dilute solution. The equation is adequate for solutions of low I, but is modified to take account of the finite size of ions in solutions of higher I (Drever, 1997).

1.3.3 Precipitation and dissolution reactions

1.3.3.1 Equilibrium chemistry of precipitation and dissolution

Dissolution and precipitation reactions may be represented as

$$A_aB_b(s) = aA^{n+}(aq) + bB^{m-}(aq)$$

The equilibrium constant for this kind of reaction, often referrred to as the solubility product, is given by

$$K_{sp} = \{A^{n+}\}^a\{B^{m-}\}^b$$

where {} represent activities. The standard-state values of K_{sp} have been determined experimentally for many substances, and so, for any solution of ions A^{n+} and B^{m-}, if K_{sp} is known, it is possible to express the tendency of that solution to precipitate or dissolve $A_aB_b(s)$ by reference to the ratio

$$\{A^{n+}\}^a\{B^{m-}\}^b / K_{sp}$$

This ratio is often expressed in logarithmic form as the saturation index (SI), i.e,

$$SI = \log [\{A^{n+}\}^a\{B^{m-}\}^b / K_{sp}]$$

A solution is undersaturated with respected to the solid phase, and will tend to dissolve it when $SI < 0$. Conversely, a solution is oversaturated and will tend to precipitate the solid phase when $SI > 0$. The equilibrium state is represented by $SI = 0$ (Drever, 1997).

1.3.3.2 Precipitation

In the absence of a pre-existing solid phase, and only when a solution is strongly oversaturated with respect to a given compound, there is incipient formation of a very fine crystalline precipitate with a disordered lattice – known as the 'active' form of the compound. This form persists in metastable equilibrium with the solution, and converts slowly to the more stable, ordered, inactive form of the compound. The active forms of compounds have greater solubilities, due to their small particle size and resulting greater interfacial energy (Stumm & Morgan, 1996).

At low degrees of oversaturation, nucleation (incipient precipitation) can only take place if there is some means of minimising the interfacial energy of the active form of the incipient precipitate. This is commonly accomplished by nucleation taking place in contact with some other solid phase (Drever, 1997).

Apart from thermodynamic considerations, it is known that precipitation may be inhibited by the interference of other species in solution. In the case of gypsum, dissolved humic substances can retard or prevent precipitation from a oversaturated solution. This is thought to occur because of the adsorption of humic anions onto gypsum crystal nuclei, effectively coating the crystal and isolating it from the solution (Van den Ende, 1991). It has been suggested that, in acid soils, the dissolution (and precipitation) of gypsum crystals might also

be similarly inhibited by the coating of the crystals with aluminium phosphate (Frenkel et al., 1989).

1.3.4 Ion exchange and chemisorption

Soil colloids (finely divided clay minerals, oxide minerals and organic matter) possess electrical charge on their surfaces and thus tend to adsorb ions from solution onto their charged surfaces. The process of adsorption may be reversible or irreversible. The cation (or anion) exchange capacity (CEC or AEC) of a mineral is the quantity of cations or anions reversibly adsorbed per unit weight of the mineral (McBride, 1994). The units used here for ion exchange capacity are millimoles of charge per kilogram ($mmol_c/kg$).

Most clay minerals possess a permanent negative surface charge by virtue of their molecular structure, which allows for either isomorphous substitution of metal cations of different charge or vacancies (missing cations), so that clays have a net deficit of positive charge in their structure (McBride, 1994). Kaolinite ($Al_2Si_2O_5(OH)_4$), a clay mineral common in deeply weathered soils of temperate to tropical climates, has little or no permanent negative surface charge, but silanol groups on the edges of clay molecule surfaces are likely to adsorb cations, as follows:

$$\equiv Si\text{-}OH \quad = \quad \equiv Si\text{-}O^- + H^+ \qquad (1)$$

$$\equiv Si\text{-}O^- + M(H_2O)_y^{n+} \quad = \quad \equiv Si\text{-}O^-\text{---}\ M(H_2O)_y^{n+} \qquad (2)$$

where ≡Si-OH represents a silanol group and $M(H_2O)_y^{n+}$ a hydrated cation. The bond (---) formed between the silanol group and the cation is electrostatic and the cation is exchangeable, as it would be if bonded to a negatively charged clay surface site. It can be seen that reaction (1) is a pH dependent process, and that both (1) and (2) would tend to occur less at lower pH (McBride, 1994).

Kaolinite also has edge sites of the form $>M\text{-}OH_2^{+½}$, where M is typically Al^{3+}. These sites are essentially identical to the surface functional groups associated with Fe, Mn and Al oxides and hydroxides commonly found in soils. These sites tend to be weakly acidic, and their average surface charge is pH dependent, i.e.

$$>M\text{-}OH_2^{+½} \quad = \quad >M\text{-}OH_2^{-½} + H^+$$

The surface charge is thus positive at low pH and negative at higher pH, and hence these minerals possess CEC at high pH and AEC at low pH (McBride, 1994). Of particular interest for this study is the known tendency of kaolinite to adsorb sulphate ions, specifically but reversibly, at these edge sites (Mott, 1981).

Oxides and hydroxides of Fe, Al and Mn also form, specific, non-reversible, or slowly reversible inner-sphere complexes with anions by a process of ligand exchange, which can be written as

$$>M\text{-}OH + A^{n-} = >M\text{-}A^{n-1} + OH^-$$

where the anion A^{n-} exchanges for the hydroxyl group. This reaction is enhanced at low pH by the protonation of the hydroxyl group, i.e.,

$$>M\text{-}OH + H^+ = >M\text{-}OH_2$$

After protonation, the water molecule is less strongly bonded to the metal than the hydroxyl group and ligand exchange is favoured (McBride, 1994).

1.3.5 The effects of irrigation with saline mine water on soil chemistry

1.3.5.1 The build-up of soil salinity

Irrigation with saline water may result in the accumulation of dissolved mineral salts in the soil solution, i.e., an increase in soil salinity (Thellier et al., 1990). Soil salinity has negative effects on plant growth – it decreases the availability of water to plants, and leads to reduced rates of germination and growth (Tanji, 1990). The salinization of the overlying soils may result in groundwater becoming saline. Water draining from the root zone inevitably has higher concentrations of dissolved salts than irrigation water, as a result of evapotranspiration, and this saline deep drainage water must inevitably influence

groundwater quality. Salinization of the groundwater is more likely if the irrigation water is itself saline, or soluble salts are present in the unsaturated zone (Suarez, 1989).

Changes in the chemistry of the soil solution in soils irrigated with saline water depend on numerous interdependent multi-phase chemical interactions, including:

- the dissolution and precipitation of minerals,
- the formation of inorganic and organic co-ordination compounds in solution (i.e., ion pairing),
- the adsorption and exchange of ions and ligands,
- interactions between the liquid and gas phase (e.g., the influence of the partial pressure of CO_2 on calcite solubility) and
- reduction and oxidation reactions. (Jurinak, 1990).

1.3.5.2 The effects of irrigation with high-sulphate water on soil chemistry

Theoretically, the precipitation and dissolution of gypsum is likely to control the concentrations of Ca^{2+} and SO_4^{2-} in the soil solutions of soils irrigated with water with high concentrations of these ions (Papadopoulos, 1987). However, it has been found that the concentrations of Ca^{2+} and SO_4^{2-} in soil solutions after irrigation with high-sulphate water can be higher than would be expected from the solubility of gypsum (Papadopoulos, 1986). One explanation of this is the observation by Oster and Frenkel (1980) that gypsum solubility is higher in sodic soils than in water, as a result of the cation exchange phase acting as a sink for Ca^{2+} ions.

1.3.5.3 Sodic soils and dispersive behaviour

The phenomenon of dispersivity of soils, where clay aggregates are broken down and transported by water into soil pores, thus reducing soil permeability, has been extensively studied, in particular the prevalence of this behaviour in soils with high levels of exchangeable Na, known as sodic soils (e.g. McBride, 1994; Levy, 1999; Sumner 1993). Soil sodicity can be induced by irrigation with water having a high ratio of Na to Ca and Mg, usually measured as the Sodium Adsorption Ratio (SAR), while irrigation waters dominated by dissolved Ca and Mg salts tend to maintain good soil physical properties by flocculating

and aggregating soil particles (Thellier et al., 1990). Sodic soils that are exposed to rainfall or irrigated with water of a low ionic strength tend to behave dispersively. However, Sumner (1993) has pointed out that dispersive behaviour also occurs in non-sodic soils, where aggregates are mechanically disrupted by the impact of rain drops, for example, and the soil solution has a low enough ionic strength to inhibit flocculation.

1.3.6 The use of gypsum on soils

1.3.6.1 Amelioration of dispersive soils

Gypsum has been used to remedy dispersive behaviour in soils for many years (Sumner, 1993, Shainberg et al., 1989). Applied to the soil as a solid, it is sufficiently soluble to raise the soil solution's ionic strength to levels which enhance clay flocculation, as well as to gradually replace Na with Ca on clay exchange sites, thus reducing the soil's sodicity. Sumner (1993) notes that gypsum application can actually increase clay dispersion in acid soils, by reducing the activity of Al^{3+} in the soil solution, effectively reducing its ionic strength. In addition, Ca^{2+} displaces Al^{3+} from cation exchange sites, reducing the strength of interlayer electrostatic forces. Possible mechanisms by which gypsum application reduces Al^{3+} activity in the soil solution are discussed in section 1.3.6.2 below.

1.3.6.2 Amelioration of subsoil acidity

Recently, much evidence has been presented on the beneficial effects of gypsum in counteracting soil acidity (Sumner, 1993; Toma et al., 1999; Wang et al., 1999). In particular, gypsum may be more effective than lime at combating acid subsoils. Root growth is inhibited by acid conditions in the subsoil, through the toxic effects of Al (more soluble at low pH) and typically, a deficiency of Ca. This results in shallow rooting, and hence a vulnerability to drought (Shainberg et al., 1989). Gypsum applied to the soil surface is sufficiently soluble that Ca^{2+} and SO_4^{2-} ions penetrate the subsoil, providing Ca to the roots and reducing the activity of soluble Al. A variety of mechanisms have been proposed to explain the observed reduction in Al activity, and include the "self-liming effect", in which SO_4^{2-} ions displace OH^- ions from anion exchange sites on Fe-oxide minerals, resulting in the

precipitation of $Al(OH)_3$ (Reeve & Sumner, 1972), the precipitation of basic Al sulphates (e.g. jurbanite, $AlOHSO_4$ and alunite, $KAl_3(SO_4)_2(OH)_6$), the co-sorption of Al^{3+} onto Fe-oxide surfaces which have increased negative surface charge due to the sorption of SO_4^{2-}, and the formation of the $AlSO_4^+$ ion pair, which is less toxic than Al^{3+} (Sumner, 1993, Shainberg et al., 1989). It has also recently been shown that these effects of gypsum are long lasting, and may persist for decades (Toma et al., 1999).

1.3.6.3 Other chemical effects of gypsum application to soils

Gypsum has been widely observed to cause leaching of exchangeable Mg^{2+}, and in many cases the leaching of exchangeable K^+. Some laboratory studies have also indicated that gypsum application results in the leaching of dissolved Si (Shainberg et al., 1989). As would be expected from the application of the salt of a divalent cation, displacement of Na^+ and NH_4^+ from cation exchange sites has been observed. The leaching of NO_3^- and Cl^- is likely as the divalent sulphate ion is preferentially adsorbed on the surfaces of positively charged colloids. The application of gypsum has been observed to cause the pH of soils to rise slightly, but the evidence is equivocal (Shainberg et al., 1989).

1.3.6.4 Gypsum and plant nutrition

Gypsum has been used as a fertilizer for at least 200 years, and is likely to become increasingly important as a source of sulphur where soils are naturally acidic, and the application of the more commonly used source of agricultural S, ammonium sulphate, would be undesirable, because of its acidifying effects (Shainberg et al., 1989).

Gypsum is widely used as a Ca fertilizer for peanut cultivation, and also for other crops and soil conditions where agricultural lime is an unsuitable source of Ca. For example, potatoes grown in sandy, acid soils of the west coast of South Africa are fertilized with gypsum, since the use of lime as a Ca fertilizer results in a rise in soil pH conducive to the potato disease scab (Shainberg et al., 1989).

The most important plant nutritional problem related to the use of gypsum is the deficiency in Mg observed in crops grown on gypsum-treated soils. It has also been occasionally found that crops grown on these soils develop a K deficiency. These effects are probably due to the preferential exchange of Ca for these ions on cation exchange sites, and their leaching to a depth in the profile where their availability to plants is reduced (Shainberg et al., 1989).

2 Methods

2.1 Sampling and preparation of soil samples

Soil samples were collected from irrigation pivots Major, Four and Tweefontein at Kleinkopje during mid-June 2000. A geological drill rig fitted with a 100 mm diameter push-tube soil corer, 600 mm in length, was used to obtain complete cores of soil from surface to a depth of 3 metres in each of the irrigated fields. Additional cores were obtained from outside each of the three pivots, in areas not irrigated with mine water* (Figure 2.1). Each soil core was divided into 200 to 300 mm long sub-samples and bagged. The samples were dried in air at room temperature (22°C). The air-dried soil was gently disaggregated to pass through a 2 mm sieve. Homogeneous splits were analysed using the methods described below.

2.2 Saturated paste extracts

The method used was that of Rhoades (1982), with slight modifications. Distilled water was gradually added to 200-300 g of air-dried soil, while stirring, until saturation with water was achieved. The saturated soil paste was allowed to stand for 24 hours before analysis. The pH of the paste was measured using a Metrohm 691 pH meter by inserting the pH electrode directly into the paste and allowing the pH reading to settle to a constant value. The soil paste was transferred to a Buchner funnel and an extract obtained from the paste by suction through Whatman No.1 filter paper. Alkalinity was determined by potentiometric titration of 5 or 10 ml of each extract against 0.01M HCl to a pH of 4.5. The titration was carried out using a Radiometer-Copenhagen TTT85 titrator and autoburette system. The remaining

---

* A single soil core was obtained from each irrigation treatment area and from each non-irrigated area. It is possible that these cores are not representative of the soils in these areas in one or more respects. Collection and analysis of replicate cores would have been necessary to assess the magnitude of sampling uncertainty. Unfortunately, time and cost considerations prohibited this, and in spite of this limitation on the study, it is considered that the results presented here are a reasonable assessment of chemical conditions and processes in these soils.

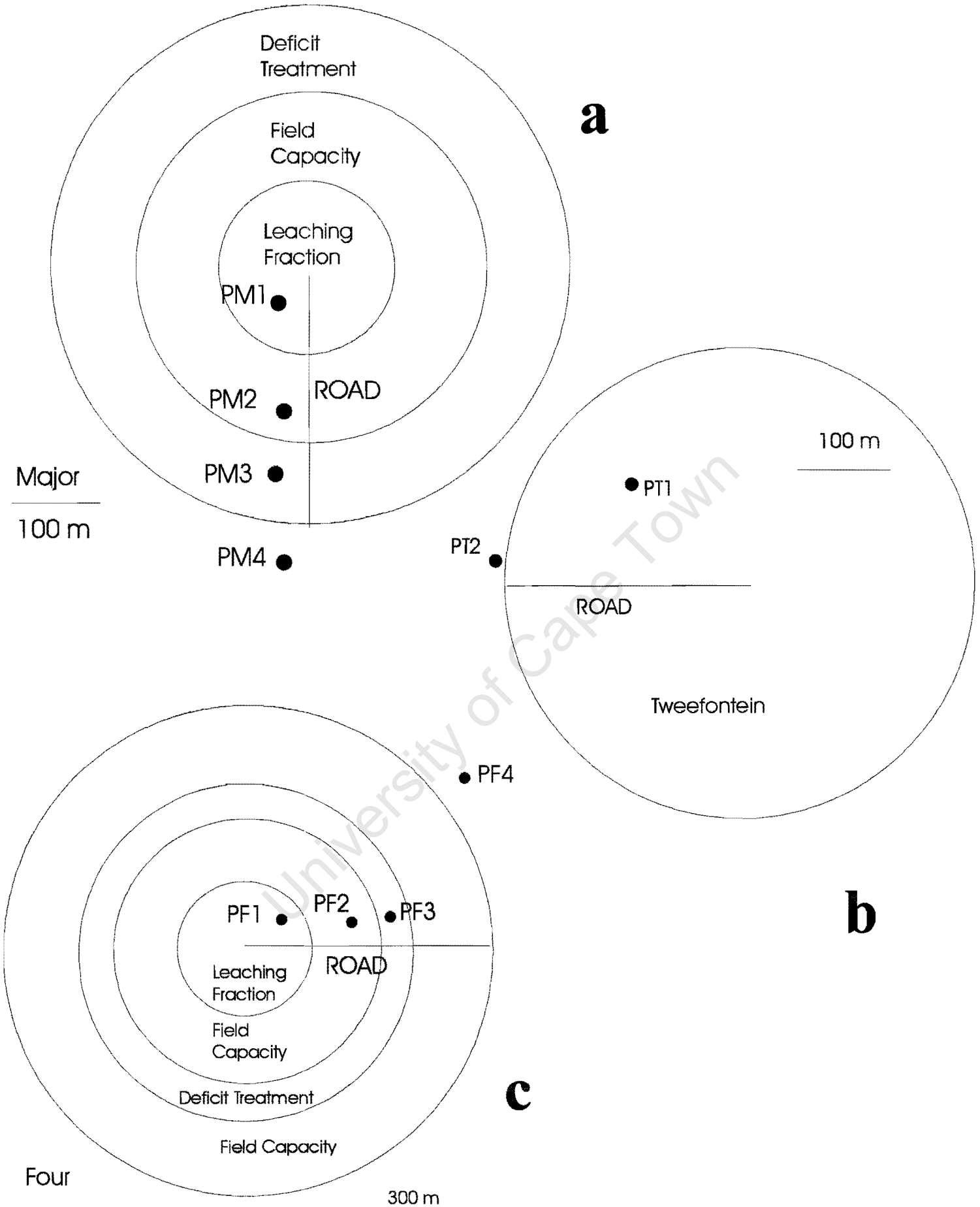

Figure 2.1: Positions of the soil cores collected in pivots Major (a), Tweefontein (b) and Four (c) at Kleinkopje.

extract was then filtered through a 0.45 µm cellulose acetate filter, and its electrical conductivity measured using a Crison Micro CM 2201 electrical conductivity meter. Major anion (F^-, Cl^-, SO_4^{2-}, NO_2^-, NO_3^-, PO_4^{3-}) and cation (Li^+, Na^+, K^+, Ca^{2+}, Mg^{2+} and NH_4^+) concentrations in the extracts were determined by ion chromatography, using a Dionex DX300 series suppressed IC system with AI-450 software (Table 2.1). The samples were diluted to electrical conductivities below 100 µS/cm before analysis.

Table 2.1: Specifications of the Dionex DX300 series ion chromatograph used in the analyses of saturated paste extracts and phosphate-extractable sulphate extracts.

	Anion Unit	Cation Unit
Sample loop capacity	**50 µl**	**25 µl**
Separator Column	**AS14**	**CS12A**
Guard Column	**AG4A**	**CG12A**
Eluant	**3.5 mM Na_2CO_3 + 1 mM $NaHCO_3$**	**22N H_2SO_4**
Eluant flow rate	**1.2 ml/min**	**1.0 ml/min**
Suppressor	**ASRS-I-4 mm**	**CSRS-I-4 mm**

The dissolved organic carbon content of the samples was determined by colorimetry at the Council for Scientific and Industrial Research's Division of Water Technology, located in Stellenbosch. In the method used, dissolved organic carbon in an aliquot of sample is oxidised to CO_2 by the addition of potassium persulphate and exposure to UV light. The CO_2 released is allowed to diffuse through a gas-permeable membrane into phenolpthalein solution, causing the solution to change colour. The relationship between the phenolpthalein solution's absorbance of light at 590 nm and DOC concentration is established by calibration with solutions of known DOC concentration (Mike Louw, laboratory head, CSIR, pers. comm., 2000).

2.3 Soil pH

In addition to the pH measurements made in the saturated pastes, soil pH was measured in soil and water, and soil and 1M KCl suspensions, following the method of the Non-Affiliated Soil Analysis Working Committee (1990). A suspension of

10g of air-dried soil and 25 ml of distilled water was stirred vigorously for 5 seconds, then allowed to stand for 50 minutes. The suspension was stirred again for 5 seconds and allowed to stand for 10 minutes. The pH of the suspension was measured, using a Metrohm 691 pH meter, by inserting the pH electrode into the supernatant and taking the reading after 30 seconds. To determine the pH in 1M KCl, the same procedure was followed, substituting a 1M KCl solution for distilled water.

2.4 Exchangeable cations

2.4.1 Exchangeable acidity

A slight variation of the method of Thomas (1982) was used to determine the soils' exchangeable acidity (i.e., $Al^{3+} + H^{+}$). A suspension of of 2.5 g of soil in 25 ml of 1M KCl was shaken for 4 minutes and centrifuged for 2 minutes. The supernatant liquid was transferred to a conical flask, and potentiometrically titrated against 0.01M NaOH to the phenolpthalein end-point (pH = 8.3) using a Radiometer-Copenhagen TTT85 titrator and a Brand digital burette. The molar quantity of NaOH added to the soil extract is stoichiometrically equivalent to the acidity extracted from the soil.

2.4.2 Exchangeable Ca, Mg, Na and K by 0.1 M ammonium acetate extraction and atomic absorption spectrometry

The method of Thomas (1982) was used. A suspension of 5 g of soil in 25 ml of 0.1 M ammonium acetate solution was shaken for 30 minutes, then centrifuged at 2000 rpm for 10 minutes. The supernatant was transferred into 50 ml volumetric flasks. Another 25 ml of ammonium acetate were added to the centrifuge tubes and the procedure repeated. The volumetric flasks were filled to the 50 ml mark with additional ammonium acetate solution. After filtration through Whatman No.1 filter paper, the Ca, Mg, K and Na concentrations in the extracts were determined by flame atomic absorption spectrometry (FAAS) in the Department of Chemical Engineering at the University of Cape Town, using a Varian Spectra AA30 spectrometer.

2.5 Grain-size analysis

A weighed portion (about 20 g) of dried soil sample was wet-sieved through a 63 μm sieve to separate the sand fraction. The sand was transferred to a beaker, air-dried and weighed. The – 63 μm (silt and clay) fraction was transferred to a 500 ml beaker, to which was added 10 ml of 3% sodium hexametaphosphate solution, to enhance clay dispersion. The silt and clay was thoroughly disaggregated using a Virsonic 475 ultrasonic cell disruptor at 20% power for 30 seconds. The silt and clay suspension was allowed to settle for 2-3 hours and the supernatant was transferred to a centrifuge tube and centrifuged at 6000 rpm for 5 minutes, to collect the clay size fraction for characterisation of clay mineralogy by XRD. The procedure was repeated several times until the supernatant was clear after settling. The settled silt fraction was dried and weighed. The mass of the clay fraction was determined by difference.

2.6 Clay mineralogy

Air-dried slurry mounts of the separated clay fraction were prepared on glass slides during the grain-size determination and analysed using a Philips X-ray diffractometry system with a Cu tube ($\lambda(K\alpha)$ = 1.54056 Å), running at 40 kV/25mA. Scans were carried out over a 2θ range of 4-75°, with a step size of 0.03°. Mineral peaks of minerals were identified using Moore and Reynolds (1997).

2.7 Organic carbon

Total organic carbon content of the soils was determined by a colorimetric variation of the Walkley-Black dichromate oxidation method (Baker, 1976). Potassium dichromate was used to oxidise carbon in the soils, by heating in the presence of sulphuric acid

$$2K_2Cr_2O_7 + 3C + 8H_2SO_4 = 3CO_2 + 2Cr_2(SO_4)_3 + 2K_2SO_4 + 8H_20$$

and the concentration of reduced Cr^{3+}, stoichiometrically proportional to the original carbon content, was determined colorimetrically.

Sucrose was used to prepare a number of standards with carbon concentrations of between 0 mg/ml and 12.5 mg/ml. Aliqots of standard or 1 g samples of soil were transferred to digestion tubes to which were added 2 ml water, 10 ml 5% potassium dichromate and 5 ml concentrated H_2SO_4. The tubes were place in a digestion block and the mixture allowed to react at 150°C for 30 minutes. After cooling, 50 ml of 0.4% $BaCl_2$ solution were added to each tube. The tubes were left to stand overnight. The absorbance of the supernatant at 600 nm was measured using a spectrophotometer. A calibration curve was constructed from the measured absorbances of the standard solutions, and the C content of the unknown samples determined by comparison with the calibration curve.

2.8 Phosphate-extractable sulphate

A variation of the method of Tabatabai (1982) was used to determine the concentration of adsorbed sulphate in the soils. Saturation of the soils with an excess of PO_4^{3-} was used to displace adsorbed sulphate into solution, and its concentration was determined by ion chromatography.

A suspension of 5 g of soil in 25 ml of a 0.01 M $Ca(H_2PO_4)_2$ solution was shaken for 16 hours. The suspension was centrifuged and filtered though Whatman No.1 filter paper. It was necessary to dilute the extract 10 times with distilled water to reduce its concentration (as measured by electrical conductivity) to a level suitable for analysis by ion chromatography. The extracts were analysed using the same Dionex DX300 series ion chromatograph used for analysis of the saturated paste extracts. The high concentration of phosphate in the extracts resulted in some overlap of the phosphate and sulphate peaks. For samples in which the sulphate concentrations were less than about 2 mg/l in the diluted extracts, it was impossible for the analytical software to resolve the sulphate peak. The results for these samples are indicated as being below the analytical detection limit.

2.9 Chemical equilibrium modeling of the soil solution

PHREEQC, a thermodynamic equilibrium computer model (Parkhurst and Appelo, 1999) was used to determine the speciation of the major constituents of the saturated paste extracts, and the state of saturation of the saturated paste extracts with respect to gypsum. In the analyses performed in this research, PHREEQC calculated solute activities using the WATEQ Debye-Hückel equation :

$$\log \gamma_i = -\frac{Az_i^2\sqrt{\mu}}{1+Ba_i^o\sqrt{\mu}} + b_i\mu$$

Where γ_i is the activity coefficient of species i, z_i is the ionic charge of aqueous species i, μ is the ionic strength of the solution and A and B are constants dependent only on temperature. In the WATEQ Debye-Hückel equation a_i^o and b_i are ion-specific parameters fitted from empirical activity coefficient data (Parkhurst and Appelo, 1999). Relevant thermodynamic data are tabulated in Appendix C, along with example input and output files for PHREEQC.

The saturation index (SI) of a solid phase is calculated according to:

$$SI = \log (IAP/K_{sp})$$

where IAP is the ion activity product of the relevant solute ions, and K_{sp} is the solubility product, i.e. the equilibrium constant of the phase in equilibrium with an aqueous solution (Drever, 1997).

2.10 Measurement of the gypsum content of the soils

The method of increasingly dilute aqueous soil extracts (J.D.Oster, University of California, Riverside, pers. comm., 2000) was used to determine the gypsum content of the soils. For each of the two soil samples with the highest gypsum saturation indices (PM2 200-400 mm and PM2 400-600 mm), five soil-water suspensions with different water:soil ratios were prepared in 50 ml PVC centrifuge tubes, by adding MilliQ de-ionised water to sub-samples of soil. The water:soil ratios used were 1:1 (20 g soil : 20 ml water), 1:2 (10 g soil : 20 ml water), 1:5 (4 g soil : 20 ml water), 1:10 (2 g soil : 20 ml water) and 1:20 (1 g soil : 20 ml water). The suspensions were shaken by a mechanical shaker for 18 hours, then centrifuged at 6000 rpm for 10 minutes. The supernatant was filtered through a 0.45 μm cellulose acetate filter and its ionic composition determined using the Dionex DX300 series ion chromatograph described in Section 2.2. PHREEQC (Parkhurst & Appelo, 1999) was used to calculate the gypsum saturation indices of the extracts.

Finely ground sub-samples of the two soil samples with the highest gypsum saturation indices (PM2 200-400 mm and PM2 400-600) were analysed by XRD. The samples were subjected to a slow-step scan over the major gypsum diffraction peak at 7.61 Å (Dixon & Weed, 1985). The scan covered the 2θ angular interval corresponding to d-spacings between 6.5 Å and 8.5Å with a step-size of 0.005°, and a dwell time of 2.5 s per step.

2.11 Estimation of analytical accuracy

The principal indicators of analytical accuracy are bias and precision. No determination of analytical bias was made for any of the procedures described above, but in most cases, the analytical precision was estimated using duplicates, as described by the American Public Health Association et al. (1995). Duplicate analyses of a number of randomly chosen samples, representing about 10% of the total number of samples, were carried out. The difference between duplicates is denoted as R. The mean R value for a particular analytical procedure is $\underline{R}$. The standard deviation (s) is estimated as:

$s = \underline{R}/1.128$

Total uncertainty(U), at the 95% confidence level, is estimated as:

$U = (2s^2 + B^2)^{½}$

where B is analytical bias. Assuming B = 0, this simplifies to:

$U = \sqrt{2}\ s$

Any result (x) can thus be expressed as $x \pm U$.

In cases where the analytical results of different samples differed greatly in magnitude, relative forms of the above expressions were used, and U is expressed as a percentage.

3 Results

3.1 Physical description of samples

3.1.1 Appearance of soils during sampling

The soil cores were described as they were being collected in the field, in terms of their colour, moisture content and textural features (Table 3.1).

Table 3.1: Description of sample appearance (textural classification from Skopp, 1999). A tick next to a row indicates that the sample representing this depth interval was included in the chemical analyses discussed in the rest of this chapter.

	Depth interval (mm)	Samples taken in Pivot Major (irrigated to field capacity) Core PM2		Depth interval (mm)	Sample taken just outside Pivot Major (non-irrigated) Core PM4
✓	0-200	Moist, brown sandy loam.	✓	0-300	Slightly moist, brown sandy loam.
✓	200-420	Moist, reddish-brown sandy loam.			
✓	420-600	Moist, reddish-brown sandy loam with grey mottles.	✓	300-600	Slightly moist, reddish-brown sandy loam.
	600-900	Moist, reddish-brown sandy loam.		600-900	Slightly moist, reddish brown sandy loam.
✓	900-1100	Saturated, reddish-brown, sandy clay loam with grey mottles and iron concretions.	✓	900-1200	Moist, brownish-red sandy clay loam.
	1100-1300	Saturated, reddish-brown, sandy clay loam with iron concretions.			
✓	1300-1500	Saturated, red, sandy clay loam with reddish-yellow mottles and iron concretions.	✓	1200-1500	Saturated, brownish-red sandy clay loam with grey mottles.
	1500-1800	Saturated, red, sandy clay loam with reddish-yellow mottles and iron concretions.		1500-1800	Saturated, brownish-red sandy clay loam with grey mottles & a few soft iron concretions.
✓	1800-2100	Moist, mottled greyish-yellow/reddish-brown clay loam with black root fibres.	✓	1800-2100	Moist, brownish-red, clay loam with iron concretions.
	2100-2400	Moist, mottled greyish-yellow/reddish-brown clay loam with black root fibres.		2100-2400	Moist, brownish-red, clay loam with yellowish-grey mottles and iron concretions.
	2400-2700	Moist, mottled greyish-yellow/reddish-brown clay loam with sandy reddish-yellow lens.		2400-2700	Saturated, greyish-yellow, gravelly clay loam with angular gravel fragments.
✓	2700-3000	Moist, mottled greyish-yellow/reddish-brown, sandy clay loam with iron concretions.	✓	2700-3000	Saturated, mottled, greyish yellow, red and black weathered sandstone.

Table 3.1: Description of sample appearance (continued)

Depth interval (mm)	Sample taken from Pivot Four (irrigated to field capacity) Core PF2	Depth interval (mm)	Sample taken from just outside Pivot Four (non-irrigated) Core PF4
✓ 0-300	Slightly moist, dark brown sandy loam.	✓ 0-300	Slightly moist, dark brown sandy loam.
✓ 300-600	Moist, reddish-brown sandy loam.	✓ 300-600	Slightly moist, dark reddish-brown sandy loam.
600-900	Moist, reddish-brown sandy loam.	600-900	Moist, brownish-red sandy loam.
✓ 900-1200	Moist, reddish-brown sandy clay loam.	✓ 900-1200	Moist, brownish-red sandy loam.
1200-1500	Very moist, reddish-brown sandy clay loam.	1200-1500	Moist, brownish-red sandy clay loam with soft iron concretions.
✓ 1500-1800	Saturated, reddish-brown sandy clay loam.	✓ 1500-1800	Moist, brownish-red sandy clay loam with soft iron concretions.
1800-2100	Saturated, brownish-red sandy clay loam with dark brown mottles.	1800-2100	Moist, brownish-red sandy clay loam with soft iron concretions and a few small grey linear mottles.
✓ 2100-2400	Saturated, brownish-red sandy clay loam with dark brown mottles.	✓ 2100-2400	Very moist, brownish-red sandy clay loam with soft iron concretions and a few small, grey linear mottles.
2400-2700	Saturated, brownish-red sandy clay loam with "veins" of weathered sandstone.	2400-2700	Moist, brownish-red sandy clay loam with soft iron concretions and larger grey mottles.
✓ 2700-3000	Saturated, brownish-red sandy clay loam with "veins" of weathered sandstone.	✓ 2700-3000	Moist, brownish-red sandy clay loam with soft iron concretions and grey linear mottles, giving sample a veined appearance.
✓ 3000-3300	Moist, mottled, light grey, yellow and brownish-red sandy clay loam with a few iron concretions and a few gravel fragments.	✓ 3000-3300	Moist, brownish-red sandy clay loam with soft iron concretions and grey linear mottles which give sample a veined appearance.
		3300-3600	Moist, brownish-red sandy clay loam with a few hard iron concretions and quartz gravel and grey linear mottles which give sample a veined appearance.

Depth interval (mm)	Sample taken in Pivot Tweefontein (irrigated to field capacity). Core PT1	Depth interval (mm)	Sample taken just outside Pivot Tweefontein (non-irrigated) Core PT2
✓ 0-300	Slightly moist, red sandy loam.	✓ 0-300	Dry, reddish brown sandy loam.
✓ 300-600	Moist, brownish-red sandy loam.	✓ 300-600	Dry, reddish brown sandy loam.
600-700	Moist, brownish-red sandy loam and black coaly shale mine spoil.	600-900	Moist, mixed brown and reddish-brown sandy loam.
		900-1200	Moist, mixed brown and reddish-brown sandy loam.
		1200-1300	Black and grey coaly shale mine spoil.

3.1.2 Grain-size (textural) analysis of the irrigated soil profiles

The clay and silt contents of the irrigated soils from both pivots Major and Four increased with depth (Figure 3.1). In pivot Major, the clay content increased from 17.6% in the 0-300 mm sample to 32.4% in the 1800-2100 mm sample, with a slight decrease to 28.4% in the 2700-3000 mm sample. The silt content followed a similar trend, increasing from 13.7% in the topsoil to 23.5% in the 1800-2100 mm sample, followed by a slight drop to 19.5% in the 2700-3000 mm sample. In pivot Four, the clay content increased from 17.8% in the topsoil to 32.0% in the 3000-3300 mm sample, and silt increased from 11.5% in the topsoil to 18.1% in the 3000-3300 mm sample.

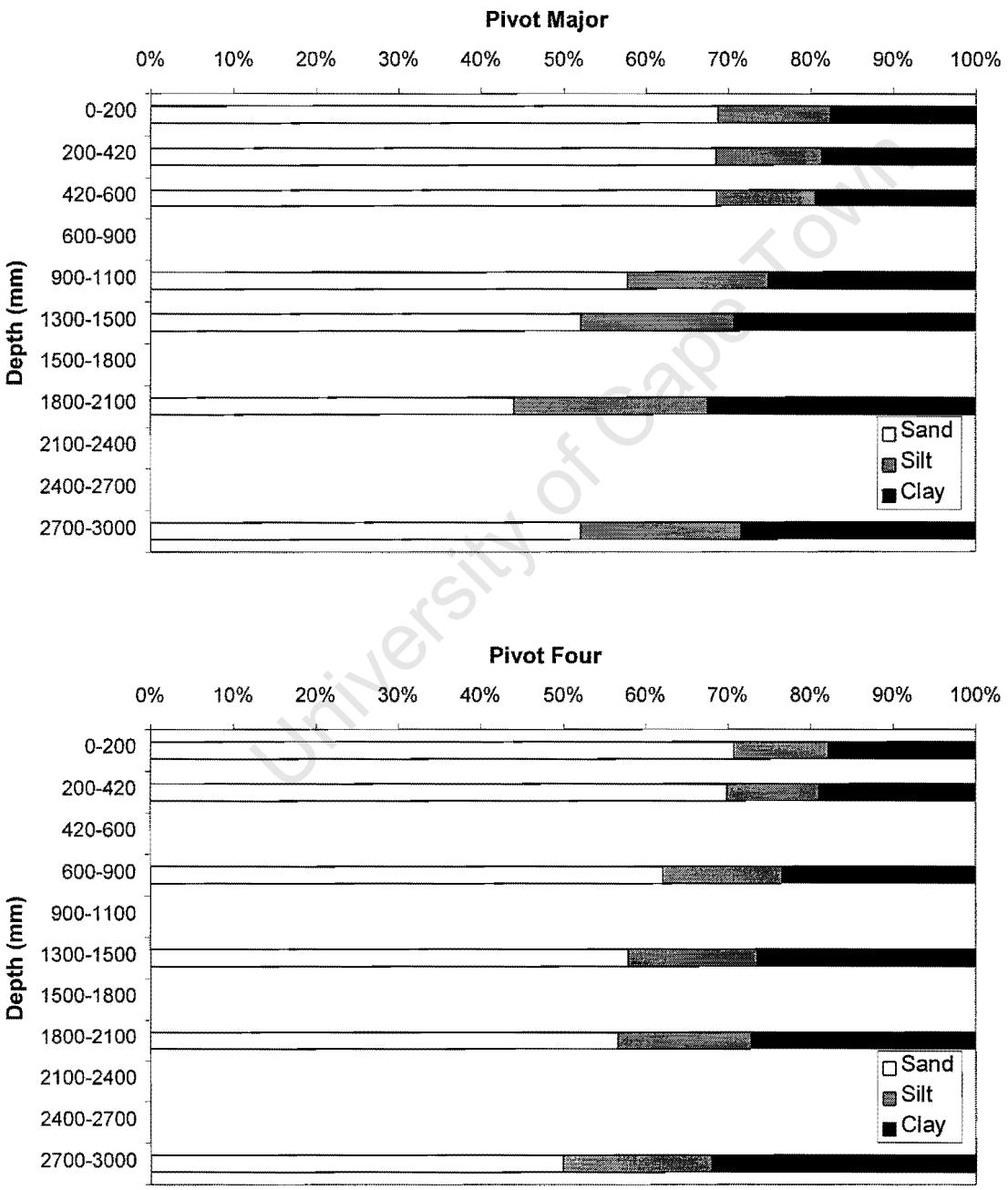

Figure 3.1: Grain-size distribution versus depth for the irrigated soils in pivots Major and Four.

3.1.3 Clay mineralogy

XRD results indicate that the soils' clay fraction is dominated by kaolinite. Mica is the next most abundant clay mineral. Small quantities of goethite and haematite are present.

3.2 Soil solution composition from saturated paste extracts

3.2.1 Electrical conductivity (EC) of saturated paste extracts

The electrical conductivities of saturated paste extracts indicate that the irrigated soils have higher soluble salt contents than the non-irrigated soils (Figure 3.2).

3.2.1.1 Pivot Major

The electrical conductivity (EC) of the irrigated soil increases with depth to a maximum value of 2.4 dS/m in the 400-600 mm sample, then decreases rapidly through the remainder of the profile. In the non-irrigated soil, however, the EC profile has a bimodal appearance, with twin peaks of 0.5 dS/m and 0.6 dS/m in the topsoil and 900 to 1500 mm depth intervals, respectively.

3.2.1.2 Pivot Tweefontein (irrigated)

The highest EC's were measured in the 300-600 mm samples from both irrigated and non-irrigated soils. The irrigated soil's EC in this sample (2.0 dS/m) is almost an order of magnitude greater than that of the non-irrigated sample (0.3 dS/m).

3.2.1.3 Pivot Four

In the irrigated soil, the EC increases gradually from the topsoil to peak at 1.1 dS/m in the 1500-1800 mm sample, and decreases gradually toward the base of the profile. In contrast, the EC of the non-irrigated soil is highest in the topsoil (0.75 dS/m) and decreases rapidly with depth.

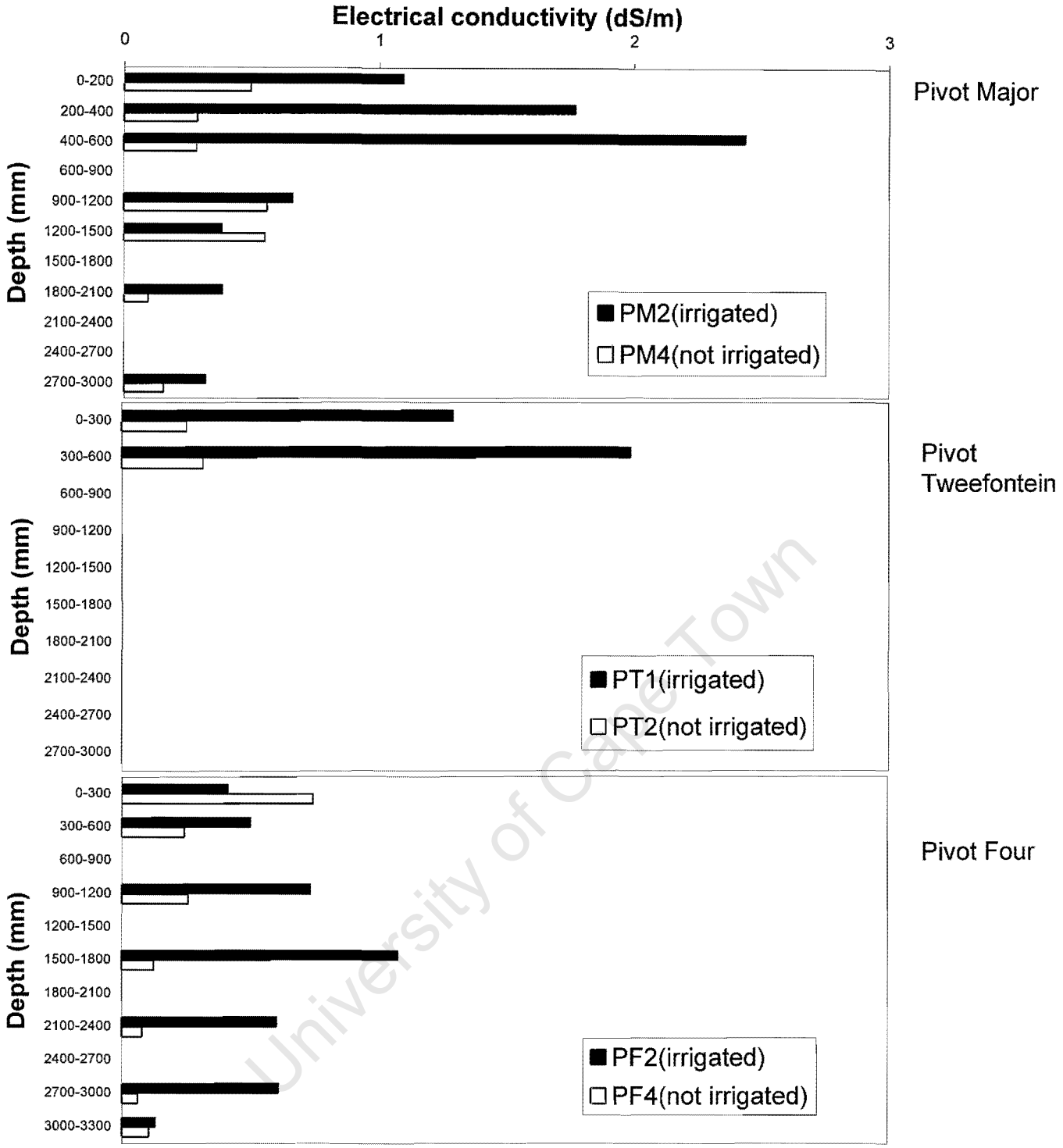

Figure 3.2: Electrical conductivity of saturated paste extracts (no estimate of analytical uncertainty was made for these measurements).

3.2.2 Soluble calcium, magnesium and sulphate

The ionic constituents of the saturated paste extracts, especially Ca^{2+} (Figure 3.3) Mg^{2+} (Figure 3.4) and SO_4^{2-} (Figure 3.5) follow the EC patterns.

3.2.2.1 Pivot Major (irrigated)

These ions follow the EC pattern in this soil. The peak concentrations measured (Ca^{2+} = 9.3 $mmol_c/kg$, Mg^{2+} = 3.4 $mmol_c/kg$, SO_4^{2-} = 6.0 $mmol_c/kg$) in this soil occur in the 400-600 mm sample, after a gradual rise from the topsoil, and are the highest values measured in this study.

3.2.2.2 Pivot Major (not irrigated)

Magnesium and sulphate ions in this profile follow the EC pattern, while calcium deviates from it to some extent. The highest concentrations of Mg^{2+} and SO_4^{2-} in this soil profile occur in the 900-1200 mm sample – i.e., 0.9 $mmol_c/kg$ Mg^{2+} and 0.2 $mmol_c/kg$, SO_4^{2-}. Calcium, on the other hand has its peak (0.7 $mmol_c/kg$) in the 0-300 mm sample, although it has a secondary peak of 0.6 $mmol_c/kg$ in the 900-1200 mm sample. Concentrations of all the ions drop sharply with depth 1200 mm.

3.2.2.3 Pivot Tweefontein (irrigated)

The ions also have a similar pattern to EC in this profile, except that the Mg^{2+} measured in the 0-300 mm sample is much lower than would be predicted by the EC pattern. The greatest concentrations (Ca^{2+} = 2.5 $mmol_c/kg$, Mg^{2+} = 2.2 $mmol_c/kg$, SO_4^{2-} = 3.6 $mmol_c/kg$) occur in the 300-600 mm sample.

3.2.2.4 Pivot Tweefontein (not irrigated)

All the ions follow the EC pattern for this profile. The peak concentrations (Ca^{2+} = 0.3 $mmol_c/kg$, Mg^{2+} = 0.2 $mmol_c/kg$, SO_4^{2-} = 0.4 $mmol_c/kg$) occur in the 300-600 mm sample.

3.2.2.5 Pivot Four (irrigated)

Again, the ions follow the pattern indicated by EC measurements. The peak concentrations (Ca^{2+} = 2.4 $mmol_c/kg$, Mg^{2+} = 1.6 $mmol_c/kg$, SO_4^{2-} = 2.8 $mmol_c/kg$) occur in the 1500-1800 mm sample, after gradually increasing from the topsoil, and decrease toward the base of the profile. However, the concentrations of sulphate measured in the samples from 2100 mm to 3300 mm are much lower than would be predicted by the EC pattern.

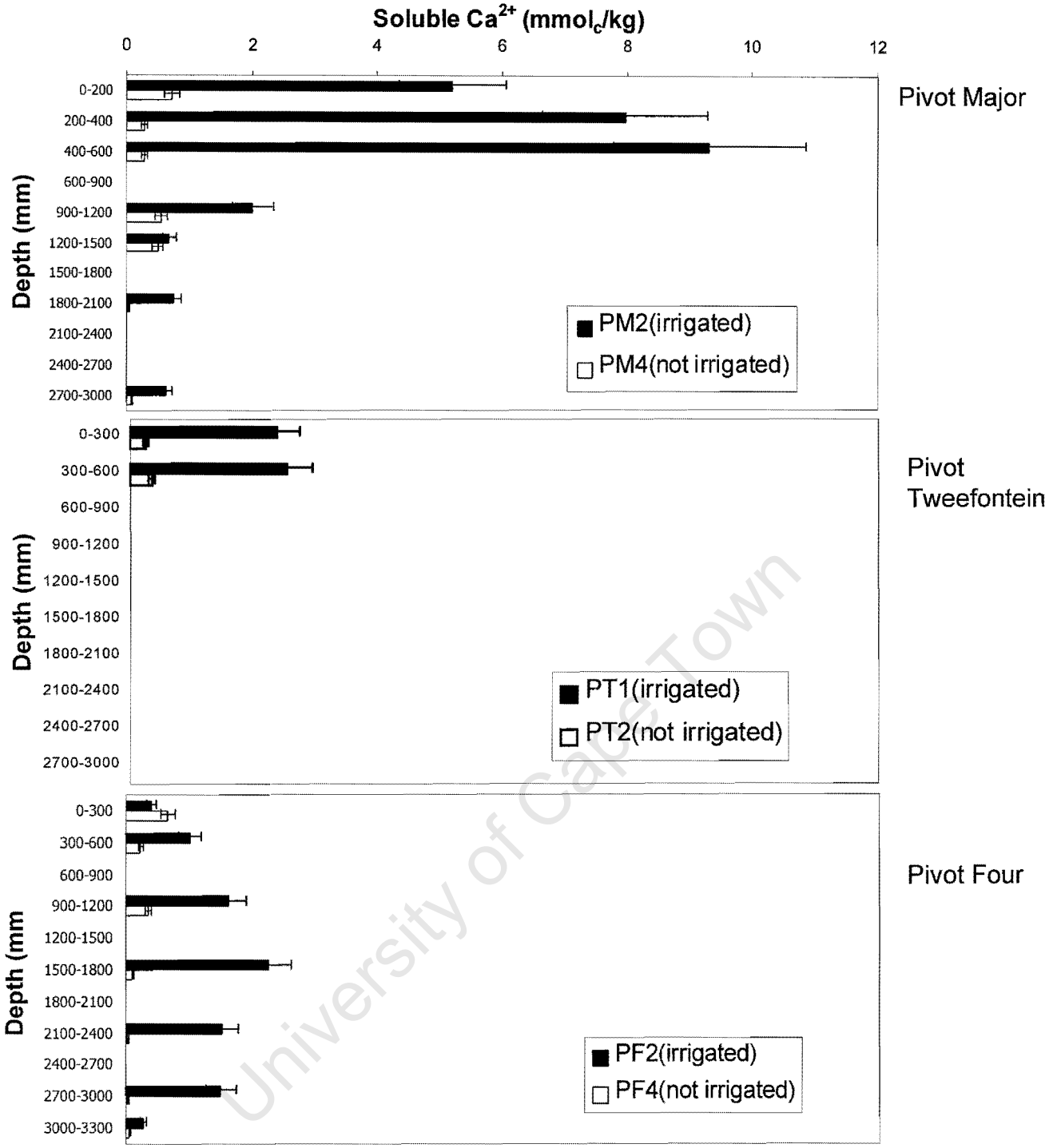

Figure 3.3: Soluble calcium in saturated paste extracts. Error bars indicate analytical uncertainty at the 95% confidence level. Missing results indicate that the sample for that depth interval was not analysed. Results are given in $mmol_c$ per kg of soil.

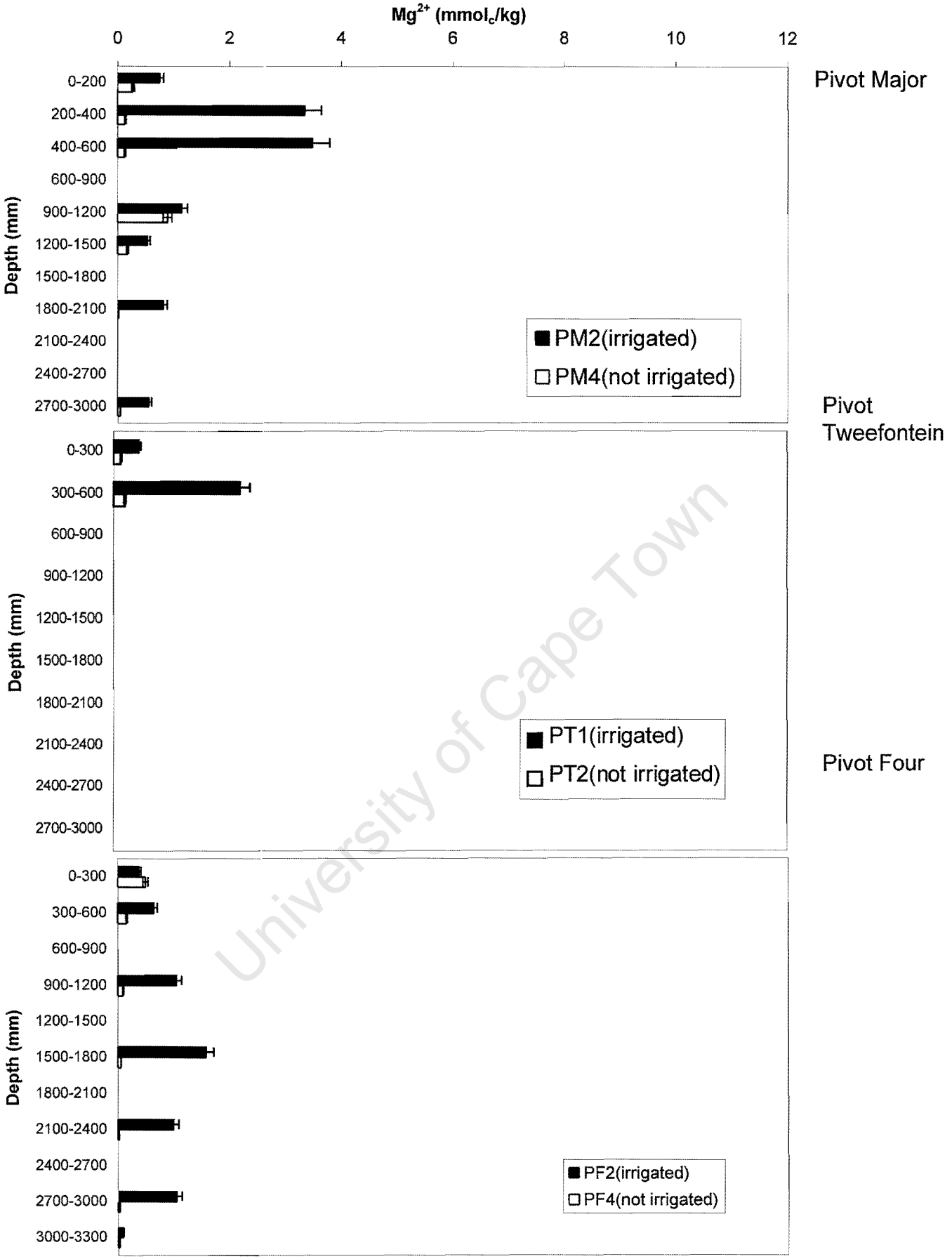

Figure 3.4: Soluble magnesium in saturated paste extracts. Error bars indicate analytical uncertainty at the 95% confidence level. Missing results indicate that the sample for that depth interval was not analysed. Results are given in $mmol_c$ per kg of soil.

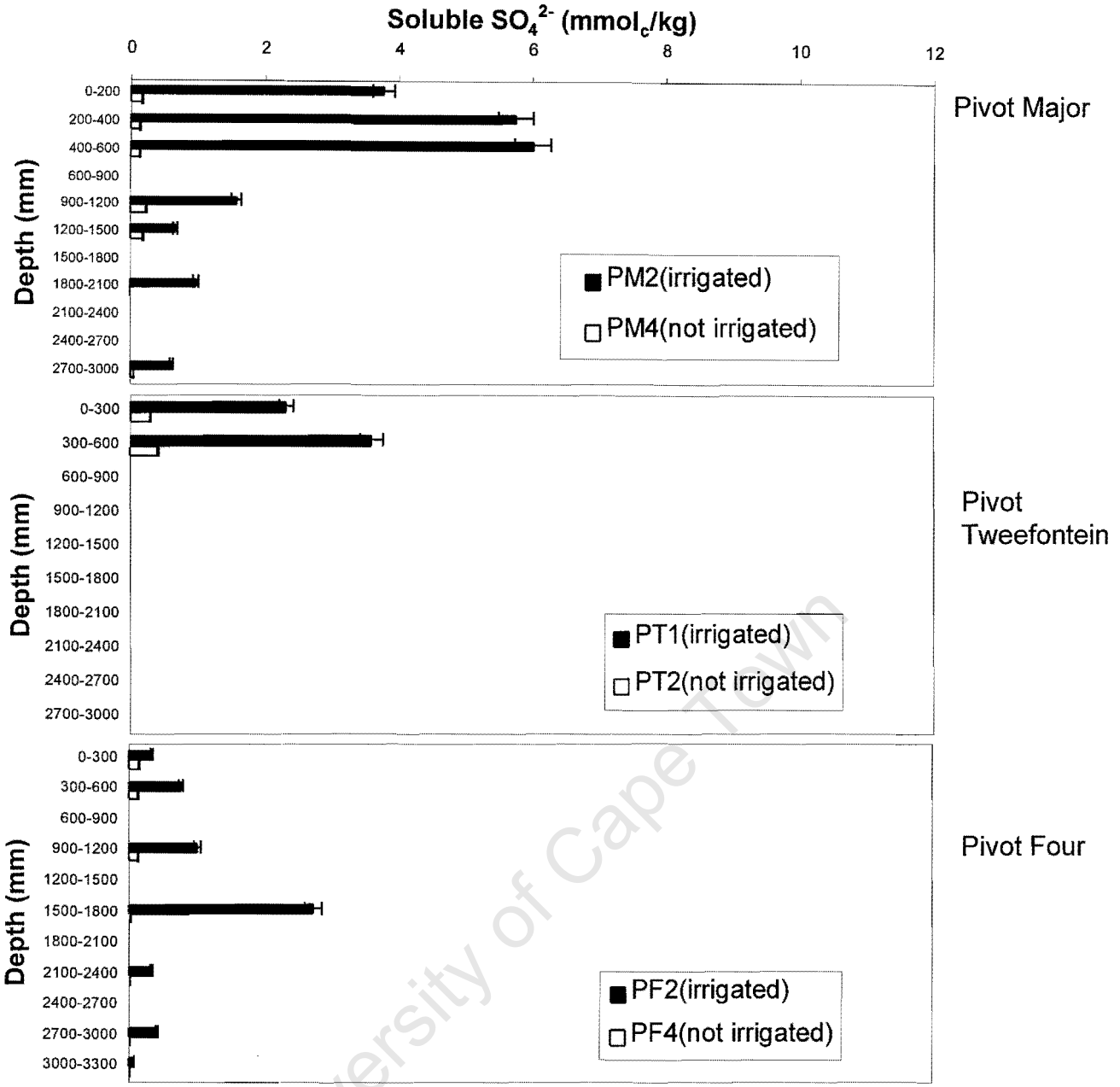

Figure 3.5: Soluble sulphate in saturated paste extracts. Error bars indicate analytical uncertainty at the 95% confidence level. Missing results indicate that the sample for that depth interval was not analysed. Results are given in mmol$_c$ per kg of soil.

3.2.2.6 Pivot Four (not irrigated)

Calcium and magnesium follow the EC pattern, while sulphate is somewhat different from it. The highest concentrations (Ca^{2+} = 0.7 $mmol_c/kg$, Mg^{2+} = 0.5 $mmol_c/kg$, SO_4^{2-} = 0.2 $mmol_c/kg$) occur in the topsoil, and the concentrations of the cations fall sharply with depth. Both Ca^{2+} and Mg^{2+} values in this sample exceed that of the corresponding sample in the irrigated part of pivot Four.

The pattern of sulphate concentration behaves differently to EC in that, although concentrations in the 300 – 1200 mm zone are lower than that in the topsoil, they do not differ greatly from it. There is a sharp drop in concentration in the 1500-1800 mm sample, and, unlike the other ions, no increase in the deepest (3000-3300 mm) sample.

3.2.3 Soluble sodium, chloride, potassium and nitrate

The monovalent ions Na^+ (Figure 3.6), Cl^- (Figure 3.7), K^+ (Figure 3.8) and NO_3^- (Figure 3.9) are usually present in smaller concentrations than Ca^{2+}, Mg^{2+} and SO_4^{2-} in these soils. They do not always follow the trends indicated by the EC data as closely as the divalent ions.

3.2.3.1 Pivot Major

The highest concentrations of Na^+ , Cl^- , K^+ and NO_3^- in the irrigated profile are found in the 400-600 mm sample (Na^+ = 4.2 $mmol_c/kg$, Cl^- = 3.3 $mmol_c/kg$, K^+ = 0.3 $mmol_c/kg$, NO_3^- = 1.0 $mmol_c/kg$). The non-irrigated profile differs by having its highest concentrations of Na^+ and Cl^- in the 1200-1500 mm sample (Na^+ = 0.8 $mmol_c/kg$, Cl^- = 0.7 $mmol_c/kg$), and the highest NO_3^- concentrations in the 900 - 1200 mm sample (NO_3^- = 0.9 $mmol_c/kg$). The highest K^+ concentration in the non-irrigated profile occurs in the topsoil (K^+ = 0.1 $mmol_c/kg$).

3.2.3.2 Pivot Tweefontein

The concentrations of Na^+ , Cl^- , K^+ and NO_3^- are higher in the irrigated soil. Sodium peaks at 0.3 $mmol_c/kg$ in the 300-600 mm sample, while the maximum values of Cl^- and K^+ concentration occur in the topsoil (Cl^- = 0.1 $mmol_c/kg$ and K^+ = 0.1 $mmol_c/kg$. Nitrate concentrations in both the 0-300 mm and 300-600 mm samples are equal within analytical precision (NO_3^- = 0.1 $mmol_c/kg$). In the non-irrigated soil, the concentrations of all four of these ions in the 0-300 mm sample are equal to their concentrations in the 300-600 mm sample, within analytical precision (Na^+ = 0.08 $mmol_c/kg$, Cl^- = 0.15 $mmol_c/kg$, K^+ = 0.03 $mmol_c/kg$, NO_3^- = 0.05 $mmol_c/kg$).

3.2.3.3 Pivot Four

The maximum concentrations of Na^+, Cl^- and NO_3^- in the irrigated profile occur in the 2100 mm to 3000 mm zone. (Na^+ = 1.0 $mmol_c/kg$, Cl^- = 1.3 $mmol_c/kg$, , NO_3^- = 0.6 $mmol_c/kg$), while potassium has its peak in the 0-300 mm sample (K^+ = 0.6 $mmol_c/kg$). In contrast, the maximum concentrations of K^+, Cl^- and NO_3^- in the non-irrigated profile are found in the topsoil (K^+ = 0.3 $mmol_c/kg$, NO_3^- = 0.7 $mmol_c/kg$), Cl^- = 0.8 $mmol_c/kg$), and that of Na^+ in the 300-600 mm sample (0.2 $mmol_c/kg$).

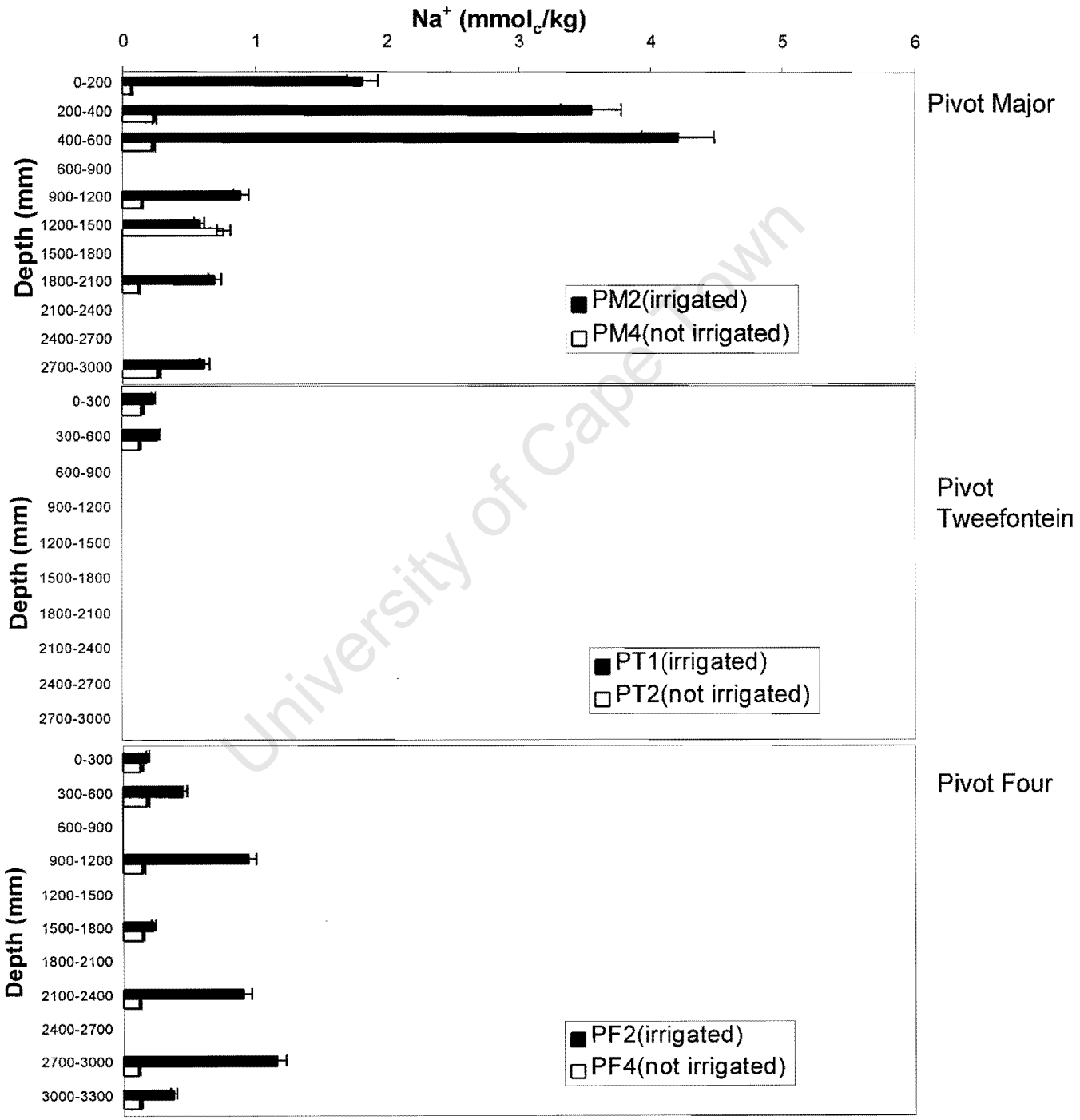

Figure 3.6: Soluble sodium in saturated paste extracts. Error bars indicate analytical uncertainty at the 95% confidence level. Missing results indicate that the sample for that depth interval was not analysed. Results are given in $mmol_c$ per kg of soil.

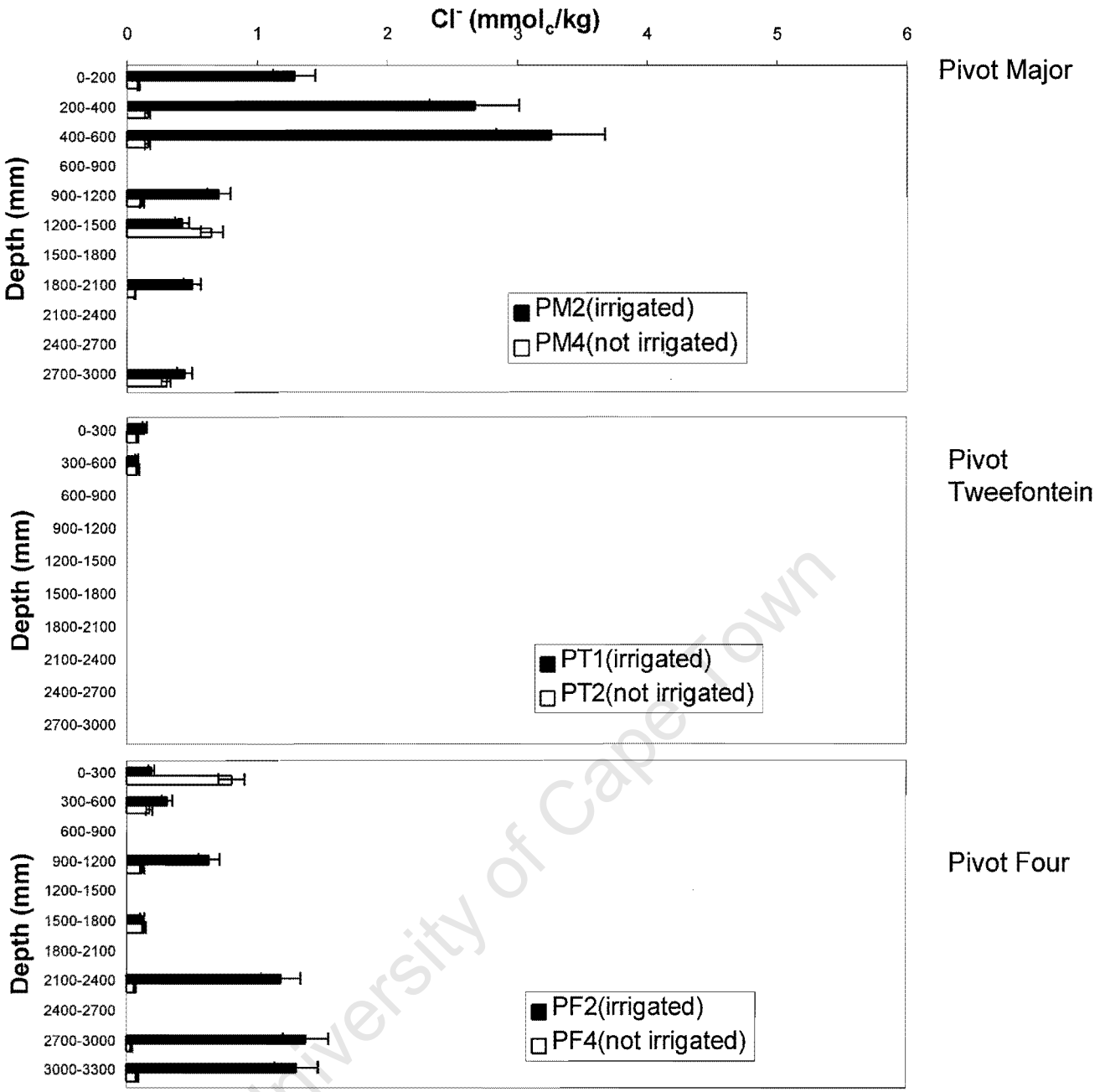

Figure 3.7: Soluble chloride in saturated paste extracts. Error bars indicate analytical uncertainty at the 95% confidence level. Missing results indicate that the sample for that depth interval was not analysed. Results are given in mmol$_c$ per kg of soil.

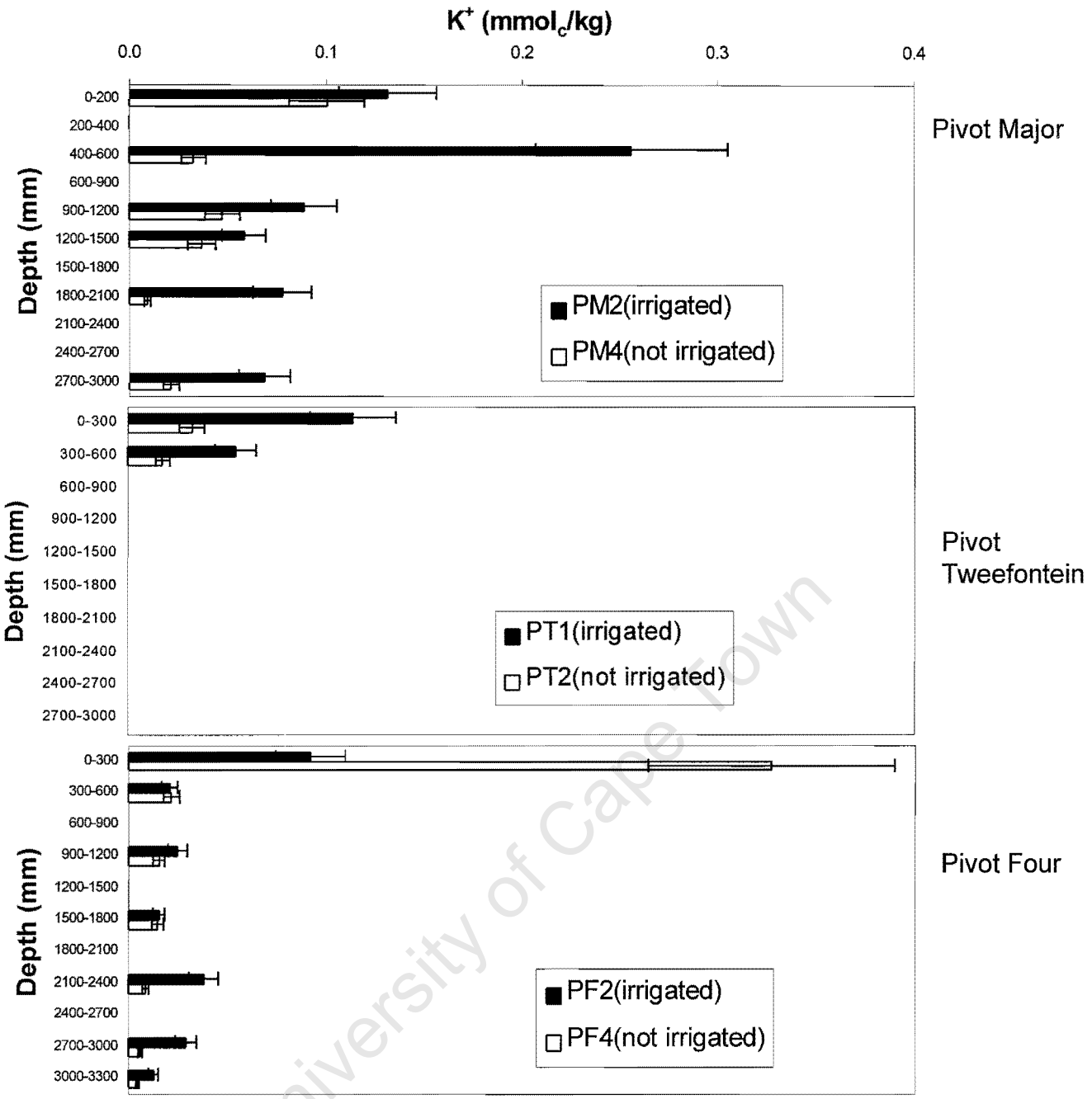

Figure 3.8: Soluble potassium in saturated paste extracts. Error bars indicate analytical uncertainty at the 95% confidence level. Missing results indicate that the sample for that depth interval was not analysed. Results are given in $mmol_c$ per kg of soil.

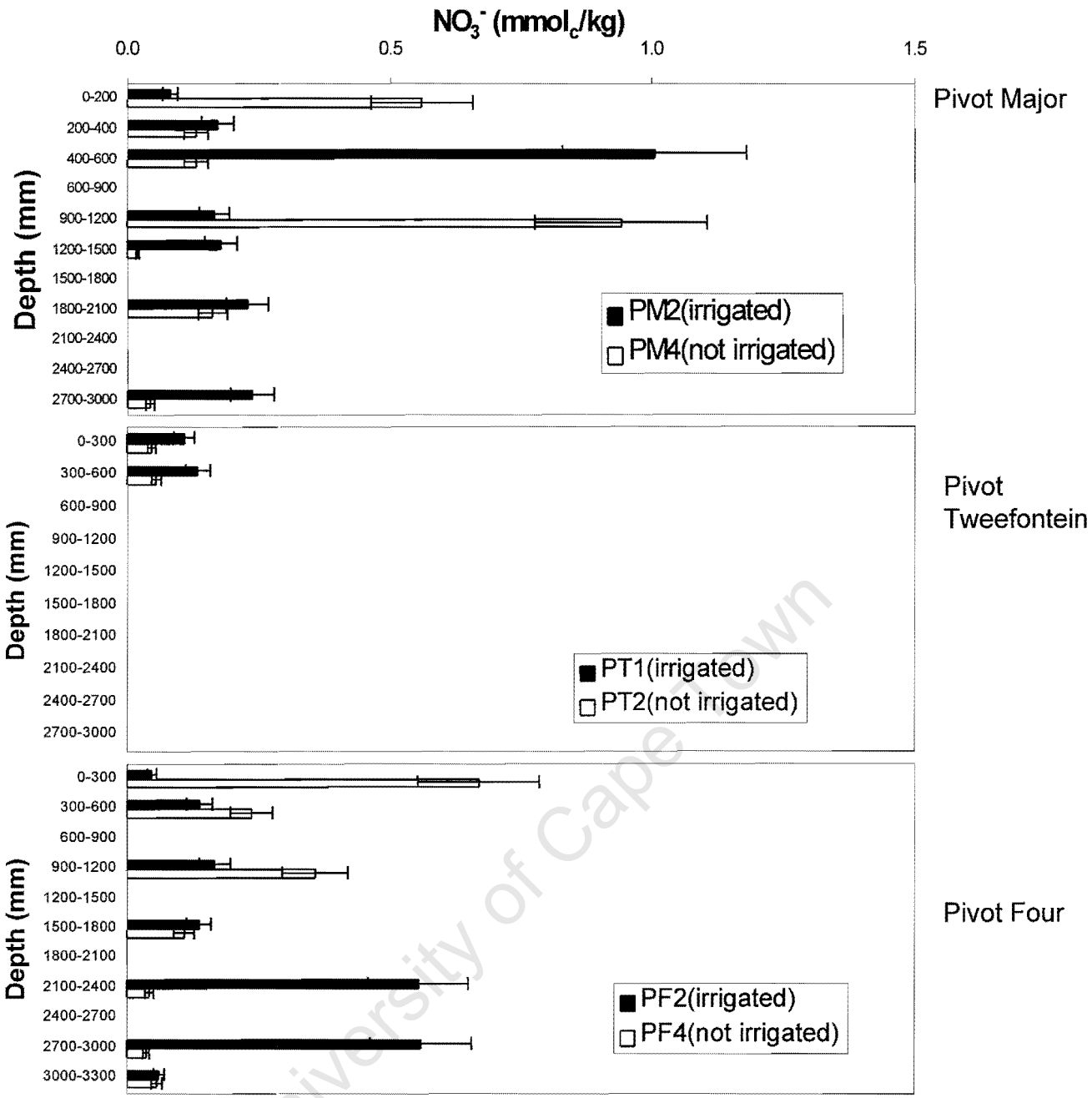

Figure 3.9: Soluble nitrate in saturated paste extracts. Error bars indicate analytical uncertainty at the 95% confidence level. Missing results indicate that the sample for that depth interval was not analysed. Results are given in mmol$_c$ per kg of soil.

3.2.4 Ammonium, alkalinity and soluble organic carbon (Tables 3.2, 3.3 & 3.4)

These constituents of the soil solution show no clear relation to EC patterns. Ammonium has the highest concentration measured in this study (0.4 $mmol_c/kg$) in the 0-200 mm sample of irrigated soil in pivot Major, and a secondary peak (0.06 $mmol_c/kg$ in the 1800-2100 mm sample of the same profile. It reaches its highest value in the irrigated soil from pivot Four deep in the profile, at 2100-2400 mm (0.09 $mmol_c/kg$). It occurs only in the topsoil (0-300 mm) samples of the non-irrigated soil profiles. It is not detectable in the samples from pivot Tweefontein.

Alkalinities of the soil solutions are generally low, between 0.0 and 0.1 $mmol_c/kg$ (0.0 to 0.3 $mmol_c$/litre of saturated paste extract), the exception being the topsoil (0-200 mm) sample from the the irrigated soil in pivot Major, which has an alkalinity of 0.2 $mmol_c/kg$ (0.7 $mmol_c$/litre of saturated paste extract).

Soluble organic carbon consistently has its maximum value in the topsoil samples (ranging from 5.1 to 26.3 mg/kg), and declines with depth to minima of between 4.0 and 7.0 mg/kg.

Table 3.2: NH_4^+ concentration in saturated paste extracts Missing results indicate that the sample for that depth interval was not analysed. Results are given in $mmol_c$ per kg of soil (bdl = below detection limit). Analytical precision was not determined for these results.

Sample position	Depth interval(mm)	$mmol_c/kg$	Sample position	Depth interval(mm)	$mmol_c/kg$
Pivot Major	0-200	bdl	Pivot Major	0-300	0.09
(irrigated to field	200-420	0.44	(non-irrigated)	300-600	0.01
capacity)	420-600	bdl	Core PM4	600-900	
Core PM2	600-900			900-1200	0.08
	900-1100	bdl		1200-1500	bdl
	1100-1300			1500-1800	
	1300-1500	0.04		1800-2100	0.06
	1500-1800			2100-2400	
	1800-2100	0.06		2400-2700	
	2100-2400			2700-3000	bdl
	2400-2700				
	2700-3000	0.04			
Pivot Four	0-300	0.02	Pivot Four	0-300	0.02
(irrigated to field	300-600	bdl	(non-irrigated)	300-600	bdl
capacity)	600-900		Core PF4	600-900	
Core PF2	900-1200	bdl		900-1200	bdl
	1200-1500			1200-1500	
	1500-1800	0.03		1500-1800	bdl
	1800-2100			1800-2100	
	2100-2400	0.09		2100-2400	bdl
	2400-2700			2400-2700	
	2700-3000	bdl		2700-3000	bdl
	3000-3300	bdl		3000-3300	bdl
Pivot Tweefontein	0-300	bdl	Pivot Tweefontein	0-300	bdl
(irrigated to field	300-600	bdl	(non-irrigated)	300-600	bdl
capacity)			Core PT2		
Core PT1					

Table 3.3: Alkalinity of saturated paste extracts. Missing results indicate that the sample for that depth interval was not analysed. Results are given in $mmol_c$ per kg of soil. The analytical uncertainty for these results is 32% at the 95% confidence level.

Sample position	Depth interval(mm)	$mmol_c/kg$	Sample position	Depth interval(mm)	$mmol_c/kg$
Pivot Major	0-200	0.2	Pivot Major	0-300	0.1
(irrigated to field	200-420	0.0	(non-irrigated)	300-600	
capacity)	420-600	0.0	Core PM4	600-900	
Core PM2	600-900			900-1200	
	900-1100			1200-1500	0.1
	1100-1300			1500-1800	
	1300-1500	0.1		1800-2100	
	1500-1800			2100-2400	
	1800-2100			2400-2700	
	2100-2400			2700-3000	0.1
	2400-2700				
	2700-3000	0.1			
Pivot Four	0-300	0.1	Pivot Four	0-300	0.0
(irrigated to field	300-600	0.0	(non-irrigated)	300-600	
capacity)	600-900		Core PF4	600-900	
Core PF2	900-1200			900-1200	
	1200-1500			1200-1500	
	1500-1800	0.1		1500-1800	0.1
	1800-2100			1800-2100	
	2100-2400			2100-2400	
	2400-2700			2400-2700	
	2700-3000	0.1		2700-3000	0.0
	3000-3300			3000-3300	
Pivot Tweefontein	0-300	0.0	Pivot Tweefontein	0-300	
(irrigated to field	300-600	0.0	(non-irrigated)	300-600	0.0
capacity)			Core PT2		
Core PT1					

Table 3.4: Soluble organic carbon in saturated paste extracts. Missing results indicate that the sample for that depth interval was not analysed. Results are given in mg per kg of soil. The analytical uncertainty is 12% at the 95% confidence level.

Sample position	Depth interval(mm)	mg/kg	Sample position	Depth interval(mm)	mg/kg
Pivot Major	0-200	26.3	Pivot Major	0-300	11.6
(irrigated to field	200-420	19.0	(non-irrigated)	300-600	
capacity)	420-600	15.0	Core PM4	600-900	
Core PM2	600-900			900-1200	
	900-1100			1200-1500	5.1
	1100-1300			1500-1800	
	1300-1500	6.6		1800-2100	
	1500-1800			2100-2400	
	1800-2100			2400-2700	
	2100-2400			2700-3000	5.5
	2400-2700	7.0			
	2700-3000				
Pivot Four	0-300	12.3	Pivot Four	0-300	8.6
(irrigated to field	300-600	13.0	(non-irrigated)	300-600	
capacity)	600-900		Core PF4	600-900	
Core PF2	900-1200			900-1200	
	1200-1500			1200-1500	
	1500-1800	7.7		1500-1800	4.6
	1800-2100			1800-2100	
	2100-2400			2100-2400	
	2400-2700			2400-2700	
	2700-3000	4.6		2700-3000	4.0
	3000-3300			3000-3300	
Pivot Tweefontein	0-300	5.1	Pivot Tweefontein	0-300	
(irrigated to field	300-600	6.2	(non-irrigated)	300-600	5.2
capacity)			Core PT2		
Core PT1					

3.2.5 Assessment of the presence of gypsum in the irrigated soils

3.2.5.1 Calculation of the gypsum saturation index

The gypsum saturation index (SI) was calculated for the saturated paste extracts prepared from the irrigated soil samples using the computer program PHREEQC (Parkhurst and Appelo, 1999). The results are presented in Figure 3.10. The gypsum SI shows the same general trends with depth as the EC. All the SI values calculated are less than zero, indicating that each saturated paste extract is undersaturated with respect to gypsum.

3.2.5.2 Extraction of soluble sulphate by the method of increasing dilution

The concentration of soluble sulphate in the two soil samples with the highest gypsum saturation indices was measured by this method. The results are presented in Figure 3.11. Increasing quantities of sulphate are dissolved from the soil until the water:soil ratio reaches 10:1, where dissolved sulphate (per kg soil) remains constant.

The concentration of each of the other major ions (Ca^{2+}, Mg^{2+}, K^{+}, Na^{+}, NH_4^{+}, Cl^{-}, NO_3^{-}) in the extracts was also measured, and this data used to calculate gypsum saturation indices for each of the extracts, using PHREEQC (Parkhurst and Appelo, 1999). The results of the calculations are also presented in Figure 3.11. Again, the gypsum SI is less than zero for every extract, indicating that the solutions are all undersaturated with respect to gypsum.

3.2.5.3 Qualitative assessment of the presence of gypsum in the soils by XRD

The same samples analysed by increasing dilution (PM2 200-400 mm and PM2 400-600 mm) were analysed for gypsum by XRD. No gypsum was detected in the soil by XRD.

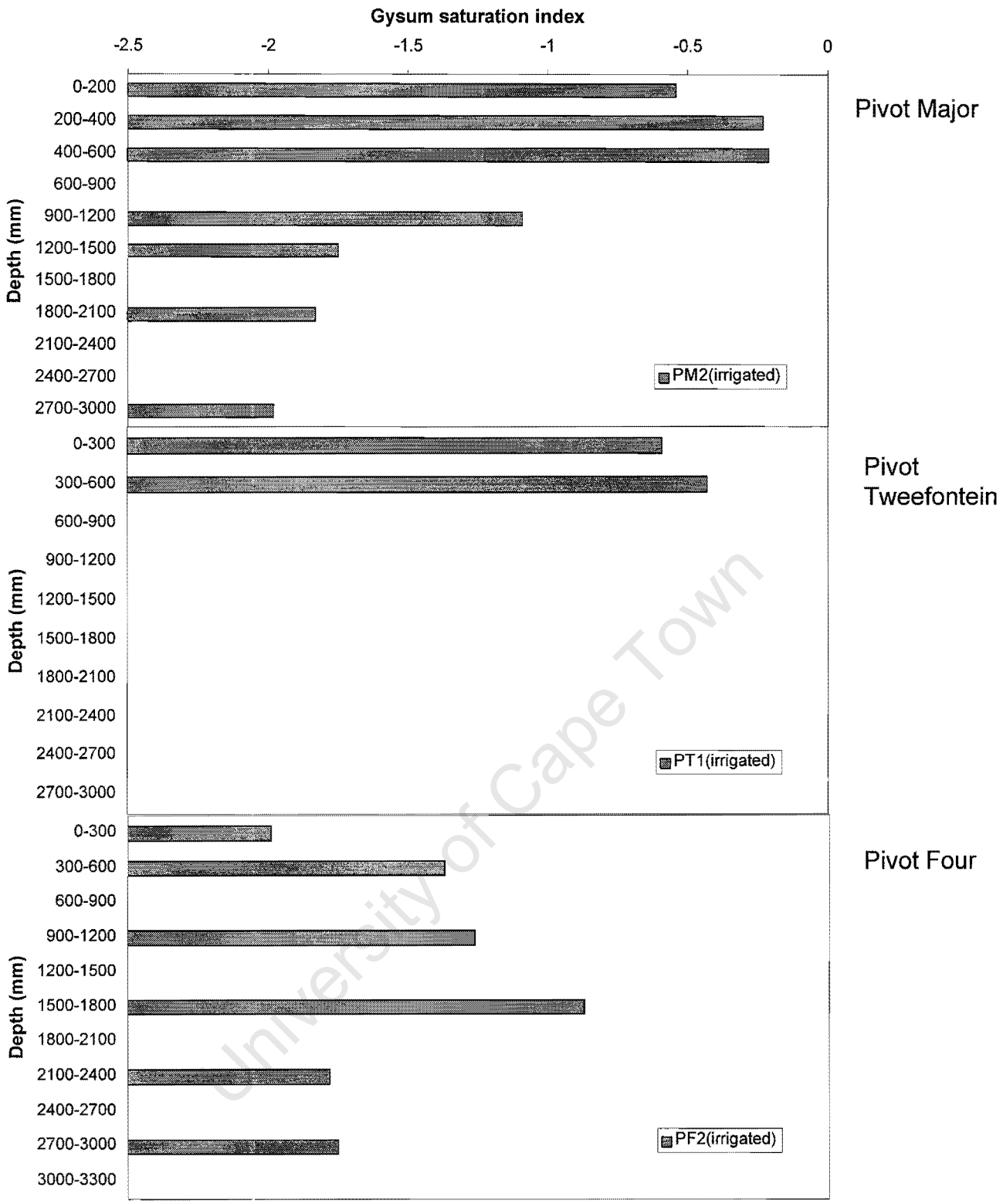

Figure 3.10: Gypsum saturation index calculated with PHREEQC (Parkhurst and Appelo, 1999). Missing results indicate that the sample for that depth interval was not analysed.

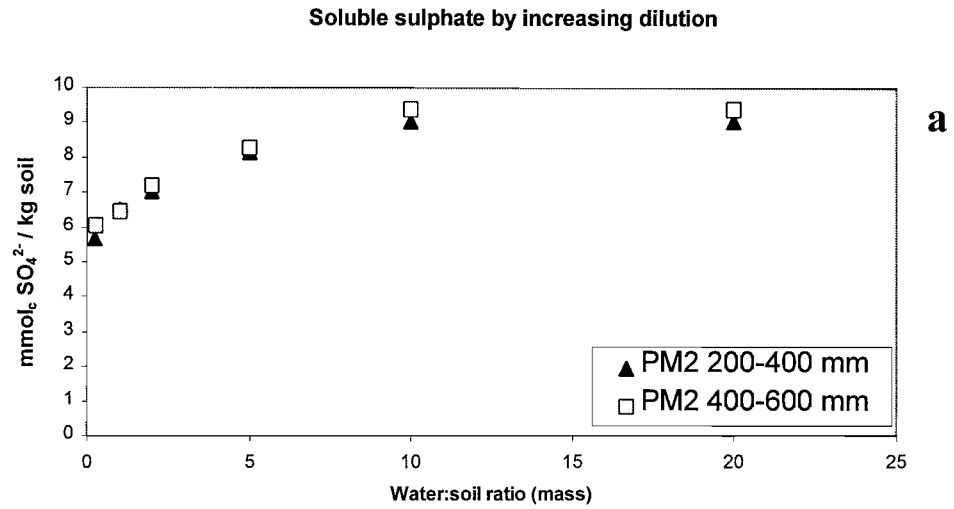

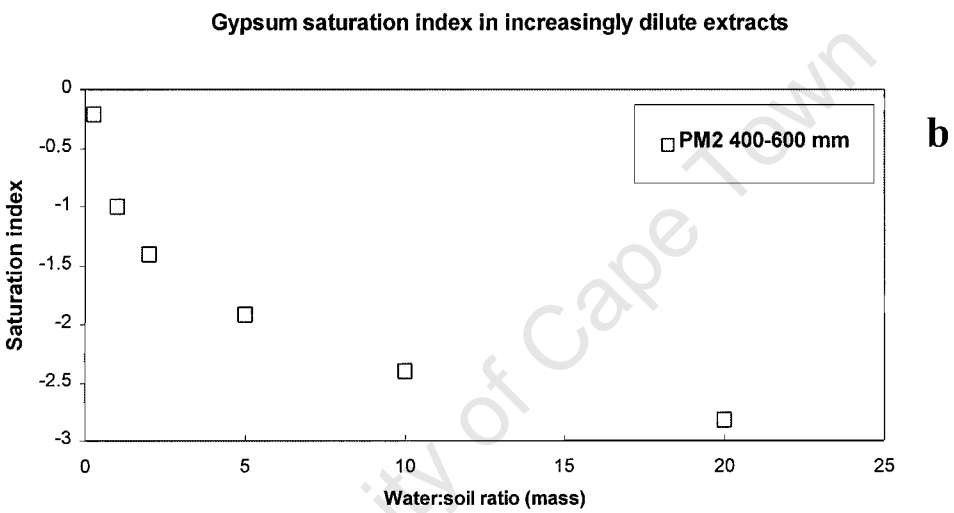

Figure 3.11: Soluble sulphate in increasingly dilute soil extracts (a) and gypsum SI for the extracts (b) for soil samples from pivot Major. The data points on the extreme left of the charts represent data from saturated paste extracts.

3.3 Soil pH

The pH of the soil samples in the saturated pastes (Table 3.5) falls between 4.5 and 5.8. pH measured in 1:2.5 1M KCl suspensions fell in the range 3.9-5.0 (Table 3.6) and pH in 1:2.5 water suspensions between 6.0 and 8.4 (Table 3.7).

In general, soil pH increases gradually with depth, but intervals where pH is elevated above this trend occur in pivot Major at 0-200 mm and 900-1100mm, and in pivot Four in at 0-300 mm and 1500-1800 mm.

Table 3.5: pH measured in saturated pastes. Missing results indicate that the sample for that depth interval was not analysed.

Sample position	Depth interval(mm)	pH	Sample position	Depth interval(mm)	pH
Pivot Major	0-200	5.7	Pivot Major	0-300	4.9
(irrigated to field	200-420	4.5	(non-irrigated)	300-600	4.7
capacity)	420-600	4.7	Core PM4	600-900	
Core PM2	600-900			900-1200	4.8
	900-1100	5.7		1200-1500	5.0
	1100-1300			1500-1800	
	1300-1500	5.3		1800-2100	5.8
	1500-1800			2100-2400	
	1800-2100	5.3		2400-2700	
	2100-2400			2700-3000	5.7
	2400-2700				
	2700-3000	5.5			
Pivot Four	0-300	5.4	Pivot Four	0-300	5.0
(irrigated to field	300-600	5.0	(non-irrigated)	300-600	5.9
capacity)	600-900		Core PF4	600-900	
Core PF2	900-1200	4.8		900-1200	5.5
	1200-1500			1200-1500	
	1500-1800	5.6		1500-1800	5.6
	1800-2100			1800-2100	
	2100-2400	5.1		2100-2400	5.7
	2400-2700			2400-2700	
	2700-3000	5.8		2700-3000	5.8
	3000-3300	5.7		3000-3300	5.6
Pivot Tweefontein	0-300	4.9	Pivot Tweefontein	0-300	5.1
(rrigated to field	300-600	5.5	(non-irrigated)	300-600	5.6
capacity)			Core PT2		
Core PT1					

Table 3.6: pH measured in 1 M KCl (1:2.5) suspensions. Missing results indicate that the sample for that depth interval was not analysed.

Sample position	Depth interval(mm)	pH	Sample position	Depth interval(mm)	pH
Pivot Major	0-200	5.0	Pivot Major	0-300	4.2
(irrigated to field	200-420	3.9	(non-irrigated)	300-600	3.9
capacity)	420-600	4.2	Core PM4	600-900	
Core PM2	600-900			900-1200	4.1
	900-1100	4.8		1200-1500	4.4
	1100-1300			1500-1800	
	1300-1500	4.5		1800-2100	4.5
	1500-1800			2100-2400	
	1800-2100	4.5		2400-2700	
	2100-2400			2700-3000	4.9
	2400-2700				
	2700-3000	4.6			
Pivot Four	0-300	4.6	Pivot Four	0-300	4.1
(irrigated to field	300-600	4.1	(non-irrigated)	300-600	5.0
capacity)	600-900		Core PF4	600-900	
Core PF2	900-1200	4.1		900-1200	4.5
	1200-1500			1200-1500	
	1500-1800	4.7		1500-1800	4.4
	1800-2100			1800-2100	
	2100-2400	4.4		2100-2400	4.2
	2400-2700			2400-2700	
	2700-3000	4.4		2700-3000	4.2
	3000-3300	4.8		3000-3300	4.3
Pivot Tweefontein	0-300	4.8	Pivot Tweefontein	0-300	4.4
(irrigated to field	300-600	4.3	(non-irrigated)	300-600	4.8
capacity)-Core PT1			Core PT2		

Table 3.7: pH measured in water (1:2.5) suspensions. Missing results indicate that the sample for that depth interval was not analysed*.

Sample position	Depth interval(mm)	pH	Sample position	Depth interval(mm)	pH
Pivot Major	0-200	6.0	Pivot Major	0-300	7.2
(irrigated to field	200-420	5.8	(non-irrigated)	300-600	6.8
capacity)	420-600	5.6	Core PM4	600-900	
Core PM2	600-900			900-1200	6.7
	900-1100	6.9		1200-1500	7.3
	1100-1300			1500-1800	
	1300-1500	6.1		1800-2100	8.3
	1500-1800			2100-2400	
	1800-2100	7.2		2400-2700	
	2100-2400			2700-3000	8.4
	2400-2700				
	2700-3000	7.3			
Pivot Four	0-300	7.2	Pivot Four	0-300	7.2
(irrigated to field	300-600	6.9	(non-irrigated)	300-600	7.8
capacity)	600-900		Core PF4	600-900	
Core PF2	900-1200	6.3		900-1200	7.5
	1200-1500			1200-1500	
	1500-1800	6.8		1500-1800	8.0
	1800-2100			1800-2100	
	2100-2400	7.1		2100-2400	8.1
	2400-2700			2400-2700	
	2700-3000	8.4		2700-3000	7.1
	3000-3300	7.9		3000-3300	8.0
Pivot Tweefontein	0-300	6.5	Pivot Tweefontein	0-300	6.9
(irrigated to field	300-600	6.2	(non-irrigated)	300-600	7.4
capacity)			Core PT2		
Core PT1					

* These pH measurements are significantly higher than would be expected from the measurements of pH in KCl and saturated pastes. These measurements may be wholly or partially incorrect, because the method used here (Non-Affiliated Soil Analysis working Committee, 1990) stipulates that the pH probe be inserted into the soil:water suspension for a period of 30 s only. This may not have been enough time for the pH reading to settle to a constant value.

3.4 Total organic carbon content of the soils

The highest total organic carbon contents occur in the topsoils, with the highest being 0.83 %, in the irrigated soil from pivot Major (Table 3.8).

Table 3.8: Total organic carbon content of the soils. Missing results indicate that the sample for that depth interval was not analysed.

Core position	Depth interval (mm)	Organic carbon (weight %)	Core position	Depth interval (mm)	Organic carbon (weight %)
Pivot Major	0-200	0.83	Pivot Major	0-300	0.65
(irrigated to field	200-420	0.25	(not irrigated)	300-600	0.33
capacity)	420-600	0.48	Core PM4	600-900	
Core PM2	600-900			900-1200	0.34
	900-1100	0.26		1200-1500	0.21
	1100-1300			1500-1800	
	1300-1500	0.09		1800-2100	0.08
	1500-1800			2100-2400	
	1800-2100	0.10		2400-2700	
	2100-2400			2700-3000	0.09
	2400-2700				
	2700-3000	0.12			
Pivot Four	0-300	0.50	Pivot Four	0-300	0.47
(irrigated to field	300-600	0.20	(not irrigated)	300-600	0.26
capacity)	600-900		Core PF4	600-900	
Core PF2	900-1200	0.12		900-1200	0.10
	1200-1500			1200-1500	
	1500-1800	0.10		1500-1800	0.10
	1800-2100			1800-2100	
	2100-2400	0.09		2100-2400	0.03
	2400-2700			2400-2700	
	2700-3000	0.00		2700-3000	0.03
	3000-3300	0.05		3000-3300	0.04
Pivot Tweefontein	0-300	0.32	Pivot Tweefontein	0-300	0.18
(irrigated to field	300-600	0.26	(not irrigated)	300-600	0.10
capacity)- Core PT1			Core PT2		

3.5 Exchangeable cations

3.5.1 Exchangeable acidity (EA)

Exchangeable (1M KCl extractable) acidity results are given in Figure 3.12. These measurements indicate the sum of exchangeable H^+ and Al^{3+} which can be extracted from the soil by 1M KCl. The results range between 0 (below analytical detectability) to 11 $mmol_c/kg$. The irrigated soil profiles have generally lower exchangeable acidities than the soils which have not been irrigated.

3.5.1.1 Exchangeable acidity of the irrigated soils

In Pivot Major, EA is low in the topsoil (0-200 mm) but has its highest value in the 200-400 mm sample (EA=5 $mmol_c/kg$), then declines with depth, except for a slight upturn in the deepest sample (2700-3000 mm). In pivot Tweefontein, EA is below the analytical detection limit in the 0-300 mm sample, and has a value of 3 $mmol_c/kg$ in the 300-600 mm sample. In pivot Four, EA increases from a low level in the topsoil to peak at 5 $mmol_c/kg$ in the 900-1200 mm sample. The EA of the profile then declines somewhat before rising to a second high point of 5 $mmol_c/kg$ in the deepest sample analysed, 3000-3300 mm.

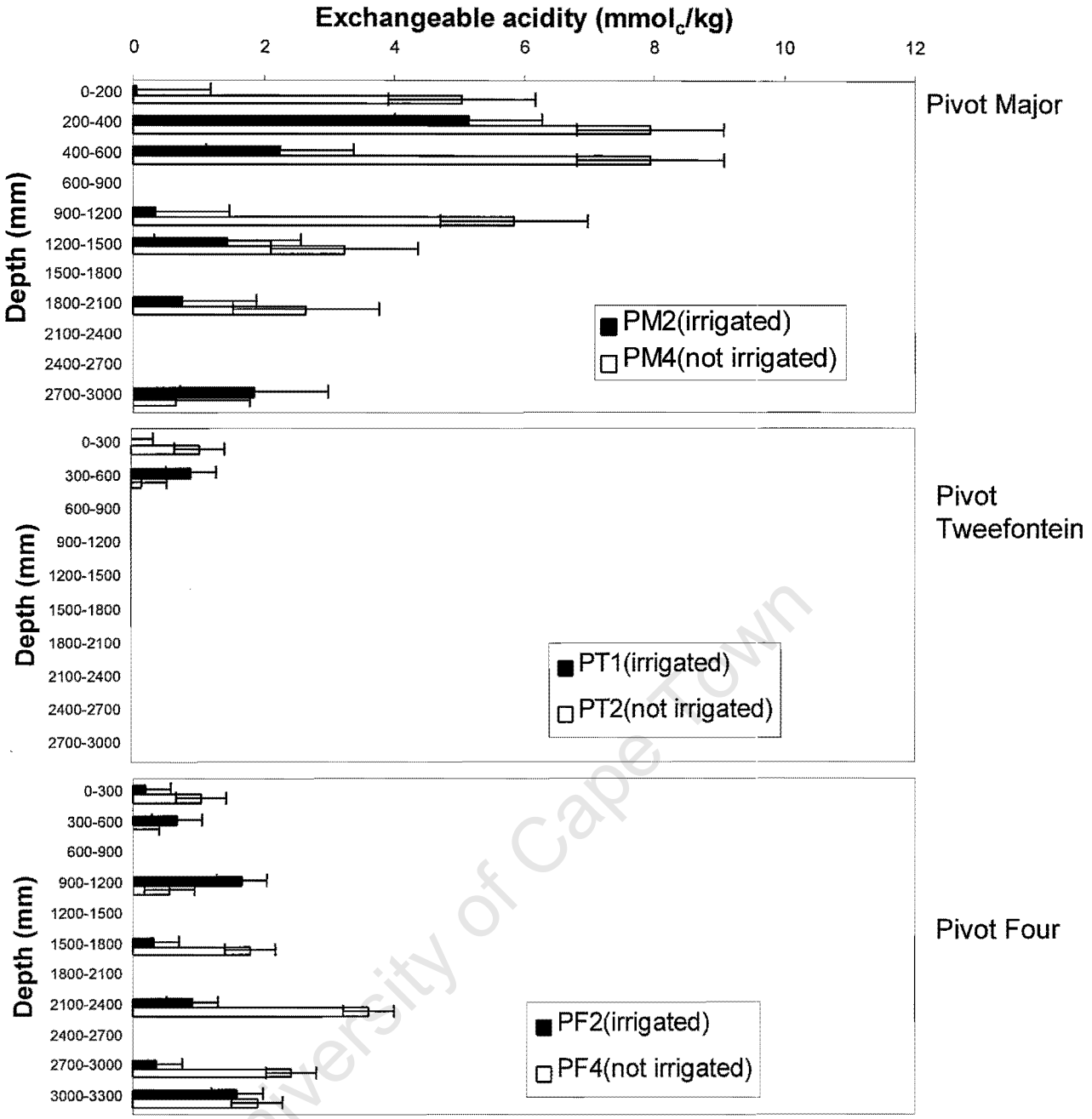

Figure 3.12: 1M KCl extractable acidity. Error bars indicate analytical uncertainty at the 95% confidence level. Missing results indicate that the sample for that depth interval was not analysed. Results are given in mmol$_c$ per kg of soil.

3.5.1.2 Exchangeable acidity of the non-irrigated soils

Pivot Major's EA peaks in the 400-600 mm sample at 8 mmol$_c$/kg and decreases steadily with depth. In Pivot Tweefontein, the greatest EA occurs in the topsoil (3 mmol$_c$/kg). Pivot Four shows a gradual increase in EA with depth, which attains its highest value (11 mmol$_c$/kg) in the 2100-2400 mm sample. This is the highest EA measured in this study.

3.5.2 Ammonium acetate extractable cations

The exchangeable cations Ca^{2+}, Mg^{2+}, Na^{+} and K^{+} have been extracted from these samples with 0.1 M ammonium acetate. The results represent the sum of soluble and exchangeable cations, and will be referred to in the text as *extractable* cations. The results are shown in Figures 3.13, 3.14, 3.15 and 3.16.

3.5.2.1 Extractable cation results for the irrigated soils

In pivot Major, extractable calcium peaks in the 0-200 mm sample (31.3 $mmol_c/kg$) and declines with depth. Extractable Mg^{2+}, in contrast, increases with depth, attaining its highest value in the 1800-2100 mm sample (17.0 $mmol_c/kg$), before falling rapidly below this depth. Extractable K^{+} appears to reach its maximum (3.4 $mmol_c/kg$) in the 2700-3000 mm sample, but no clear trend is apparent in this sample (considering the low analytical precision for this ion).

Extractable Na^{+} appears to increase with depth, but, again, analytical precision is insufficient to identify any clear trend.

In the soils from pivot Tweefontein, extractable Ca^{2+} is highest in the topsoil (20.7 $mmol_c/kg$), while extractable Mg^{2+} is highest in the 300-600 mm sample (8.3 $mmol_c/kg$). Extractable K^{+} peaks in the 0-300 sample (2.1 $mmol_c/kg$), while extractable Na^{+} has equal values (within analytical precision) in both samples taken from this soil (2 $mmol_c/kg$).

The soil samples from pivot Four have a bimodal distribution of extractable Ca^{2+} with depth. The first peak (12.0 $mmol_c/kg$) is found in the 0-300 mm sample and the second (13.6 $mmol_c/kg$) in the 1500-1800 mm sample. Extractable Mg^{2+} increases with depth and reaches its greatest value (11.1 $mmol_c/kg$) in the deepest sample (3000-3300 mm). Extractable K^{+} is highest (2.1 $mmol_c/kg$) in the 0-300 mm sample and decreases with depth, while it is not apparent, within analytical precision, how extractable Na^{+} behaves in the profile, but has values between 2 and 3 $mmol_c/kg$.

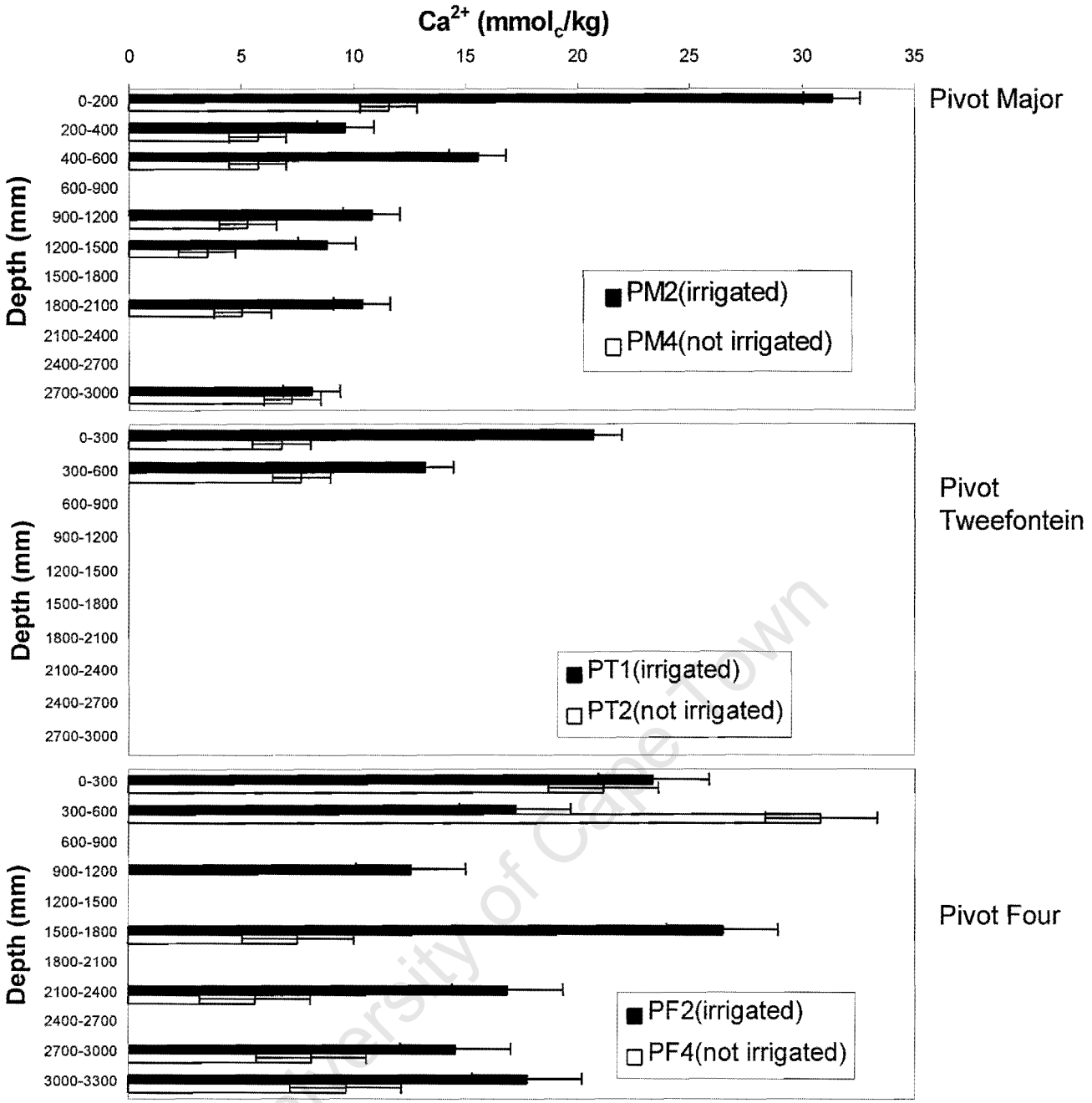

Figure 3.13: Ammonium acetate extractable Ca^{2+}. Error bars indicate analytical uncertainty at the 95% confidence level. Missing results indicate that the sample for that depth interval was not analysed. Results are given in $mmol_c$ per kg of soil.

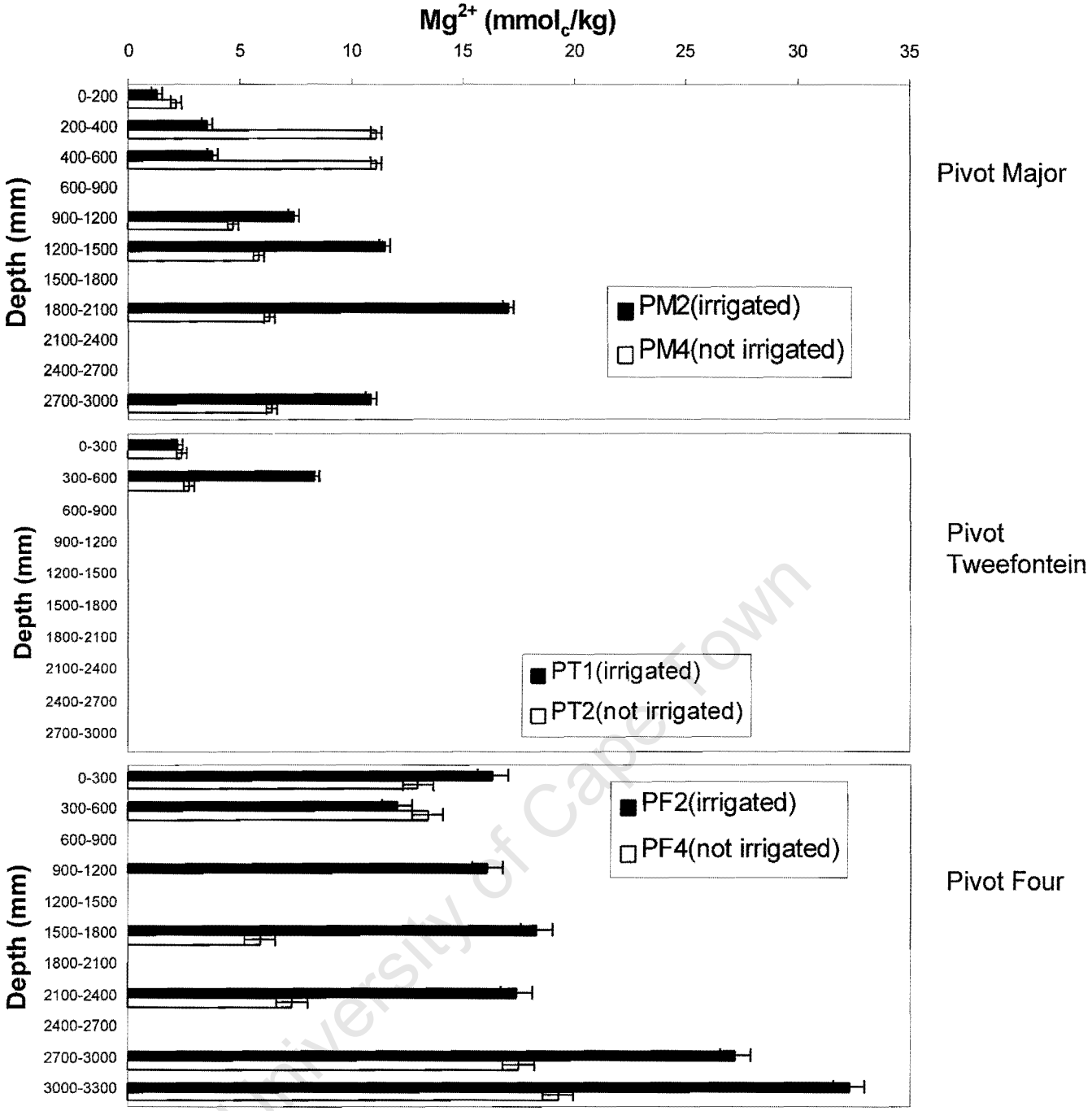

Figure 3.14: Ammonium acetate Mg^{2+}. Error bars indicate analytical uncertainty at the 95% confidence level. Missing results indicate that the sample for that depth interval was not analysed. Results are given in $mmol_c$ per kg of soil.

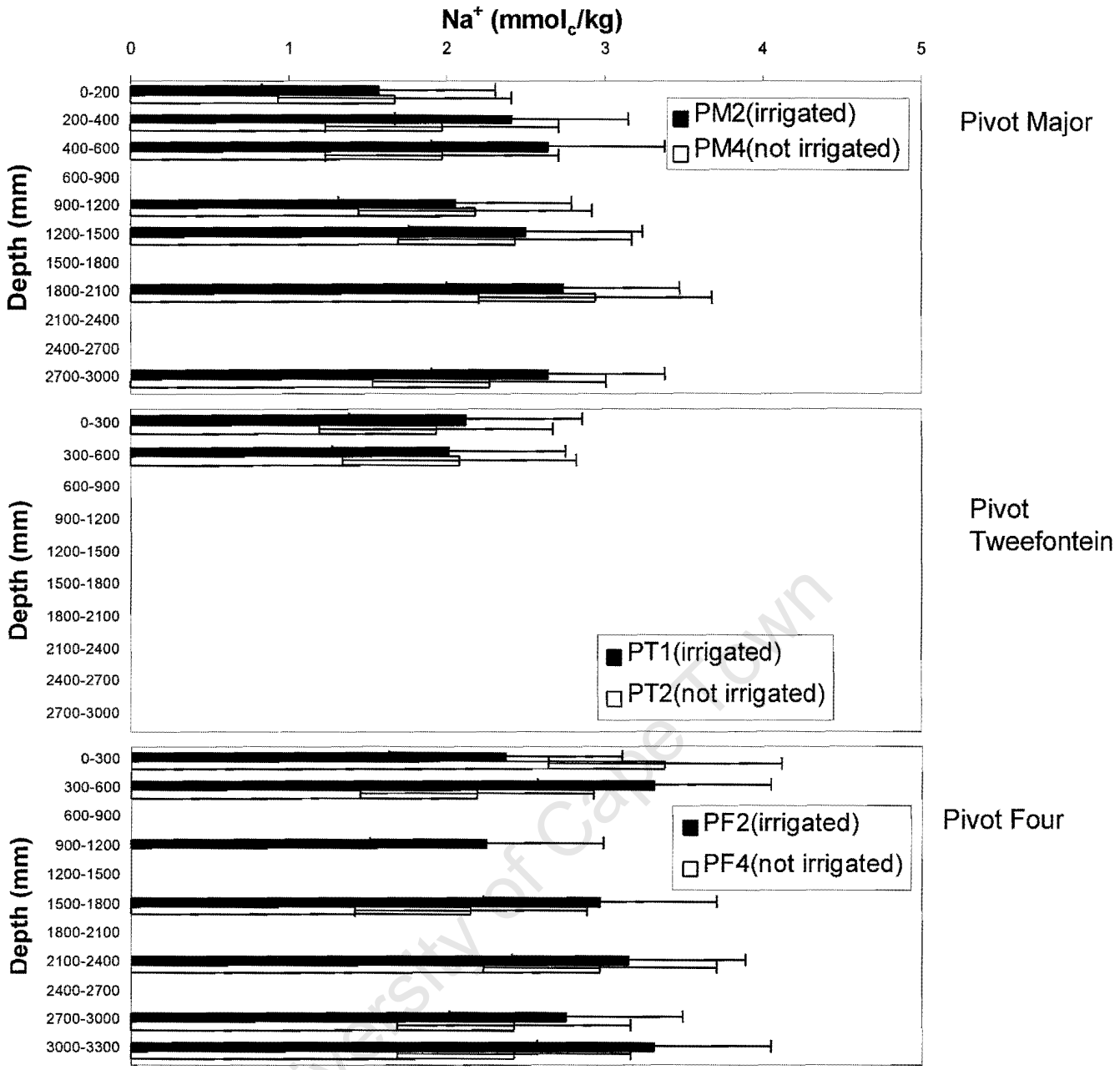

Figure 3.15: Ammonium acetate extractable sodium Na^+. Error bars indicate analytical uncertainty at the 95% confidence level. Missing results indicate that the sample for that depth interval was not analysed. Results are given in $mmol_c$ per kg of soil.

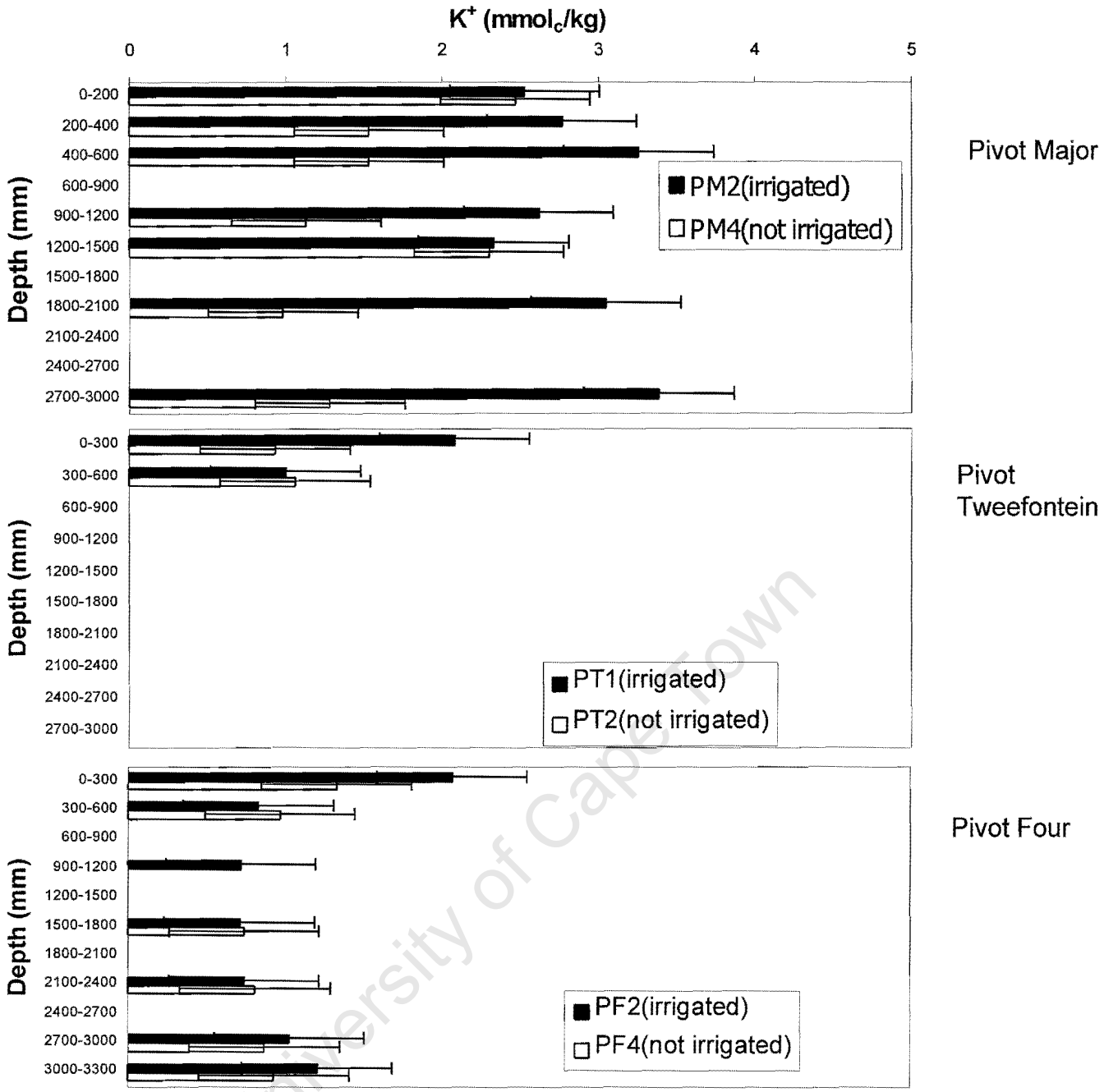

Figure 3.16: Ammonium acetate extractable K^+. Error bars indicate analytical uncertainty at the 95% confidence level. Missing results indicate that the sample for that depth interval was not analysed. Results are given in $mmol_c$ per kg of soil.

3.5.2.2 Extractable cation results for the non-irrigated soils

The pivot Major soil has its highest value of extractable Ca^{2+} in the 0-300 mm sample (11.6 $mmol_c/kg$), and its greatest extractable Mg^{2+} value in the 300-600 mm sample (11.1 $mmol_c/kg$). Extractable K^+ has a bimodal trend, peaking in the 0-300 mm sample (2.5 $mmol_c/kg$), decreasing with depth to 1200 mm and peaking again in the 1500-1800 mm sample (2.3 $mmol_c/kg$) before decreasing again. In the case of extractable Na^+, it is again impossible to identify any trend, but it has a magnitude between 1 and 3 $mmol_c/kg$.

Extractable Ca^{2+} in pivot Tweefontein has a value of 7.2 $mmol_c/kg$ in both the 0-300 mm and 300-600 mm samples, and extractable Mg is equal to 2.7 $mmol_c/kg$ in both soil samles. Similarly, K^+ has a value of 1.0 $mmol_c/kg$ and extractable Na^+ equals 2 $mmol_c/kg$, in both these samples.

In pivot Four, extractable Ca^{2+} is greatest in the 300-600 mm sample (15.9 $mmol_c/kg$) and decreases with depth, while extractable Mg^{2+} peaks at 3000-3300 mm, at the base of the profile (6.6 $mmol_c/kg$). Extractable K^+ appears to reach its maximum (1.3 $mmol_c/kg$) in the topsoil (0-300 mm) sample, but it is not possible to identify any definite trend within the limits of analytical precision, as is the case with extractable Na^+, which has values between 1 and 3 $mmol_c/kg$.

3.6 Adsorbed sulphate

Sulphate adsorbed on soil particle surfaces has been extracted from the soils with a 0.01 M calcium phosphate solution (Figure 3.17). These phosphate-extractable sulphate results represent the *sum* of adsorbed and soluble sulphate, and are referred to below as *extractable* sulphate. The concentrations of extractable sulphate in the irrigated soils exceed those in the soils which have not been irrigated with mine water.

3.6.1 Extractable sulphate in the irrigated soils

In pivot Major, extractable sulphate peaks in the 400-600 mm sample at 12 $mmol_c/kg$, and remains approximately constant between 6 and 7 $mmol_c/kg$ between 1200 mm and 3000 mm. In pivot Tweefontein, the greatest extractable sulphate concentration occurs in the 300-600 mm interval (15 $mmol_c/kg$). Pivot Four's peak extractable sulphate concentration peaks in the 1500-1800 mm sample at 16 $mmol_c/kg$ sample. It is below the analytical detection limit in both the 0-300 mm sample and the 2700-3000 mm samples.

3.6.2 Extractable sulphate in the non-irrigated soils

In most samples from non-irrigated profile from pivot Major, extractable sulphate is below the analytical detection limit. The highest concentrations (7 $mmol_c/kg$) are found in the 900-1500 mm zone. Both samples from pivot Tweefontein have

extractable sulphate concentrations of 6 $mmol_c/kg$. In pivot Four, the extractable sulphate peak occurs in the 900-1200 mm sample. Below this depth the extractable sulphate concentrations are relatively constant at 3 $mmol_c/kg$, to a depth of 3000 mm, dwindling to below the detection limit in the deepest (3000-3300 mm) sample.

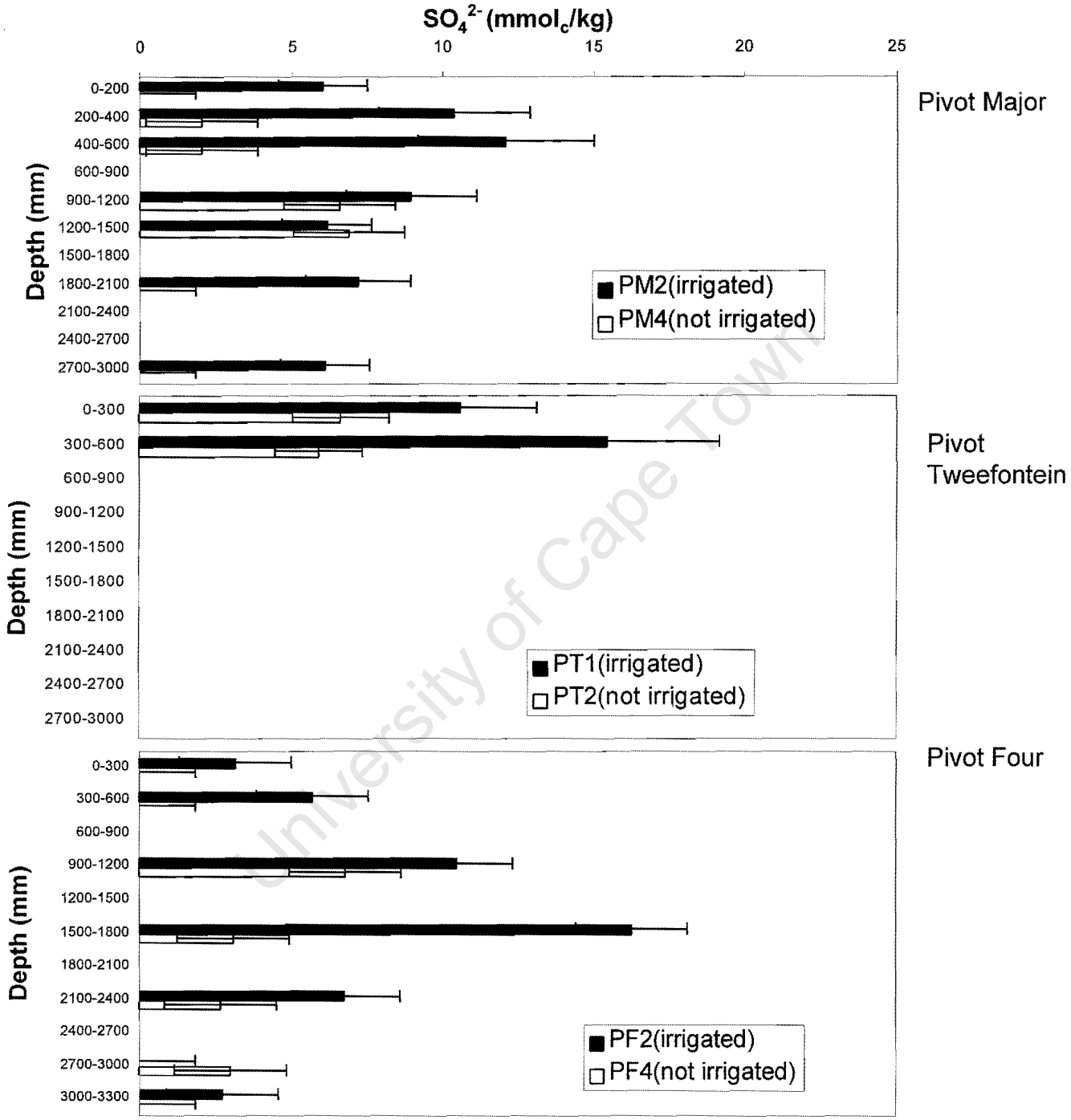

Figure 3.17: Phosphate-extractable sulphate. Error bars indicate analytical uncertainty at the 95% confidence level. Error bars which begin at zero indicate results below the detection limit. Missing results indicate that the sample for that depth interval was not analysed. Results are given in $mmol_c$ per kg of soil.

4 Discussion

The key motivation for the recent research into irrigation with mine water at Kleinkopje, and elsewhere, has been to assess whether agricultural crop lands are a suitable disposal medium for the salts dissolved in mine water. The potential for developing this practice beyond the research phase hinges upon how effectively the mine water's solute load can be retained by soils. Even if solute retention in the soils is not permanent, it should at least be such that the retained salts are released only gradually to the groundwater system, so as to minimise the impact of the salt input on groundwater quality. This chapter is a discussion of solute retention in the soils examined in this study.

Summary of chapter

The following discussion opens with a solute mass balance calculation for the irrigated soil in which the quantities of solute retained in the soils are compared with the total quantities added. Next, the spatial distribution of retained solutes and the most important mechanisms of solute retention, namely cation exchange and anion exchange or anion chemisorption are discussed.

The work of Annandale et al. (1999) suggests that the precipitation of gypsum in the upper metre of the soil profile will retain the bulk of incoming Ca^{2+} and SO_4^{2-} dissolved in saline mine water. However, it was not possible to confirm the presence of gypsum in the soil samples analysed in this study, and it is concluded that the mineral is a less important sink for Ca^{2+} and SO_4^{2-} than clay and sesquioxide adsorption sites. Possible reasons for these contradictory results are discussed.

Next, the concentrations of ions in the soil solution are discussed. It appears likely that the concentrations in the soil solution of all the ions considered in this study are controlled by surface reactions such as ion exchange, rather than by the dissolution and precipitation of solid phases.

The discussion ends with some speculation about the future chemical evolution of the soils irrigated with saline mine water. In particular, the likelihood of long-term gypsum precipitation in the soil is discussed.

4.1 Solute mass balance calculations

The total quantity of each solute ion applied to the soil by irrigation has been calculated using the quantities of irrigation water applied (Figure 1.3, p.1-5) and its ionic composition (Table 1.1, p.1-7). Where water quality data are not available (i.e., for Ca, Mg, Na, Cl and K for most of 1998 and some irrigation periods in 1999), the concentrations of these ions have been estimated by interpolation between measurements and a consideration of the relative proportions of the ions in solution. It was assumed that the relative proportions of the major ions and sulphate (the concentration of which was measured regularly) were approximately constant. The water quality and quantity data used, and an example calculation, are presented in Appendix B. The total quantities of solute ions applied to the irrigated soils since the beginning of the field trials at Kleinkopje are presented in the first column of Table 4.1.

In order to compare the solute input with soil solute reservoir, the total quantities of the major solutes, present in the soils as adsorbed and soluble species, have been estimated from the analytical data. Ammonium acetate-extractable cation data were considered to represent the sum of exchangeable and soluble cations. Phosphate-extractable sulphate was taken as an estimate of the sum of soluble and adsorbed sulphate. Chloride and alkalinity measurements made in saturated paste extracts were considered to represent the concentrations of these species in the soil solution.

The concentrations of these components have been measured in, or normalised to units of $mmol_c/kg$ soil, in samples of soil representing depth intervals of 200 mm or 300 mm. For the purpose of comparing these results with the total solute quantities added to the soil, the total quantity of each of the major ions present in a column of soil, extending from the surface to the depth of the deepest sample analysed, with a surface area of 1 m^2, has been calculated. The soils were assumed to have dry bulk

densities of 1500 kg/m^3 for pivots Major and Four, and 1600 kg/m^3 for pivot Tweefontein, at all depths. These values are based on measurements made by Lorentz et al. (2000) of the bulk densities of topsoil and subsoil samples taken from these sites. It is likely that bulk density of these soils increases with depth, associated with a greater clay content and soil compaction. The total calculated quantity of retained solute ions, originally measured per unit mass of soil, would also increase with bulk density. However, the increase would not significantly alter the results.

Table 4.1: Results of the solute balance calculation - total quantities of solutes added in irrigation water and total quantities of exchangeable and/or soluble ions detected analytically in the irrigated and non-irrigated soils. All data are in units of moles of charge per square metre (mol_c/m^2). The indicated confidence limits are at 95%, and are derived from an estimate of analytical precision.

Pivot Major Depth of soil core: 3000 mm	**Solute added by irrigation (mol_c/m^2)**	**Total quantity in irrigated soil from the surface to depth of the deepest sample (mol_c/m^2).**	**Total quantity in non-irrigated soil from the surface to depth of the deepest sample (mol_c/m^2)**
Ca^{2+}	25.7	52.7±8.9	27.2±4.6
Mg^{2+}	15.7	45.2±2.2	28.4±1.4
SO_4^{2-}	39.3	35.0±8.4	10.5±2.5
Na^+	1.4	11.1±3.2	10.6±3.0
Cl^-	0.5	4.6±0.9	1.0±0.1
K^+	0.3	13.1±2.8	6.7±1.4
Total Alkalinity	1.6	0.3±0.1	0.2±0.1
Pivot Tweefontein Depth of soil core: 600 mm			
Ca^{2+}	22.4	16.3±2.8	6.9±1.2
Mg^{2+}	19.2	5.0±0.2	2.4±0.1
SO_4^{2-}	43.3	12.5±3.0	6.0±1.5
Na^+	2.7	2.0±0.6	1.9±0.6
Cl^-	1.1	0.1±0.01	0.1±0.01
K^+	0.5	1.5±0.3	1.0±0.2
Total Alkalinity	1.8	0.03±0.01	0.03±0.01
Pivot Four Depth of soil core: 3300 mm			
Ca^{2+}	6.9	46.4±7.8	26.8±4.5
Mg^{2+}	5.9	32.6±1.6	16.2±0.8
SO_4^{2-}	12.4	37.0±8.8	13.5±3.2
Na^+	0.8	14.2±4.1	10.3±3.0
Cl^-	0.3	3.5±0.5	0.8±0.1
K^+	0.1	4.7±1.0	3.6±0.8
Total Alkalinity	0.5	0.2±0.1	0.2±0.1

A number of soil samples were omitted from the analyses, so the concentrations of the various ions in those samples were estimated by linear interpolation between analysed samples above and below them. The calculation method is presented in Appendix B. The results of the calculations are given in Table 4.1.

The quantity of each solute ion retained by the irrigated profiles is greater than or equal to the quantity retained by the non-irrigated soils. Furthermore, if it is assumed that the non-irrigated profiles represent background or pre-irrigation concentrations of these components, then the difference between the irrigated and non-irrigated profiles is an estimate of the quantity of each solute added by irrigation and retained by the soils (Table 4.2).

Table 4.2: Comparison of solute ions added by irrigation with an estimate of solute ions retained in the irrigated soils above background. Negative values indicate that the non-irrigated soils have a higher concentration of that component. Uncertainties have been estimated by the addition of the uncertainties of the measurements made in the irrigated and non-irrigated soils, i.e
$(A \pm U_A) - (B \pm U_B) = (A-B) \pm (U_A + U_B)$.

Pivot Major	Solute added by irrigation (mol_c/m^2)	Estimate of solute retained above background (mol_c/m^2)
Ca^{2+}	25.7	25.4±13.5
Mg^{2+}	15.7	16.7±3.2
SO_4^{2-}	39.3	24.6±10.9
Na^+	1.4	0.6±6.2
Cl^-	0.5	3.6±1.0
K^+	0.3	6.4±4.2
Total Alkalinity	1.6	0.1±0.2
Pivot Tweefontein		
Ca^{2+}	22.4	9.3±4.0
Mg^{2+}	19.2	2.6±0.3
SO_4^{2-}	43.3	6.5±4.5
Na^+	2.7	0.1±0.6
Cl^-	1.1	0.03±0.02
K^+	0.5	0.5±0.5
Total Alkalinity	1.8	-0.01±0.02
Pivot Four		
Ca^{2+}	6.9	19.7±12.3
Mg^{2+}	5.9	16.4±2.4
SO_4^{2-}	12.4	23.4±12.0
Na^+	0.8	3.9±7.1
Cl^-	0.3	2.7±0.6
K^+	0.1	1.0±1.8
Total Alkalinity	0.5	0.07±0.2

Assuming that the quantities of solute added are known without error, and that the the quantities of solute retained are known within the confidence limits estimated from analytical precision, the following remarks can be made:

In pivot Major, all the added Ca^{2+}, Mg^{2+} and Na^{+} have been retained in the soils. There is less sulphate retained in the soils than has been added. This suggests that some of the added sulphate has migrated below a depth of 3 m. Potassium and chloride concentrations in the soil are in excess of the quantities added. This could indicate higher pre-irrigation levels of these solutes.

In pivot Tweefontein, only the 600 mm thick soil capping on the rehabilitated mining area has been analysed, in contrast to soil thicknesses of up to 3.3 m in the natural soils. Not surprisingly, there is a smaller total quantity of every solute ion retained in this thin soil layer than in the 3 m to 3.3 m thick natural profiles. There is also less of every solute ion in the soil than was added by irrigation, except for K^{+}, which all seems to have been retained. Unlike the other pivots, Tweefontein is situated on a considerable slope, with the sampling sites located on the higher ground. This suggests that either the added solutes have been transported down into the mine spoil, to be retained there or migrate further down, or that considerable quantities of solutes have migrated down-slope, with surface or sub-surface water flow. In the latter case, the dissolved components would either have left the pivot area via its engineered surface drainage system, or have accumulated in the lower lying parts of the pivot.

In pivot Four, the retained quantities of Ca^{2+}, SO_4^{2-}, Na^{+} and K^{+} are equivalent to those added, within the uncertainty of the data. The quantities of Mg^{2+} and Cl^{-} present in the soil after correction for their background levels are higher than those added. Apart from relatively high levels of uncertainty in this calculation, one possible explanation for the high concentrations of these ions is the lateral movement of groundwater from neighbouring regions of irrigated soil. If the soil core was collected in an area which represents a local depression in the water table, there would be a net accumulation of solute ions moving in laterally from adjacent irrigated areas. This would elevate the observed solute concentrations above those expected for vertical water movement. Another explanation is simply that there is

considerable variation in the local soils' natural content of adsorbed and soluble ions – i.e., the irrigated soil was sampled in an area with naturally elevated levels of magnesium and chloride.

The quantities of total alkalinity in all of the soils are far lower than the quantities added. Both irrigated and non-irrigated soils have similarly low quantities of total alkalinity, which suggests that these soils are well buffered, probably by their exchangeable acidity (Figure 3.12). Exchangeable acidity is lower in the irrigated soils, and it is possible that some has been consumed by neutralisation reactions with the added alkalinity. However, it is more likely that the influx of sulphate ions is the most significant cause of the reduction in exchangeable acidity (see section 4.2.3.5).

Although the results of these calculations seem fairly reasonable, it should be noted that a number of samples from each soil profile were not analysed. In pivot Major, samples representing 40% of the total core lengths were omitted. In pivot Four, 36% of each soil core has not been analysed. Linear interpolation between known samples was used to fill these gaps, so that the total quantity of solute retained by the column of soil represented by each core could be estimated.

It is quite possible that the estimates of concentrations in the unknown samples are significantly different from the true values. Hence, the estimates given above for the total quantities of each solute ion retained could be significantly in error. In consequence, the results of these calculations are considered as a first approximation only, and no firm conclusions can be based upon them.

4.2 The spatial distribution and retention of adsorbed ions

The vertical distribution of solutes retained in the soil profile, and the mechanisms of solute retention has implications for crop nutrition and the effect of irrigation with mine water on groundwater quality. The location, relative abundance and mode of retention of a given species in the profile will determine whether it is available to plant roots, and whether it is likely to dissolve or desorb into groundwater. As discussed in the Introduction, the movement of solutes in a soil profile, and hence their distribution at any given time is controlled by the hydrodynamic processes of advection and dispersion, and chemical processes of molecular diffusion and sorption (Leij & Van Genuchten, 1999). While hydrological processes are undoubtedly important controlling factors in the distribution of solute ions in the soil profiles discussed here, a detailed discussion of water flow in these soils is beyond the scope of the present study. With regard to chemical controls of solute distribution in the profiles, the data presented here strongly suggest that cation exchange and anion adsorption are the most important.

4.2.1 Variation of effective cation exchange capacity with depth

The adsorption and exchange of cations on soil surfaces is an important process in the retention of cations in soils (McBride, 1999). The data presented here suggest that the effective cation exchange capacity of these soils varies with depth. Some possible reasons for this are discussed below.

The exchangeable basic cations (Ca^{2+}, Mg^{2+}, Na^{+} and K^{+}) in both pivots Four and Major tend to be present in lower concentrations between the depths of 900 mm and 1500 mm, in both irrigated and non-irrigated soils. Higher concentrations of these exchangeable cations occur above and below this zone. This suggests that the soils have a lower cation exchange capacity between depths of 900 mm and 1500 mm. The effective cation exchange capacity (ECEC) of the soils has been calculated as the sum of ammonium acetate extractable cations (at pH = 7) and KCl extractable acidity (Figure 4.1).

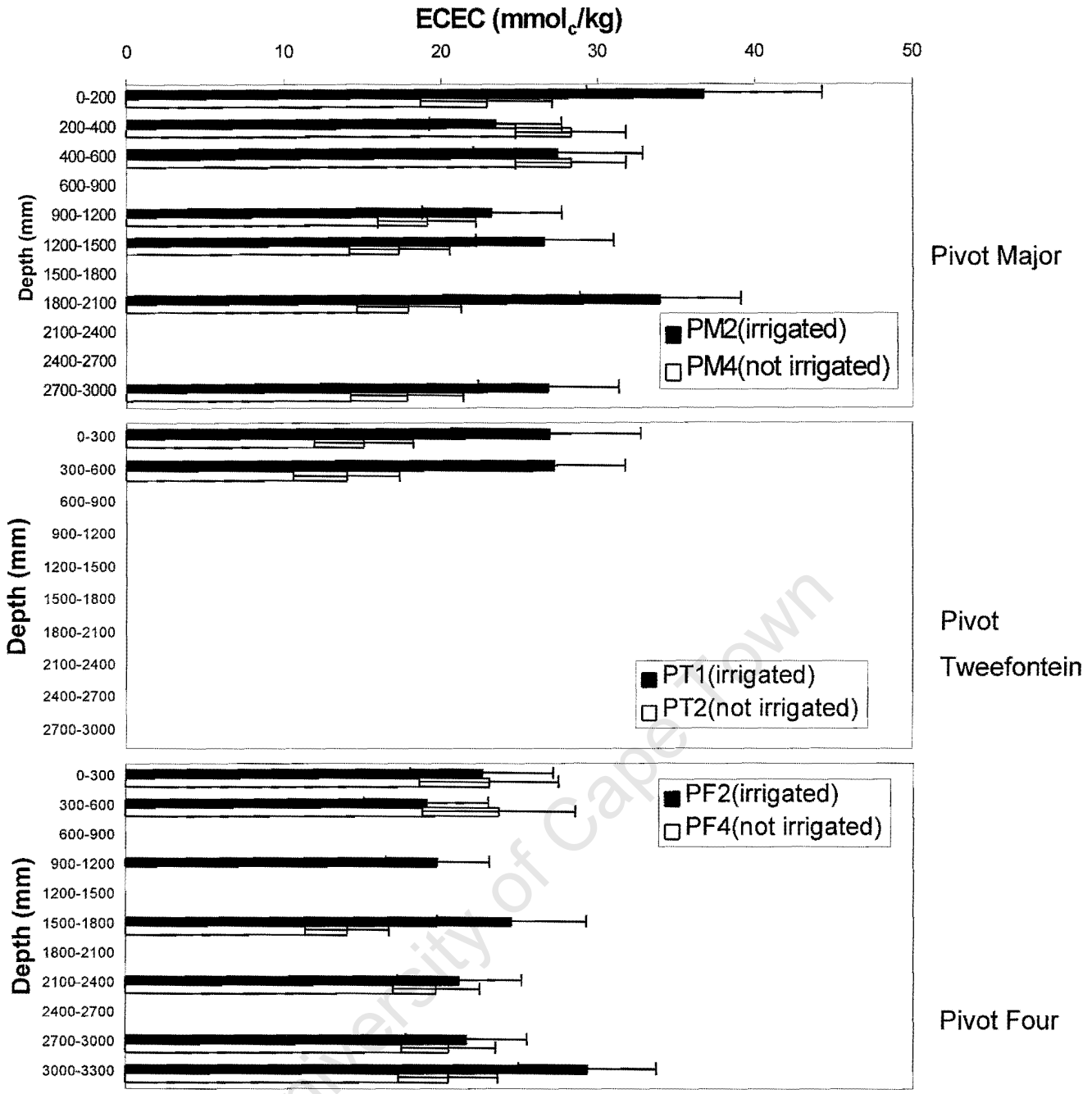

Figure 4.1: Effective cation exchange capacity, calculated as the sum of ammonium acetate extractable cations and KCl extractable acidity for soil profiles, plotted against depth in the profile. The error bars indicate confidence limits calculated from analytical precision estimates at the 95% confidence level. Missing data points indicate that the sample representing that depth interval was not analysed.

The ECECs vary with depth between 20 and 40 $mmol_c/kg$ for the irrigated soils and between 15 and 25 $mmol_c/kg$ for the non-irrigated profiles. Although the ECECs in the profiles tend to be lower in the 900 mm to 1500 mm zone, this tendency is not as obvious as it is if the exchangeable basic cations are considered separately from exchangeable acidity. Unlike the exchangeable basic cation data, the exchangeable acidity data show that in both soil profiles from pivot Four, and in the non-irrigated soil from pivot Major, there are high levels of exchangeable acidity between 900 mm and 1500 mm. In contrast, the irrigated soil profile from pivot Major, which has been under irrigation with saline mine water for the longest period of any soil considered here, has low levels of both exchangeable acidity *and* exchangeable basic cations in the 900 mm to 1500 mm zone. The role of sulphate in reducing exchangeable acidity (discussed in section 4.2.3.5) could provide an explanation for the simultaneous reduction of ECEC and exchangeable acidity in this soil profile. The formation of ternary complexes (McBride, 1994, p. 152) could be important, in particular a complex of the form SO_4-Al-clay, as this would result in a reduction in exchangeable acidity without Al ions desorbing from cation exchange sites. Shainberg et al. (1989) mention the co-sorption of Al^{3+} and SO_4^{2-} as a possible mechanism for the observed reduction in exchangeable acidity of gypsum-treated soils, although they consider the most likely sorbed complex to be of the form Al-SO_4-sesquioxide.

A more important cause of the variation in ECEC with depth seems to be the distribution of organic matter and clay-sized particles in the profile. There is a positive correlation between ECEC and total organic carbon in the soils for the topsoil and subsoil (0-600 mm zone) in both irrigated and non-irrigated profiles (Figure 4.2).

According to McBride (1994), the empirical expression

$$CEC\ (mmol_c/kg\ organic\ matter) = -600 + 500pH$$

estimates the cation exchange capacity of soil organic matter. This relationship suggests a contribution of about 20 $mmol_c/kg$ of cation exchange capacity from organic matter in these top- and subsoils, which have organic carbon concentrations

of 0.25 to 0.8 % and pH values close to 5 (assuming total organic carbon is 50-58% of soil organic matter by mass – Baldock & Nelson, 1999).

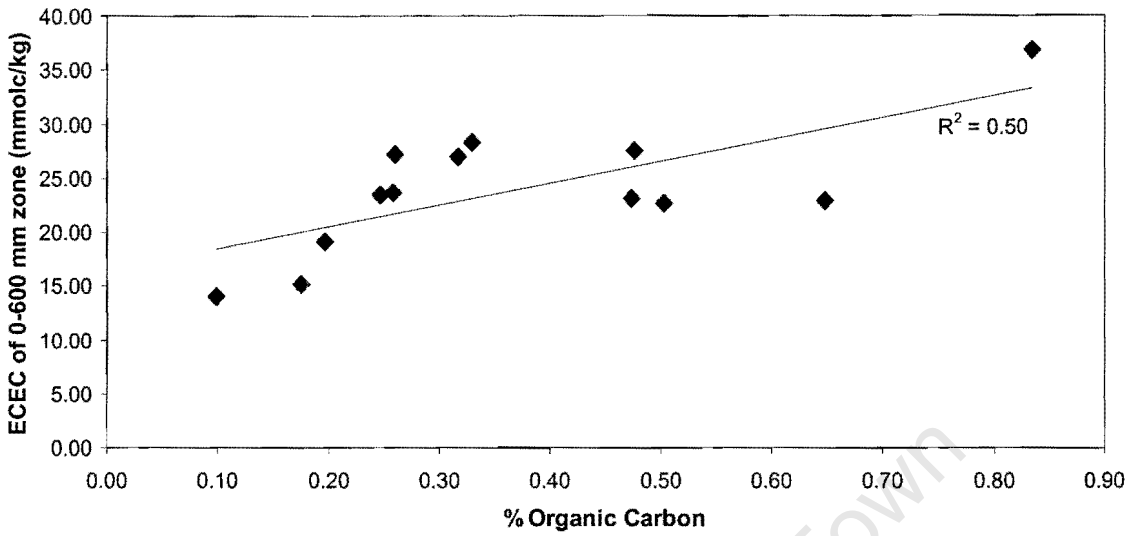

Figure 4.2: Mass percentage total organic carbon measured in soil samples representing the top 600 mm of the soil profiles for both irrigated and non-irrigated soils, plotted against the samples' effective cation exchange capacities (ECEC).

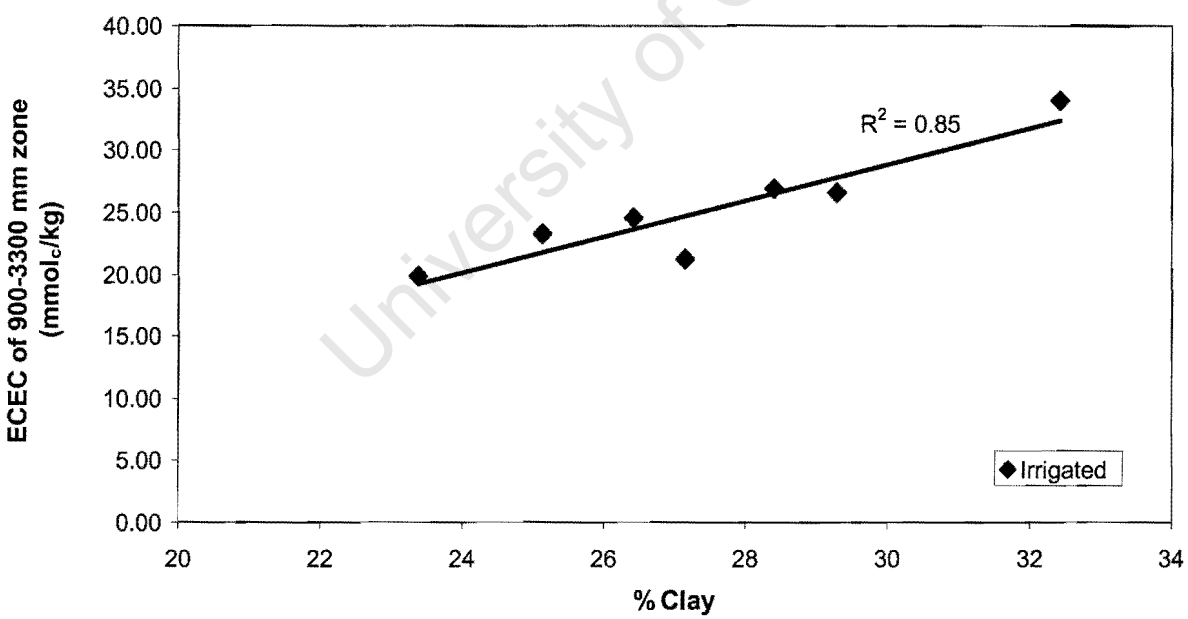

Figure 4.3: Mass percentage clay measured in soil samples representing the soil profiles between 900 mm and 3300 mm depth for irrigated soils, plotted against the samples effective cation exchange capacity (ECEC).

Below 900 mm in the irrigated profiles, clay content is positively correlated with ECEC (Figure 4.3) Clay contents of the non-irrigated soils have not been measured. Kaolinite and illite dominate the clay fraction, and the measured ECECs indicate that the clay minerals themselves have ECECs of 50 to 100 $mmol_c/kg$ clay, values that are within the usual range expected for illite and kaolinite (McBride, 1994).

ECEC and soil pH appear to be independent of one another (Figure 4.4). There is ample evidence that cation exchange capacity rises with pH (McBride, 1994), but ECEC need not behave this way. In the irrigated soils, the influx and subsequent adsorption of Ca^{2+} and Mg^{2+} would have raised the ECEC, but may have simultaneously lowered the pH as exchangeable Al^{3+} and H^{+} were displaced into solution.

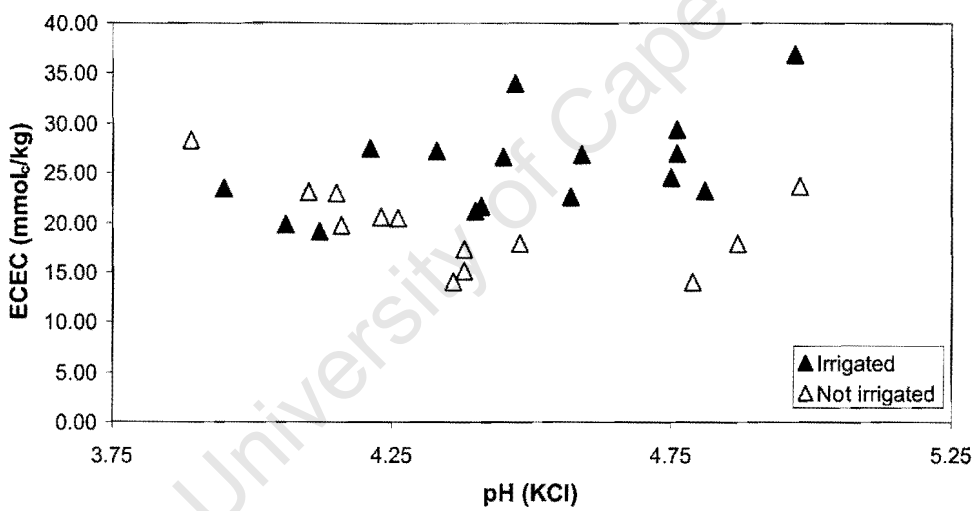

Figure 4.4: The effective cation exchange capacity of irrigated and non-irrigated soils plotted against soil pH measured in 1:2.5 soil:1M KCl suspensions.

The inference that can be drawn from these relationships is that the higher ECECs in the upper 900 mm and lower 1500 mm are attributable to higher organic matter or clay content. Conversely, lower ECECs occur where the soil is poor in both clay and organic matter.

4.2.2 The displacement of exchangeable Mg^{2+} by Ca^{2+}

The observed tendency in these soils for calcium to dominate the exchangeable cation suite in the upper half of the profiles, and magnesium to be dominant in the lower half (Figure 4.5) can be explained by these ions' relative affinity for cation exchange sites.

In general, the tendency of cations to be adsorbed on clay exchange sites is given by the Hofmeister series:

$Ba^{2+} > Sr^{2+} > Ca^{2+} > Mg^{2+}$

i.e, the affinity of an ion for a negatively charged surface increases with its non-hydrated radius (Stumm & Morgan, 1996). This has also been shown to hold for cation exchange sites on soil organic matter (McBride, 1994). This tendency has resulted in the preferential adsorption of calcium over magnesium as irrigation water percolates into the soil, and the displacement of previously adsorbed magnesium ions by incoming calcium ions. The result is a downward migration of Mg^{2+} in the soil profile, with the bulk of it being adsorbed only when its concentration in

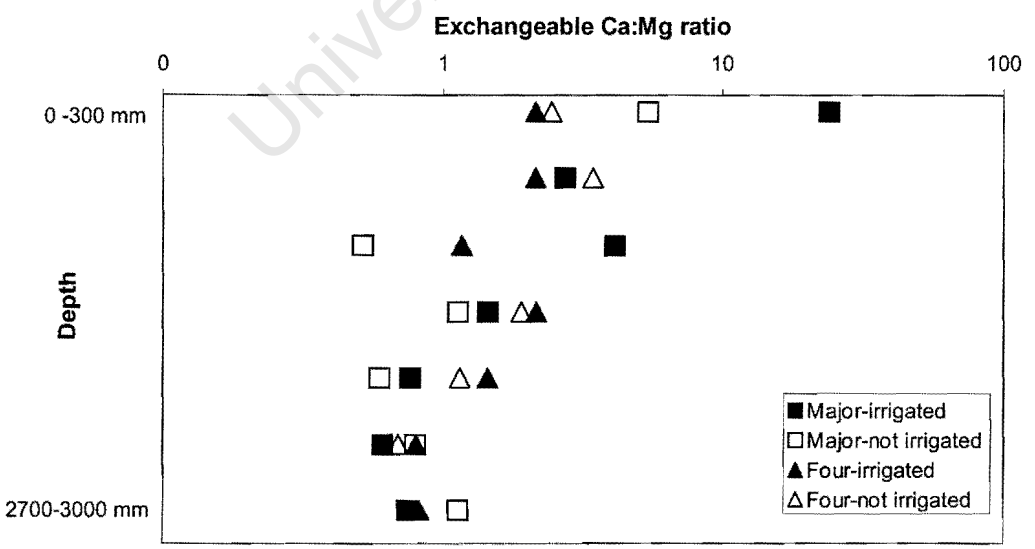

Figure 4.5: The ratio of exchangeable Ca to exchangeable Mg in the soil samples from pivots Major and Four (pivot Tweefontein is omitted because the samples only represent the top 600 mm of soil).

solution is high enough relative to Ca^{2+}. Similarly, exchangeable Na^{+} and K^{+} tend to increase with depth relative to Ca^{2+} (Figure 4.6), although exchangeable K^{+} exhibits more complex behaviour in pivot Four – probably the result of specific adsorption of K^{+} on the interlayer sites of mica minerals (Sposito, 1989, p.133) resulting in its being less easily exchangeable than Na^{+} or Mg^{2+}.

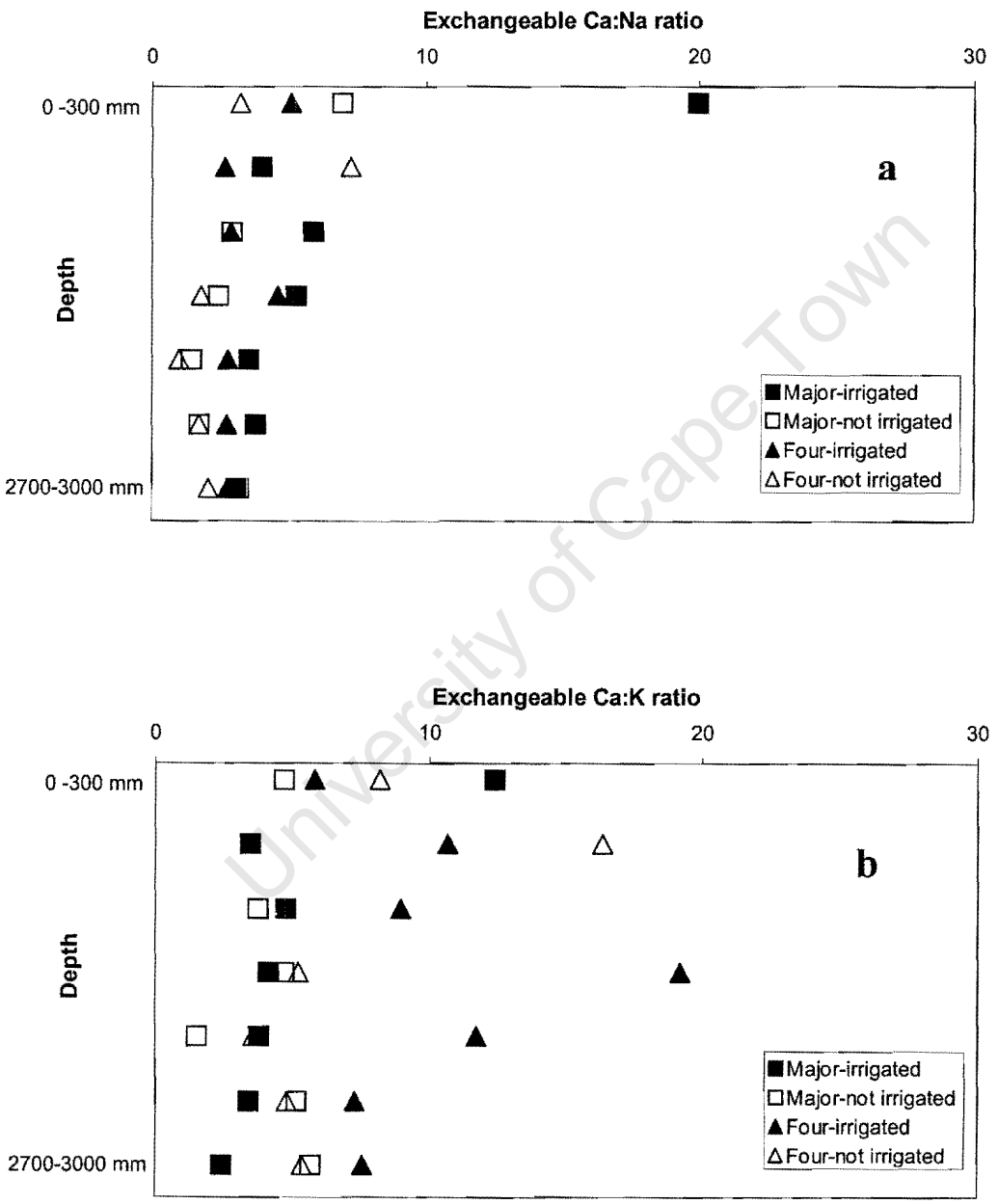

Figure 4.6: The ratio of exchangeable Ca to exchangeable Na (a) and K (b) in the soil samples from pivots Major and Four (pivot Tweefontein is omitted because the samples only represent the top 600 mm of soil).

The displacement of other exchangeable ions by calcium is observed in *both* the irrigated *and* non-irrigated soils (although soluble and adsorbed concentrations are greater in the irrigated soils). This is apparently a natural tendency in the soils, not a phenomenon specific to irrigation with mine water. However, the high concentrations of Ca^{2+} in the irrigation water have accelerated this natural trend. Exchangeable Mg^{2+} levels in the upper 600 mm of the irrigated profile from pivot Major are significantly lower than in the non-irrigated soil, while the reverse holds for the deeper part of the soil profile. Similar trends can be seen in pivots Four and Tweefontein. As a result, less magnesium will be available to plants in the irrigated soils, and there is likely to be an increased rate of leaching of Mg^{2+} into the groundwater.

4.2.3 Sulphate adsorption

As discussed in the Introduction, sulphate adsorption takes place on the positively charged surfaces of the hydroxides of Fe and Al, and is enhanced by conditions of low pH. Sulphate may form irreversible inner-sphere complexes on these surfaces. Kaolinite reversibly adsorbs sulphate at its positively-charged edge sites. Sulphate adsorption is most favoured at a pH of 2, and decreases with rising pH (Mott, 1981), becoming negligible above a pH of 6 (Tabatabai, 1982).

4.2.3.1 Sulphate adsorption and pH

Phosphate-extractable sulphate data appear to be independent of soil pH (Figure 4.7). This is probably because the movement and accumulation of sulphate in the soil profiles is controlled by soil water movement (section 4.2.3.2), and soil zones of different pH have not been exposed to the same concentrations of solube sulphate. An accurate picture of pH dependence of sulphate sorption in these soils can only be obtained from sorption experiments in which the soils are equilibrated with sulphate solutions at various pH values. The difference between soil pH measured in a salt solution and that measured in water (ΔpH) has been used as an index of soil surface charge (Rowell, 1994). There is a positive correlation between ΔpH and phosphate-

extractable sulphate, which is reasonably significant for the irrigated soils – if the two highest extractable sulphate results are omitted (Figure 4.8). However, this is probably a reflection of a more fundamental relationship between sulphate adsorption and exchangeable acidity (section 4.2.3.5), not surface charge, since ΔpH is not independent of exchangeable acidity.

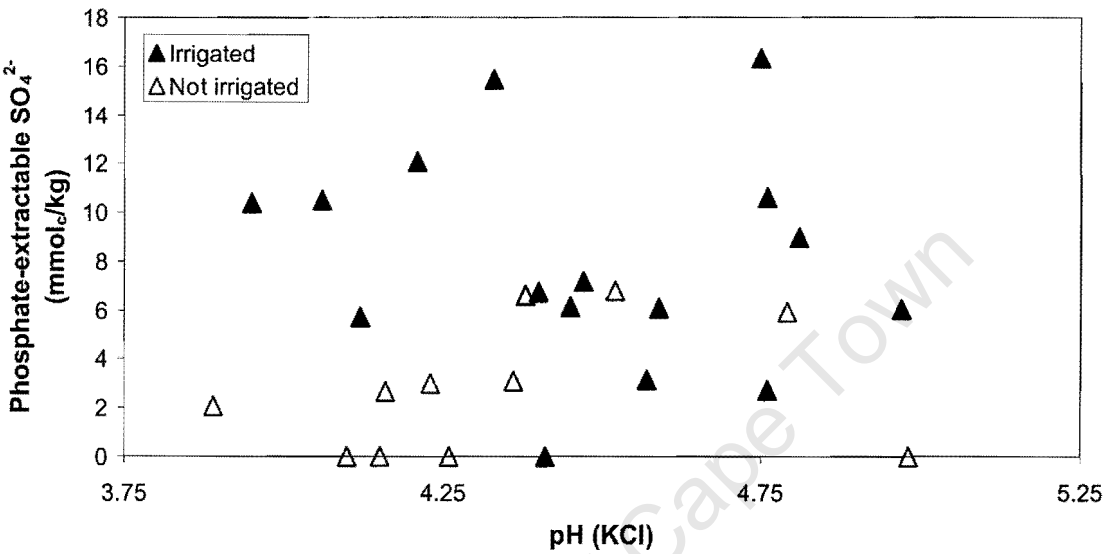

Figure 4.7: The soil pH in 1:2.5 1M KCl suspensions plotted against phosphate-extractable sulphate.

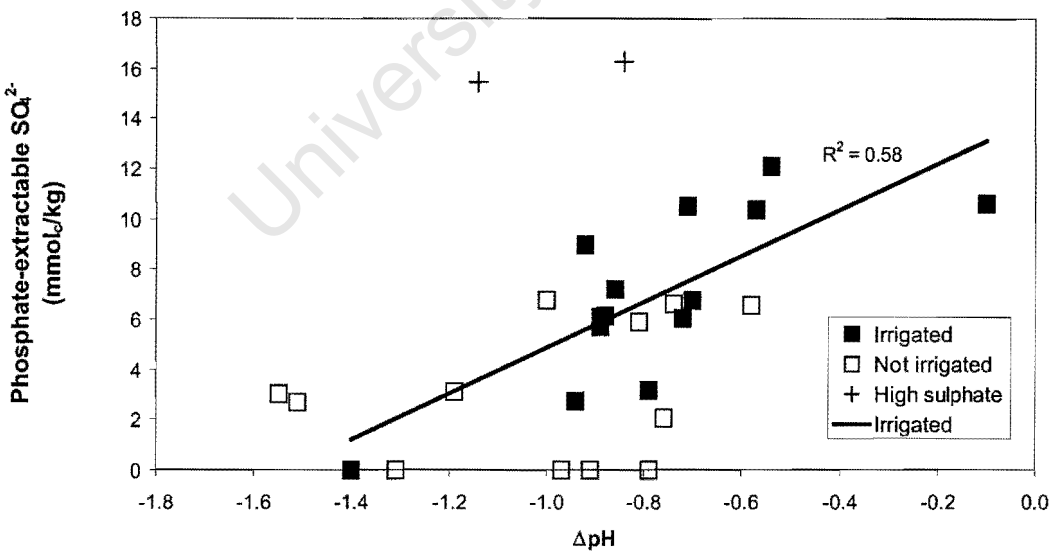

Figure 4.8: The difference between soil pH measured in a 1:2.5 1M KCl suspension and soil pH measured in saturated paste (ΔpH) plotted against phosphate-extractable sulphate. Two irrigated soil samples (data ponts +) with the highest extractable sulphate results (PF2 1500-1800 mm, 16.3 $mmol_c/kg$ and PT1 300-600 mm, 15.5 $mmol_c/kg$) have been omitted from the correlation line calculation, since they depart from the obvious linear trend.

4.2.3.2 The influence of soil water dynamics on the spatial distribution of sulphate

A comparison of the appearance of the soil samples in the field (Table 3.1, p.3-1), and the pattern of sulphate retention in the soil profiles suggests that peak sulphate adsorption takes place close to the water table. In pivot Major, the greatest value of phosphate-extractable sulphate was found in the 300-600 mm zone in the irrigated soil, and in the 1200-1500 mm sample in the non-irrigated soil. In both profiles, these were the shallowest samples in which grey mottling was observed. Grey mottling is often an indicator of temporary waterlogging and slightly reducing conditions, and is commonly associated with soil zones subject to water table fluctuations. Under waterlogged conditions the soil tends to lose its yellow or red colour, and become paler (often grey) as Fe^{3+} oxide minerals are reduced to soluble Fe^{2+} species.

In pivot Four, the highest sulphate concentration in the irrigated soil was found in the 1500-1800 mm sample, the shallowest sample to be described as "wet" – i.e. saturated with water. This sample probably represents the transition between the saturated and unsaturated zones in hydrological terms. The non-irrigated soil in pivot Four has its peak sulphate concentration in the 900-1200 mm sample. The sample immediately below it, representing the 1200-1500 mm depth interval, was not analysed for adsorbed sulphate, but is the shallowest sample in this core in which iron concretions were observed. Iron concretions are common in soil zones subject to seasonal waterlogging as a result of a fluctuating water table.

These associations between sulphate retention maxima and zones which represent past or present regions of hydrological transition suggest that the accumulation of sulphate in any particular region of the profile is significantly influenced by seasonal variations in the soils' water content and water flow in the soils. In particular, the influx of rain water during each wet season appears to have moved the bulk of sulphate present in upper part of the profile to the top of the saturated zone. Kleinkopje mine is situated in an area known for its high-intensity, short-duration rainstorms, and these conditions would tend to cause the rapid movement of significant volumes of rainwater through the unsaturated zone in these sandy soils.

Since sulphate adsorption, especially on kaolinite edge sites, tends to be reversible (Mott, 1981), rainwater passing through the unsaturated zone would cause sulphate to desorb and be transported down to the water table. More stagnant water flow conditions at the water table will cause a net accumulation of dissolved SO_4^{2-}. Since the quantity of SO_4^{2-} adsorbed from a solution increases with solution concentration and time (Tabatabai, 1982), there will be enhanced adsorption of sulphate close to the top of the saturated zone.

4.2.3.3 Exclusion of anions from the topsoil

It is known that anions in the soil solution tend to be excluded from soil regions with high concentrations of negative charge (such as topsoils rich in humus). This effect is thought to be the result of electrostatic repulsion which causes anions in solution to be concentrated in the centres of soil pores, where the flow velocity of the soil solution is greatest (Leij & van Genuchten, 1999). Low levels of SO_4^{2-} adsorption are observed in topsoils relative to deeper soil horizons (Tabatabai, 1982), probably beacuse of the abundance of negatively charged organic matter in topsoils. Another effect, thought to retard PO_4^{3-} sorption in topsoils, is the sorption of colloidal or dissolved humus to positively charged surfaces, effectively reducing their sorption capacity for phosphate (Mott, 1981), and presumably other anions. The relatively small concentrations of adsorbed and soluble sulphate found in both irrigated and non-irrigated soils considered here suggest that either or both of these phenomena are active.

4.2.3.4 Synergistic adsorption of Ca^{2+} and SO_4^{2-}

There is evidence in the literature for a synergistic enhancement of SO_4^{2-} sorption by Ca^{2+} adsorption (Ajwa & Tabatabai, 1995; Davis & Burgoa, 1995). A comparison of extractable Ca^{2+} and SO_4^{2-} (Figure 4.9) suggests that there may be co-sorption of calcium and sulphate, especially in the irrigated soils from pivot Major and pivot Four. An experimental study of simultaneous Ca^{2+} and SO_4^{2-} sorption behaviour in these soils would be necessary to establish the importance of this phenomenon in soils irrigated with saline mine water.

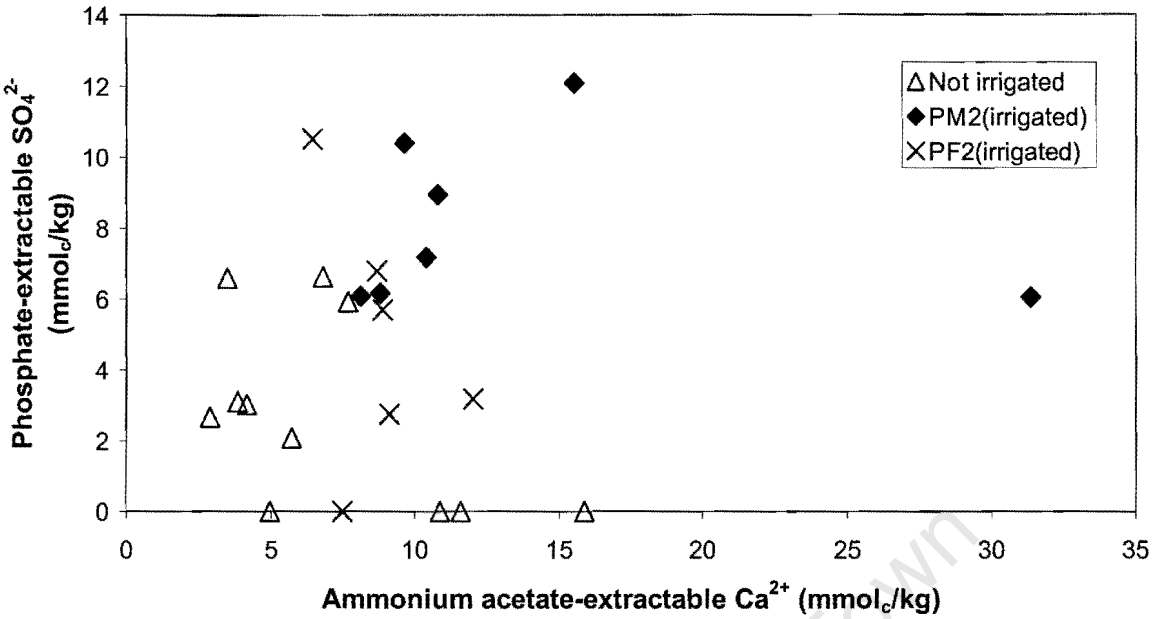

Figure 4.9: Ammonium acetate exchangeable calcium plotted against phosphate – extractable sulphate in non-irrigated soils and the irrigated soil profiles from pivots Major (PM2) and Four (PF2).

4.2.3.5 Sulphate sorption and exchangeable acidity

There appears to be an inverse relationship between 1M KCl extractable acidity and phosphate-extractable sulphate in the soils (Figure 4.10). The influx of Ca^{2+} and Mg^{2+} in irrigation water also appear to be related to the observed reduction in exchangeable acidity in the irrigated soils (Figure 4.11). While these basic cations may displace exchangeable acid cations from exchange sites, they will not neutralise the acidity. Some other mechanism must be invoked to explain the reduced exchangeable acidity of the irrigated soils. The self-liming effect, first proposed by Reeve and Sumner (1972) to explain the reduction in exchangeable acidity observed in gypsum-treated soils is a likely explanation. Reeve and Sumner (1972) proposed that SO_4^{2-} would displace hydroxyl ions from positively-charged sesquioxide sites by ligand exchange. This would cause reduced Al activity in solution as a result of the precipitation of $Al(OH)_3$.

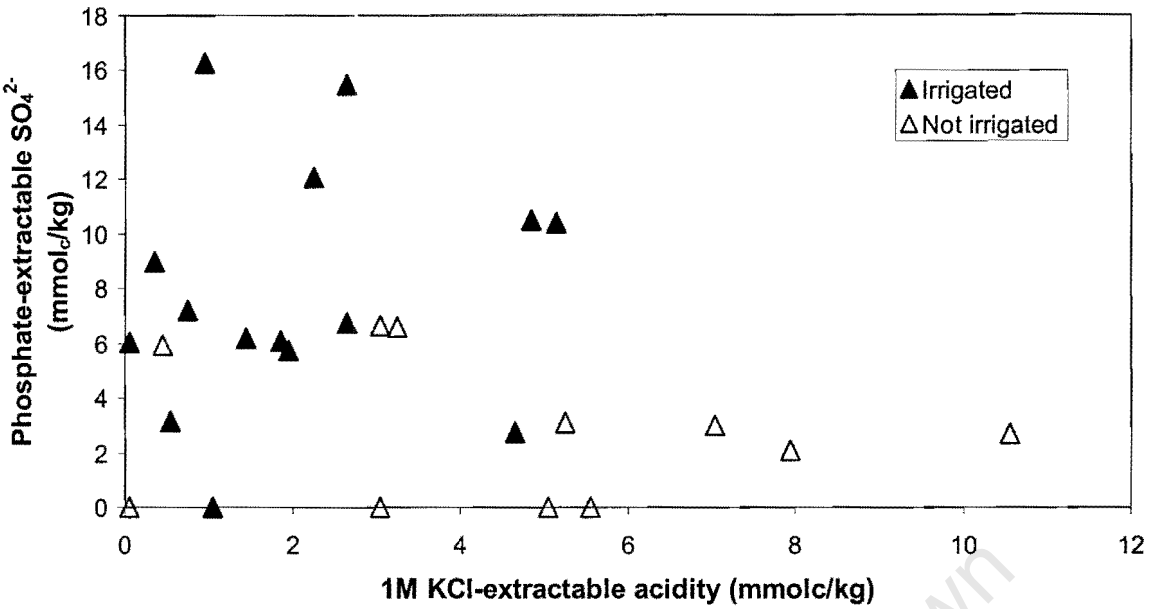

Figure 4.10: 1M KCl extractable acidity plotted against phosphate-extractable sulphate for both irrigated and non-irrigated soils.

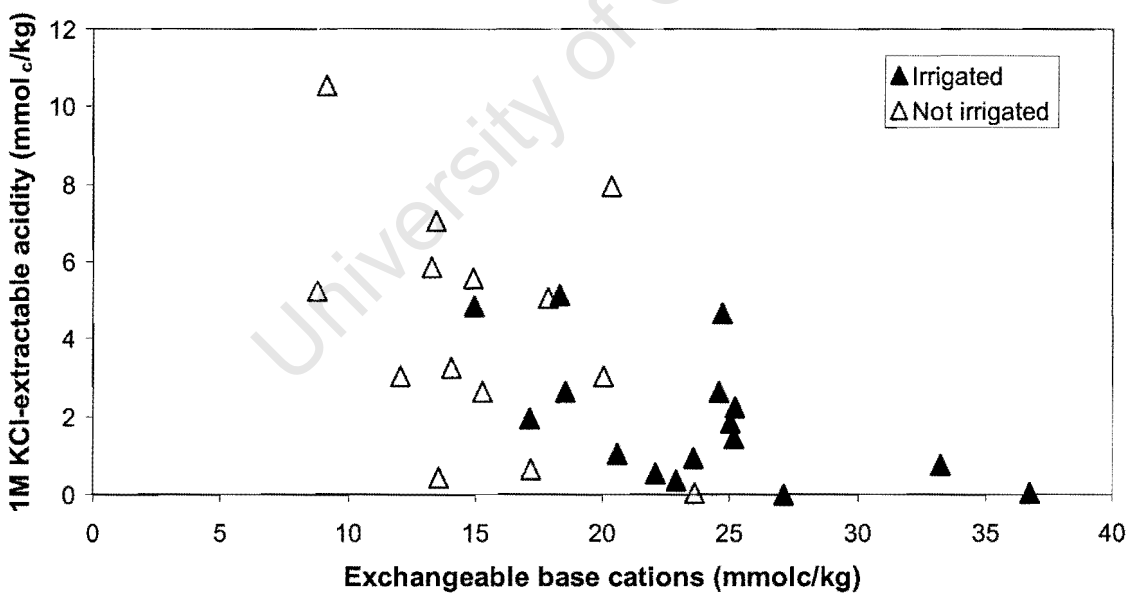

Figure 4.11: The sum of ammonium acetate extractable cations (Ca^{2+}, Mg^{2+}, Na^{+} and K^{+}) in irrigated and non-irrigated soils versus 1M KCl extractable acidity.

Sulphate addition to soils may also reduce exchangeable acidity in other ways. In particular, the formation of the $AlSO_4^+$ ion pair, and the precipitation of insoluble Al-sulphates, such as alunite ($KAl_3(OH)_6(SO_4)_2$), basaluminite ($Al_4(OH)_{10}SO_4.5H_2O$) and jurbanite ($AlOHSO_4.5H_2O$) may result in a lower activity of Al^{3+} in the soil solution (Ritchey & de Sousa, 1997, Shainberg et al., 1989). It is also possible that the adsorption of sulphate to single positively charged sites in the presence of free Al^{3+} could result in the formation of ternary complexes of the form $(=Fe\text{-}OH_2^+\text{--}SO_4^{2-})_3\text{--}Al^{3+}$, again resulting in reduced Al^{3+} activity (Drever, 1997; Shainberg et al., 1989). While the focus of the work cited above has been on the role of sulphate in reducing exchangeable acidity, the same processes result in the immobilisation of sulphate. The implication is that pre-irrigation levels of exchangeable acidity may be positively correlated with SO_4^{2-} sorption during irrigation with saline mine water.

4.3 Gypsum precipitation

Contrary to the prediction of Annandale et al. (1999) that precipitation of gypsum in the top 1.1 m of soil would be the predominant mode of solute retention in soils irrigated with saline mine water, it has not been possible to confirm the presence of gypsum in the irrigated soils. In particular, calculations of the gypsum saturation indices of saturated paste extracts of soils from the irrigated fields demonstrate their universal undersaturation with respect to gypsum (Figure 3.10, p.3-19). This suggests that only very small amounts of gypsum, if any, are present, although Van den Ende (1991) has shown that saturated paste extracts of soils can be undersaturated with respect to gypsum, while the in-situ soil solution is oversaturated, and free gypsum is present in the soils.

One possible reason for the undersaturation of these extracts was that the procedure followed during the preparation of saturated pastes may not have allowed sufficient time for equilibration with gypsum in the soils. To overcome this problem, and to ensure complete equilibration, increasingly dilute, well-equilibrated aqueous soil extracts were prepared for the two soil samples with the highest gypsum saturation indices. The results (Figure 3.11, p.3-20) indicate that the mass of sulphate dissolved per kilogram of soil increases as the soil:water ratio falls from 1:1 to 1:10, after

which no increase is detectable, indicating that all water-soluble sulphate has dissolved.

If gypsum were present in the soils, the long equilibration times used should have ensured that it would have dissolved until the solution was saturated, if gypsum were present in excess. As soil:water ratios became smaller, more gypsum would have dissolved, and hence there would have been an observed increase in soluble sulphate per unit mass of soil. When no further increase in soluble sulphate was observed with falling soil:water ratios, it could have been concluded that all the gypsum had dissolved. At every soil:water ratio before all the gypsum has dissolved, the extract should have been in equilibrium with gypsum.

The soluble sulphate data follow precisely the pattern they would if gypsum was dissolving. However, the gypsum saturation indices for *all* these extracts were negative, indicating undersaturation. The implication is that at no soil:water ratio was there any gypsum present as a solid phase, after the extracts had reached equilibrium. Thus the observed increases in dissolved sulphate with increasing dilution were not caused by the dissolution of gypsum. This data indicates strongly that sulphate solubility in these soils is not controlled by the dissolution and precipitation of gypsum, but probably by adsorption and desorption reactions at particle surfaces. The data also implies that gypsum is present only in small amounts, if at all.

Since these soils contain haematite, goethite and kaolinite, and are acidic, it is likely that much sulphate retention in these soils is by adsorption at the surfaces of those minerals. So-called soluble sulphate determined by the analysis of saturated paste extracts and increasingly dilute extracts could well reflect SO_4^{2-} desorption from adsorption sites as the equilibrium between these surfaces and the small amounts of pore water remaining in air-dried soils is disturbed by the addition of an excess of deionised water during the extraction procedures.

A similar argument can be made for each of the other water-soluble ions determined in saturated paste extracts. Given the data at hand, it is considered unlikely that any soluble or sparingly-soluble salt of the major ionic constituents of the soil solution is

the dominant sink for dissolved ions. To illustrate this, the maximum quantity of gypsum that could be present in the irrigated soil at pivot Major has been estimated:

It is assumed that all soluble SO_4^{2-} determined in the well-equilibrated 1:1 soil:water extract (Figure 3.11, p.3-20) of the soil sample closest to gypsum saturation (PM2, 400-600 mm) comes from dissolved gypsum, i.e.

$$\begin{aligned} 6.5 \text{ mmol}_c/\text{kg } SO_4^{2-} &= 3.25 \text{ mmol/kg gypsum} \\ &= 3.25 \text{ mmol/kg x } 0.172 \text{ g/mmol} \\ &= 0.56 \text{ g gypsum per kg soil} \end{aligned}$$

Assuming a bulk soil density of 1500 kg/m^3 (Lorentz et al., 2000), the maximum quantity of gypsum present in a volume of soil with a surface area of 1 m^2 and a depth of 1.1 m is

$$0.56 \text{ g/kg x } 1500 \text{ kg/m}^3 \text{ x } 1 \text{ m}^2 \text{ x } 1.1 \text{ m}$$
$$= 0.92 \text{ kg gypsum}$$

Annandale et al.(1999) predict that gypsum precipitation in the first 1.1 m of soil irrigated with saline mine water will result in the retention of most applied Ca^{2+} and a chemically equivalent quantity of SO_4^{2-}. The total quantity of Ca^{2+} applied during the irrigation of pivot Major (Table 4.1) is

$$25.7 \text{ mol}_c/\text{m}^2 \text{ } Ca^{2+} \text{ equivalent to } 12.9 \text{ moles of gypsum/m}^2$$
$$= 2.21 \text{ kg gypsum/m}^2$$

This figure is more than double the estimate of the maximum gypsum accumulation (0.92 kg/m^2) in the upper 1.1 m of soil.

Furthermore, given the much lower gypsum SI values below a depth of 1.1 m (Figure 3.10), it is unlikely that there is sufficient gypsum precipitated at depth to make up the deficit. While all of the applied Ca^{2+} has been retained in the soil profile (between 0 and 3 m – section 4.1), a maximum of 42% of the calcium retention could have been by gypsum precipitation. The balance is retained on cation exchange sites – this in the soil which is closest to equilibrium with gypsum. In

general, it is likely that the solubility of major ions in the soil solution is largely controlled by surface reactions such as ion exchange and ligand exchange.

A comment made by McBride (1999) is pertinent to the issue of the relative importance of adsorption and precipitation: "It is perhaps best to view the removal of adsorbate ions from solution, termed generically as sorption, as a continuous process that ranges from chemisorption at the low to precipitation at the high end of solubility. Unless a new solid phase can be detected, the onset of precipitation and the termination of chemisorption during sorption is usually not recognized by experimentalists."

4.4 The spatial distribution of soluble ions

As mentioned above, it is likely that the activities of most ions in the soil solution are controlled by the reactions with surface adsorption sites and not by the dissolution of solid phases. The following discussion takes this view as its starting point.

4.4.1.1 Major ions

The major ions in the soil solution (as determined by saturated paste extractions) are Ca^{2+}, Mg^{2+} and SO_4^{2-}. The spatial distributions of soluble and exchangeable calcium (Figures 3.3,p.3-7 and 3.13,p.3-26) are similar, although the lower concentrations of the soluble relative to the exchangeable ion near the bases of the profiles indicate that adsorption at these depths can be described by a different adsorption isotherm to that at shallow depths. It is likely that clay minerals provide most cation exchange sites at depth, while organic matter is the dominant reactive surface in the shallow soil, and this could explain the observed difference. Magnesium demonstrates this even more markedly (Figures 3.4,p.3-8 and 3.14,p.3-27), having its highest solubilities at the same depths as Ca^{2+}, and its lowest solubilities where its exchangeable concentration is highest. This suggests that it is only weakly held on organic matter in the topsoil. Soluble sulphate (Figure 3.5,p.3-9) correlates well with adsorbed sulphate (Figure 3.17,p.3-31) although the proportion of adsorbed to

soluble sulphate is not constant, again suggesting spatial variability in the shape of the adsorption isotherm.

4.4.1.2 Minor ions

Soluble Na^+ (Figure 3.6, p.3-12) behaves similarly to magnesium in pivot Major, with its lowest solubility where its adsorbed concentration (Figure 3.15,p.3-28) is highest. In pivot Four, the soluble concentration of Na^+ increases with depth in the irrigated soil, pointing to its higher lability relative to the divalent cations. The concentrations of soluble K^+ (Figure 3.8,p.3-14) appear to be well correlated with exchangeable concentrations (Figure 3.16,p.3-29), suggesting that its adsorption on all cation exchange sites has approximately equal strength.

The soluble anions Cl^- (Figure 3.7,p.3-13) and NO_3^- (Figure 3.9,p.3-15) tend to have higher concentrations in the irrigated soils, indicating a greater likelihood of the leaching of these ions into the groundwater from the irrigated soils. While Cl^- is known to have been added to the irrigated soils in the irrigation water, it is not known if the same is true of nitrate. Nitrate is naturally present in soils, and added as a component of fertilizer. Its relatively higher solubility in the irrigated soils is probably caused by it having been displaced from anion exchange sites by sulphate.

Soluble NH_4^+ (Table 3.2,p.3-16) is present in uniformly low concentrations in these soils, and its highest concentration is found in the 200-420 mm sample of the irrigated soil from pivot Major. This anomaly almost certainly represents the residuum of ammonium nitrate fertilizer application (Dr. N. Jovanovic, Department of Plant Production and Soil Science, University of Pretoria, pers. comm., 2000).

Alkalinities of the soil solution are also uniformly low (Table 3.3,p.3-17), with the one exception being the irrigated topsoil (0-200 mm sample) from pivot Major. The cause of this relatively elevated alkalinity (0.2 $mmol_c$/kg of soil, equivalent to 0.7 $mmol_c$/litre) is not known, but the presence of agricultural lime in the topsoil is likely, given that the land was used for commercial farming prior to the mine water irrigation experiment.

4.5 The possibility of future gypsum precipitation and accumulation in the irrigated soils

The data presented here strongly suggest that, at present, the adsorption of calcium and sulphate ions is the favoured mechanism of removing these ions from solution, and that little gypsum is present in the soils sampled. It is possible that, with continued irrigation, the adsorption sites will approach equilibrium with a soil solution which is sufficiently oversaturated with respect to gypsum for the mineral to begin to precipitate. Because of the energy barrier which retards nucleation of solid phases in solutions, the soil solution must be somewhat oversaturated with respect to gypsum before nucleation and crystallization can occur (McBride, 1994; Stumm and Morgan, 1996).

It is quite possible that gypsum precipitation already occurs in the irrigated soils during the irrigation season. However, the influx of rainwater during summer, and particularly discrete events of very intense rainfall, would tend to dissolve much of the relatively small amounts of gypsum that may have accumulated during the winter irrigation season.

Rainwater moving through the soil profile must also necessarily cause some desorption of adsorbed species from colloid surfaces. When irrigation begins again, these cation and anion adsorption sites and the soil solution would take time to regain a state which would allow gypsum to precipitate.

The extent to which the surface adsorption sites are reset toward their pre-irrigation state by each rainy season must control the timing of the onset of gypsum precipitation during the irrigation season, and thus the quantity of gypsum precipitated during the season. From the data at hand it is apparent that, even after substantial rainfall and a six-month hiatus in irrigation, the quantities of Ca^{2+} and SO_4^{2-} present on adsorption sites (and, possibly, small amounts of gypsum) in the irrigated soils can subtend concentrations of the ions in solution which are significantly greater than the non-irrigated soils. This points to minimal resetting of the system, at least in pivot Major, where soil solutions were closest to saturation

with respect to gypsum. In pivot Major, at least, it is possible that gypsum precipitated during the irrigation season immediately following the sampling carried out for this study.

The question of whether the gypsum which has precipitated (if any) in a given irrigation season will survive the subsequent rainy season is difficult to answer. It would depend on the quantity of gypsum precipitated, its distribution in the soil, its particle size, and the season's rainfall. Further experimental work would be necessary to answer the question with any degree of certainty. Possible directions for this work include investigations of calcium and sulphate adsorption in these soils, with the aim of determining the equilibrium conditions under which gypsum precipitation could take place, and field investigations of gypsum solubility during irrigation and the rainy season. The latter might potentially be carried out by burying porous containers of gypsum at different depths in the soil, and monitoring the rate of gypsum dissolution (or precipitation) by periodically determining the quantity of gypsum lost from (or added to) each container.

It should be noted, however, that even if gypsum accumulates in the upper 1.1 m of the irrigated soils, as predicted by Annandale et al. (1999), there will still be downward movement of Mg^{2+} and SO_4^{2-}, given that Mg^{2+} will continue to be more exchangeable than Ca^{2+} in the upper part of the soil profile and that the concentration of SO_4^{2-} in the irrigation water is twice that of Ca^{2+}. Furthermore, the solution which percolates from the base of a gypsiferous zone must be saturated with respect to gypsum (under equilibrium conditions), so soluble Ca^{2+} must also be present in leachate from the zone. Even if irrigation is managed such that leaching is negligible during the dry season, it is apparent from the data collected here that significant movement of the solutes added by irrigation would take place during the rainy season. In the long term, almost all of the soluble Mg^{2+}, at least half of the soluble SO_4^{2-} and some of the soluble Ca^{2+} added by irrigation must enter the groundwater system. If sustainable gyspum precipitation does not take place, then close to all of the added Mg^{2+}, Ca^{2+} and SO_4^{2-} will move into the local aquifer.

5 Conclusions

The huge volumes of mine water generated by coal mining in Mpumalanga Province, South Africa, the high potential of the province's agricultural land and the region's limited rainfall are compelling motivations for using saline mine water to irrigate crops. However, the region's agricultural and industrial importance and its low rainfall are also strong arguments in favour of the strict conservation of groundwater quality. The three goals of disposal of mine water, enhanced crop production and the protection of groundwater quality can all be reached if, as has been suggested by Annandale et al. (1999) and Barnard et al.(1998), the irrigated soils can act as sinks for the salts dissolved in saline mine water. The precipitation of gypsum is one mechanism that has been proposed for the attenuation of the salt load applied to soils irrigated with mine water (Annandale et al., 1999).

This study has considered the chemistry of soils irrigated with saline mine water at Kleinkopje Colliery, the site of ongoing field trials of mine water irrigation. Soil samples, representing entire irrigated and non-irrigated soil profiles from the surface to depths in excess of 3 m, were collected. Two natural soils (pivots Major and Four) and one rehabilitated mining area which has been backfilled with a thin (600 mm) layer of soil (pivot Tweefontein) were sampled.

5.1 A summary of the study's findings

Key results of this study are:

- Irrigated soil profiles have higher soil solution salinities, with well-defined peaks in salinity of between 1 dS/m and 2.4 dS/m in the irrigated soils and between 0.5 and 0.7 dS/m in the non-irrigated soils.

- Saturated paste extracts are undersaturated with respect to gypsum for all samples from irrigated and non-irrigated soils, as determined by saturation index calculations using PHREEQC (Parkhurst & Appelo, 1999). Subsequent

determinations of total soluble sulphate in the soils in well-equilibrated, increasingly dilute aqueous extracts, followed by a calculation of the saturation indices of these extracts could not confirm the presence of gypsum, but do not rule out the presence of very small amounts. The most likely source of soluble SO_4^{2-} in these soils is the desorption of sulphate weakly held on sesquioxide surfaces and kaolinite edge sites.

- Given that gypsum is the least soluble of the salts of the major ions in the soil solution, and gypsum is either absent from the soil samples or present in small amounts, it is likely that the activities of the major ions are controlled by reactions at charged surfaces such as cation exchange, rather than by the precipitation and dissolution of solid phases.

- Concentrations of exchangeable Ca^{2+}, Mg^{2+} and adsorbed SO_4^{2-} are higher in the irrigated soils than in the non-irrigated soils.

- The natural tendency in these soils for exchangeable Ca^{2+} to dominate cation exchange sites in the upper part of the soil profile, and exchangeable Mg^{2+} to be dominant in the lower part is exaggerated in the irrigated soils. Significantly higher ratios of exchangeable Ca^{2+} to Mg^{2+} occur in the upper 600 mm of the irrigated soils, compared with the non-irrigated soils, and much higher exchangeable Mg^{2+} concentrations are found between 1 m and 3 m in the irrigated soils.

- The generally lower concentrations of soluble cations in the saturated paste extracts deep in the profiles is in contrast to the relatively high concentrations of exchangeable cations at depth. This points to different adsorption isotherms in different parts of the profile, thus probably different cation exchange surfaces. Organic matter is probably the dominant exchange substrate in the upper part of the profile, while clay minerals are more important at depth.

- Effective cation exchange capacities (ECEC) in the irrigated soils range between 20 and 40 $mmol_c/kg$ for the irrigated soils and between 15 and 25 $mmol_c/kg$ for the non-irrigated soils.

- The soils are generally deeply leached, well-drained and acidic. The dominant clay mineral in these soils is kaolinite, with some mica and small amounts of goethite and haematite.

- The depth of occurrence of the highest concentrations of adsorbed (and soluble) sulphate appears to be associated with the transition between the saturated and unsaturated zone, pointing to the mobility of this species during the wet season.

- Exchangeable acidity is lower in the irrigated soils. Sulphate sorption may be an important cause of the observed reduction in exchangeable acidity. Conversely, higher levels of exchangeable acidity may correlate with enhanced potential for sulphate retention.

A solute mass balance (or salt balance) for the irrigated soils was estimated from the irrigation history and retained solute content of the soils. The total quantity of each solute ion applied to the soil during irrigation was calculated by integrating irrigation volume data and water quality data over the period of the irrigation experiment. It was assumed that the ammonium acetate extract results for cations, phosphate extract results for sulphate and saturated paste extracts results give a good indication of the total quantities of each ion retained by the soils. It was further assumed that the non-irrigated soils represent pre-irrigation background levels of all solutes.

The results of the salt balance calculation are different for each of the irrigated fields. In pivot Major, the quantities of solute ions retained are equivalent to those applied. In pivot Tweefontein, only a small fraction of the dissolved salts applied were retained in the 600 mm thick soil layer which caps this rehabilitated mining area. This points to solute transport by surface and subsurface flow into the drainage system, or to lower-lying parts of the field. Soil sampled in Pivot Four contains quantities of Mg^{2+} and Cl^- which exceed the quantities applied. A possible explanation for the excess of major ions retained in this sample is some kind of solute focussing mechanism. For example, the soil core may have been collected in a region corresponding to a local depression in the water table, which has caused lateral solute transport into the soil from surrounding areas. Alternatively, there may

be sufficient natural variation in the soils' ionic composition to explain the observed ion excesses.

5.2 The future chemical evolution of soils irrigated with saline mine water

It is difficult to predict, from the data at hand, whether gypsum precipitation in the irrigated soils will be a sustainable process and result in the long-term accumulation of the mineral in the soils. It is possible that gypsum does precipitate in the irrigated soils, particularly pivot Major, but it appears that flushing of the soils by rainfall during the summer dissolves gypsum formed during the irrigation season.

Whether gypsum does or does not accumulate in the soils, the soils will evolve toward a state of equilibrium with the mine water. The groundwater directly below the irrigated soils is likely to be subject to seasonal pulses of dissolved salts during the wet season, as the soils are flushed by rainfall. This will be followed by periods of low salt input during the irrigation season when leaching is kept to a minimum by irrigation management. If sustainable gypsum accumulation does occur in the soil, then quantities of leached Ca^{2+} and SO_4^{2-} will be maintained at relatively low levels, while most of the applied Mg^{2+} will eventually move into the groundwater. However, if irrigation ceases, any gypsum in the soils will gradually dissolve and its constituent Ca^{2+} and SO_4^{2-} ions will migrate into the groundwater.

The most favourable scenario for groundwater quality is one in which gypsum accumulates in the soils. The results of this study are not conclusive as to whether or not this will happen. Additional work on these soils would certainly clarify the picture. In particular, the following work is proposed:

- A careful study of calcium and sulphate adsorption in these soils to determine the conditions under which gypsum can accumulate in the presence of adsorption sites which compete for its constituent calcium and sulphate ions.

- Laboratory and field work to study the solubility of gypsum in these soils, under irrigation and natural rainfall, to establish whether gypsum is ever likely to accumulate.

In conclusion, this study has shown that there is little evidence of gypsum precipitation in these soils. Adsorption of ions onto colloid surfaces is a more important mechanism of solute retention in the soils. Irrigation with saline mine water will probably lead to the movement of significant quantities of dissolved salts into the groundwater. Most solute movement will probably take place during the seasonal flushing of the soils by rainwater. It is not known whether the rate at which the soils will release solutes into the groundwater is low enough, and the dilution effect of incoming rainwater high enough, to result in acceptably small impacts on groundwater quality. As suggested by Suarez (1989) and Oster (J.D. Oster, pers. comm., 2000) in other contexts, the best solution may be to physically stop saline leachate from irrigated fields from entering the groundwater system. This can be done by means of an engineered drainage system which collects leachate from below the root zone. This leachate could be re-used for irrigation, or disposed of in an evaporation pan. This approach may be the only way to use saline mine waters for irrigation while preserving the quality of local and regional water supplies.

6 References

AJWA, H.A. and TABATABAI, M.A. 1995. Metal-induced sulfate adsorption by soils: I. Effect of pH and ionic strength. *Soil Science.* 159(1):32-42.

AMERICAN PUBLIC HEALTH ASSOCIATION, AMERICAN WATER WORKS ASSOCIATION & WATER ENVIRONMENT FEDERATION. 1995. *Standard Methods for the examination of water and wastewater.* 19th edition. American Public Health Association. Washington DC.

ANNANDALE, J. G., JOVANOVIC, N. Z., BENADE, N. and TANNER, P. D. 1999. Modeling the long-term effect of irrigation with gypsiferous water on soil and water resources. *Agriculture, Ecosystems and Environment.* 76:109-119.

BAKER, K.D. 1976. The determination of organic carbon in soil using a probe-colorimeter. *Laboratory Practice.* 25:83-85.

BALDOCK, J.A. and NELSON, P.N. 1999. Soil organic matter, section B, chapter 2. **In:** Sumner, M.E. (Ed.). *Handbook of Soil Science.* CRC Press.Boca Raton, USA.

BARNARD, R. O., RETHMAN, N. F. G, ANNANDALE, J. G., MENTZ, W. H. and JOVANOVIC, N. Z. 1998. *The screening of crop, pasture and wetland species for tolerance of polluted water originating in coal mines.* Report to the Water Research Commission by the Department of Plant Production and Soil Science, University of Pretoria. WRC Report No. 582/1/98. Pretoria.

DAVIS, J.G. and BURGOA, B. 1995. Interactive mechanisms of anion adsorption with calcium leaching and exchange. *Soil Science.* 160(1):256-264.

DEPARTMENT OF MINES and GEOLOGICAL SURVEY. 1978. *2528 Pretoria. 1:250 000 Geological Series.* Department of Mines and Geological Survey. Pretoria.

DEPARTMENT OF WATER AFFAIRS AND FORESTRY. 1986. *Management of the water resources of the Republic of South Africa.* Department of Water Affairs and Forestry, Pretoria.

DEPARTMENT OF WATER AFFAIRS AND FORESTRY. 1995. *Geohydrological assessment of old mine workings in the Blesbokspruit catchment.* Report No. 2938/1023/1/E. Water Quality Management Series. Department of Water Affairs and Forestry. Pretoria.

DIXON, J.B. and WEED, S.B. 1989. *Minerals in Soil Environments.2nd edition.* Soil Science Society of America. Madison, Wisconsin, USA.

DREVER, J.I. 1997. *The Geochemistry of Natural Waters: Surface and Groundwater Environments. 3rd edition.* Prentice-Hall. Upper Saddle River. New Jersey. USA.

DU PLESSIS H. M. 1983. Using lime treated acid mine water for irrigation. *Water Science and Technology*. 15:145-154.

FRENKEL, H., FEY, M.V. and NOBLE, A.D. 1989. Some factors limiting the dissolution rate of phosphogypsum in acid soils. *Soil Sci.Soc.Am.J.* 53:958-961.

HALBICH, T. F. J. 1997. *The mobility of metals in acid mine drainage from abandoned coal mines.* Unpublished MSc. thesis. University of Cape Town. Cape Town.

JURINAK, J. 1990. The chemistry of salt-affected soils and waters, chapter 3. **In:** Tanji, K.K. (Ed.) *Agricultural Salinity Assessment and Management. ASCE Manuals and Reports in Engineering Practice No.71.* American Society of Civil Engineers. New York.

LEIJ, F.J. and VAN GENUCHTEN, M.Th. 1999. Solute Transport, section A, chapter 6. **In:** Sumner, M. E. (Ed.) *Handbook of Soil Science.* CRC Press. Boca Raton, USA.

LEVY, G. J. 1999. Sodicity, section G, chapter 2. **In:** Sumner, M. E. (Ed.) *Handbook of Soil Science.* CRC Press. Boca Raton, USA.

LORENTZ, S., ASCOUGH, G. and BUICK, M. 2000. *Vadose zone soil water dynamics and soil physical, hydraulic and solute transport characteristics.* Unpublished report to Water Research Commission steering committee of the mine water irrigation project. School of Bioresources Engineering and Environmental Hydrology, University of Natal.

MCBRIDE, M. B. 1994. *Environmental Chemistry of Soils.* Oxford University Press. New York and Oxford.

MCBRIDE, M. B. 1999. Chemisorption and precipitation reactions, section B, chapter 8. **In:** Sumner, M.E. (Ed.) *Handbook of Soil Science.* CRC Press. Boca Raton, USA.

MOORE, D.M. and REYNOLDS, R.C. 1997. *X-Ray Diffraction and the Identification and Analysis of Clay Minerals (Second Edition).* Oxford University Press. Oxford & New York.

MOTT, C.J.B. 1981. Anion and Ligand Exchange, chapter 5. **In:** Greenland, D.J. and Hayes, M.H.B. (Eds.) *The Chemistry of Soil Processes.* Wiley-Interscience. Chichester.

NON-AFFILIATED SOIL ANALYSIS WORK COMMITTEE. 1990. *Handbook of Standard Soil Testing Methods for Advisory Purposes.* Soil Science Society of South Africa. Pretoria.

OR, D. and WRAITH, J.M. 1999. Soil water content and water potential relationships, section A, chapter 3. **In:** Sumner, M.E. (Ed.) *Handbook of Soil Science.* CRC Press. Boca Raton, USA.

OSTER, J.D. and FRENKEL, H. 1980. The chemistry of the reclamation of sodic soils with gypsum and lime. *Soil Sci.Soc.Am.J.* 44:41-45.

PAPADOPOULOS, I. 1986. Effects of high-sulphate irrigation waters on soil salinity and yields. *Agron. J.* 78:429-432.

PAPADOPOULOS, I. 1987. Effects of residual soil salinity resulting from irrigation with sulphate waters on lettuce. *Plant & Soil.* 97:171-177.

PARKHURST, D. L. & APPELO, C. A. J. 1999. *User's Guide To Phreeqc Version 2—A Computer Program For Speciation, Batch-Reaction, One-Dimensional Transport, And Inverse Geochemical Calculations.* Water-Resources Investigations Report 99-4259. US Geological Survey, Denver, Colorado.

PAUL, O. W. 1995. *Optimizing water quality monitoring: A case study on the South African highveld.* Unpublished MSc. thesis. University of Cape Town. Cape Town.

PRETORIUS J. J. B., DOYER O. T., ANNANDALE J. G. and JOVANOVIC N. Z. 1999. *Modeling and monitoring crop production, soil properties and drainage water under centre pivot irrigation with gypsiferous mine water: Economic assessment of irrigation with gypsiferous mine water.* Unpublished progress report to the Water Research Commission. Pretoria.

REEVE, N.G. and SUMNER, M.E. 1972. Amelioration of subsoil acidity in Natal oxisols by leaching of surface-applied amendments. *Agrochemophysica.* 4:1-6.

RITCHEY, K.D. and DE SOUSA, D.M.G. 1997. Use of gypsum in management of subsoil acidity in Oxisols. **In:** Moniz, A.C., Furlani, A.M.C., Schaffert, R.E., Fageria, N.K., Rosolem, C.A. and Cantarella, H. (Eds.) *Plant-Soil Interactions at low pH: Sustainable Agriculture and Forestry Production. Proc. 4th Int.Symp. on Plant-Soil Interactions at Low pH, Belo Horizonte. Minas Gerais, Brazil, 17-24 March 1996.* Brazilian Soil Science Society. Campinas/Vicosa.

RHOADES, J.D. 1982. Soluble Salts, chapter 10. **In:** Page, A.L., Miller, R.H. and Keeney, D.R. (Eds.). *Methods of Soil Analysis, Part 2: Chemical and Microbiological Properties, Second Edition.* American Society of Agronomy, Inc. and Soil Science Society of America, Inc. Madison, Wisconsin, USA.

ROBBINS, C. H. 1991. Solute transport reactions in salt-affected soils. **In:** *Modeling Plant and Soil Systems.* Agronomy monograph No. 31. ASA-CSSA-SSSA. Madison, Wisconsin. USA.

ROWELL, D. L. 1994. *Soil Science: Methods and Applications.* Longman. UK.

SHAINBERG, I., SUMNER, M.E., MILLER, W.P., FARINA, M.P.W., PAVAN, M.A. and FEY, M.V. 1989. Use of Gypsum on Soils: A Review. *Advances in Soil Science.* 9:1-111.

SKOPP, J. 1999. Physical properties of primary particles. Chapter 1 in Sumner. M. E. (Ed.) , *Handbook of Soil Science*. CRC Press. Boca Raton.

SOIL AND IRRIGATION RESEARCH INSTITUTE. 1979. *2628 East Rand. 1:250 000 Land Type series.* Department of Agricultural Technical Services and Soil and Irrigation Research Institute. Pretoria.

SOIL CLASSIFICATION WORKING GROUP. 1991. Soil Classification: A Taxonomic System for South Africa. *Memoirs Agric. Nat. Resour. S. A. No. 15.* Soil and Irrigation Research Institute, Department of Agricultural Development. Pretoria, South Africa.

SPOSITO, G. 1989. *The Chemistry of Soils.* Oxford University Press. New York.

STUMM, W. and MORGAN, J.J. 1996. *Aquatic Chemistry: Chemical Equilibria and Rates in Natural Waters. 3rd edition.* Wiley-Interscience. New York.

SUAREZ, D.L. 1989. Impact of agricultural practices on groundwater salinity. *Agriculture, Ecosystems and Environment*. 26:215-227.

SUMNER, M. E. 1993. Gypsum and acid soils: the world scene. *Advances in Agronomy*. 51:1-32.

TABATABAI, M.A. 1982. Sulphur, chapter 28. **In:** Page, A.L., Miller, R.H. and Keeney, D.R. (Eds.). *Methods of Soil Analysis, Part 2: Chemical and Microbiological Properties, Second Edition.* American Society of Agronomy, Inc. and Soil Science Society of America, Inc. Madison, Wisconsin, USA.

TANJI, K.K. 1990. Nature and extent of agricultural salinity, chapter 1. **In:** Tanji, K.K. (Ed.) *Agricultural Salinity Assessment and Management. ASCE Manuals and Reports in Engineering Practice No.71.* American Society of Civil Engineers. New York.

THELLIER, C., SPOSITO, G. and HOLTZCLAW, K.M. 1990. Chemical effects of saline irrigation water on a San Joaquin Valley soil: I. Column studies. *J.Environ.Qual.* 19:50-55.

THOMAS, G.W. 1982. Exchangeable cations, chapter 9. **In:** Page, A.L., Miller, R.H. and Keeney, D.R. (Eds.). *Methods of Soil Analysis, Part 2: Chemical and Microbiological Properties, Second Edition.* American Society of Agronomy, Inc. and Soil Science Society of America, Inc. Madison, Wisconsin, USA.

TOMA, M. , SUMNER, M. E. , WEEKS, G. and SAIGUSA, M. 1999. Long-term effects of gypsum on crop yield and subsoil chemical properties. *Soil Science Society of America Journal.* 39:891-895.

VAN DEN ENDE, J. 1991. Supersaturation of soil solutions with respect to gypsum. *Plant and Soil.* 133:65-74.

WANG, H. L., HEDLEY, M. J., BOLAN, N. S. and HORNE, D. J. 1999. The influence of surface incorporated lime and gypsiferous by-products on surface and subsurface soil acidity. I. Soil solution chemistry. *Aust. J. Soil. Res.* 37:165-180.

Appendix A – Analytical Results

The results of all analytical work are presented in the following tables, along with, in most cases, an estimation of analytical precision. Data for some depth intervals is missing – the samples for these depth intervals were not analysed in this study. A result which is below analytical detection limits is indicated as "bdl".

Table A1: Soil pH in saturated pastes

Core position	Depth interval (mm)	Soil pH	Core position	Depth interval (mm)	Soil pH
Pivot Major	0-200	5.7	Pivot Major	0-300	4.9
(irrigated to field	200-420	4.5	(not irrigated)	300-600	4.7
capacity)	420-600	4.7	Core PM4	600-900	
Core PM2	600-900			900-1200	4.8
	900-1100	5.7		1200-1500	5.0
	1100-1300			1500-1800	
	1300-1500	5.3		1800-2100	5.8
	1500-1800			2100-2400	
	1800-2100	5.3		2400-2700	
	2100-2400			2700-3000	5.7
	2400-2700				
	2700-3000	5.5			
Pivot Four	0-300	5.4	Pivot Four	0-300	5.0
(irrigated to field	300-600	5.0	(not irrigated)	300-600	5.9
capacity)	600-900		Core PF4	600-900	
Core PF2	900-1200	4.8		900-1200	5.5
	1200-1500			1200-1500	
	1500-1800	5.6		1500-1800	5.6
	1800-2100			1800-2100	
	2100-2400	5.1		2100-2400	5.7
	2400-2700			2400-2700	
	2700-3000	5.8		2700-3000	5.8
	3000-3300	5.7		3000-3300	5.6
Pivot Tweefontein	0-300	4.9	Pivot Tweefontein	0-300	5.1
(rrigated to field	300-600	5.5	(not irrigated)	300-600	5.6
capacity)			Core PT2		
Core PT1					

Table A2: Soil pH in 1 M KCl (1:2.5) suspensions

Core position	Depth interval (mm)	Soil pH	Core position	Depth interval (mm)	Soil pH
Pivot Major	0-200	5.0	Pivot Major	0-300	4.2
(irrigated to field	200-420	3.9	(not irrigated)	300-600	3.9
capacity)	420-600	4.2	Core PM4	600-900	
Core PM2	600-900			900-1200	4.1
	900-1100	4.8		1200-1500	4.4
	1100-1300			1500-1800	
	1300-1500	4.5		1800-2100	4.5
	1500-1800			2100-2400	
	1800-2100	4.5		2400-2700	
	2100-2400			2700-3000	4.9
	2400-2700				
	2700-3000	4.6			
Pivot Four	0-300	4.6	Pivot Four	0-300	4.1
(irrigated to field	300-600	4.1	(not irrigated)	300-600	5.0
capacity)	600-900		Core PF4	600-900	
Core PF2	900-1200	4.1		900-1200	4.5
	1200-1500			1200-1500	
	1500-1800	4.7		1500-1800	4.4
	1800-2100			1800-2100	
	2100-2400	4.4		2100-2400	4.2
	2400-2700			2400-2700	
	2700-3000	4.4		2700-3000	4.2
	3000-3300	4.8		3000-3300	4.3
Pivot Tweefontein	0-300	4.8	Pivot Tweefontein	0-300	4.4
(irrigated to field	300-600	4.3	(not irrigated)	300-600	4.8
capacity)			Core PT2		
Core PT1					

Duplicate analyses for estimation of analytical precision

Sample	Result 1 Soil pH	Result 2 Soil pH	R
PM4 1200-1500 mm	4.38	4.38	0.00
PT2 300-600mm	4.79	4.79	0.00
PF2 2100-2400 mm	4.40	3.38	0.02
PF4 300-600 mm	4.98	4.89	0.09

Largest value of R taken as estimate of precision, i.e. Soil pH = stated value ± 0.09

Table A3: Soil pH in water (1:2.5) suspensions

Core position	Depth interval (mm)	Soil pH	Core position	Depth interval (mm)	Soil pH
Pivot Major	0-200	6.0	Pivot Major	0-300	7.2
(irrigated to field	200-420	5.8	(not irrigated)	300-600	6.8
capacity)	420-600	5.6	Core PM4	600-900	
Core PM2	600-900			900-1200	6.7
	900-1100	6.9		1200-1500	7.3
	1100-1300			1500-1800	
	1300-1500	6.1		1800-2100	8.3
	1500-1800			2100-2400	
	1800-2100	7.2		2400-2700	
	2100-2400			2700-3000	8.4
	2400-2700				
	2700-3000	7.3			
Pivot Four	0-300	7.2	Pivot Four	0-300	7.2
(irrigated to field	300-600	6.9	(not irrigated)	300-600	7.8
capacity)	600-900		Core PF4	600-900	
Core PF2	900-1200	6.3		900-1200	7.5
	1200-1500			1200-1500	
	1500-1800	6.8		1500-1800	8.0
	1800-2100			1800-2100	
	2100-2400	7.1		2100-2400	8.1
	2400-2700			2400-2700	
	2700-3000	8.4		2700-3000	7.1
	3000-3300	7.9		3000-3300	8.0
Pivot Tweefontein	0-300	6.5	Pivot Tweefontein	0-300	6.9
(irrigated to field	300-600	6.2	(not irrigated)	300-600	7.4
capacity)			Core PT2		
Core PT1					

Duplicate analyses for estimation of analytical precision

Sample	Result 1 Soil pH	Result 2 Soil pH	R
PM4 1200-1500 mm	7.34	7.30	0.04
PT2 300-600mm	7.10	7.22	0.12
PF2 2100-2400 mm	7.81	7.99	0.18
PF4 300-600 mm	7.44	7.39	0.05

Largest value of R taken as estimate of precision, i.e. Soil pH = stated value ± 0.18

Table A4: Electrical conductivity of saturated paste extracts

Core position	Depth interval (mm)	dS/m	Core position	Depth interval (mm)	dS/m
Pivot Major	0-200	1.095	Pivot Major	0-300	0.496
(irrigated to field	200-420	1.772	(not irrigated)	300-600	0.286
capacity)	420-600	2.440	Core PM4	600-900	
Core PM2	600-900			900-1200	0.560
	900-1100	0.661		1200-1500	0.552
	1100-1300			1500-1800	
	1300-1500	0.382		1800-2100	0.095
	1500-1800			2100-2400	
	1800-2100	0.384		2400-2700	
	2100-2400			2700-3000	0.154
	2400-2700				
	2700-3000	0.318			
Pivot Four	0-300	0.414	Pivot Four	0-300	0.748
(irrigated to field	300-600	0.503	(not irrigated)	300-600	0.244
capacity)	600-900		Core PF4	600-900	
Core PF2	900-1200	0.738		900-1200	0.260
	1200-1500			1200-1500	
	1500-1800	1.081		1500-1800	0.125
	1800-2100			1800-2100	
	2100-2400	0.604		2100-2400	0.080
	2400-2700			2400-2700	
	2700-3000	0.609		2700-3000	0.062
	3000-3300	0.130		3000-3300	0.105
Pivot Tweefontein	0-300	1.296	Pivot Tweefontein	0-300	0.253
(irrigated to field	300-600	1.993	(not irrigated)	300-600	0.317
capacity)			Core PT2		
Core PT1					

Table A5: Ca^{2+} ion concentration of saturated paste extracts

Core position	Depth interval (mm)	$mmol_c/kg$	Core position	Depth interval (mm)	$mmol_c/kg$
Pivot Major	0-200	5.2	Pivot Major	0-300	0.7
(irrigated to field	200-420	8.0	(not irrigated)	300-600	0.3
capacity)	420-600	9.3	Core PM4	600-900	
Core PM2	600-900			900-1200	0.6
	900-1100	2.0		1200-1500	0.5
	1100-1300			1500-1800	
	1300-1500	0.7		1800-2100	0.03
	1500-1800			2100-2400	
	1800-2100	0.8		2400-2700	
	2100-2400			2700-3000	0.1
	2400-2700				
	2700-3000	0.6			
Pivot Four	0-300	0.4	Pivot Four	0-300	0.7
(irrigated to field	300-600	1.0	(not irrigated)	300-600	0.2
capacity)	600-900		Core PF4	600-900	
Core PF2	900-1200	1.6		900-1200	0.4
	1200-1500			1200-1500	
	1500-1800	2.3		1500-1800	0.1
	1800-2100			1800-2100	
	2100-2400	1.5		2100-2400	0.04
	2400-2700			2400-2700	
	2700-3000	1.5		2700-3000	0.04
	3000-3300	0.3		3000-3300	0.06
Pivot Tweefontein	0-300	2.3	Pivot Tweefontein	0-300	0.2
(irrigated to field	300-600	2.5	(not irrigated)	300-600	0.3
capacity)			Core PT2		
Core PT1					

Duplicate analyses for estimation of analytical precision

Sample	Result 1 (Ca mg/l)	Result 2 (Ca mg/l)	R	Relative R
PF2,2700-3000 mm	93.8	108.8	15.0	0.148
PT1,0-300mm	237.4	212.2	25.2	0.112
T1(Dam water)	597.0	682.0	85.0	0.133
PT1,300-600mm	293.2	256.4	36.8	0.134
		Mean:	40.5	0.132
		Std.dev:		0.117 (r.s.d)
		95% Conf. interval :		16 %

Table A6: Mg^{2+} ion concentration of saturated paste extracts

Core position	Depth interval (mm)	$mmol_c$ /kg	Core position	Depth interval (mm)	$mmol_c$ /kg
Pivot Major	0-200	0.7	Pivot Major	0-300	0.3
(irrigated to field	200-420	3.3	(not irrigated)	300-600	0.1
capacity)	420-600	3.5	Core PM4	600-900	
Core PM2	600-900			900-1200	0.9
	900-1100	1.2		1200-1500	0.2
	1100-1300			1500-1800	
	1300-1500	0.5		1800-2100	0.0
	1500-1800			2100-2400	
	1800-2100	0.8		2400-2700	
	2100-2400			2700-3000	0.1
	2400-2700				
	2700-3000	0.6			
Pivot Four	0-300	0.4	Pivot Four	0-300	0.5
(irrigated to field	300-600	0.6	(not irrigated)	300-600	0.2
capacity)	600-900		Core PF4	600-900	
Core PF2	900-1200	1.0		900-1200	0.1
	1200-1500			1200-1500	
	1500-1800	1.6		1500-1800	0.1
	1800-2100			1800-2100	
	2100-2400	1.0		2100-2400	0.0
	2400-2700			2400-2700	
	2700-3000	1.0		2700-3000	0.0
	3000-3300	0.1		3000-3300	0.0
Pivot Tweefontein	0-300	0.4	Pivot Tweefontein	0-300	0.1
(irrigated to field	300-600	2.2	(not irrigated)	300-600	0.2
capacity)			Core PT2		
Core PT1					

Duplicate analyses for estimation of analytical precision

Sample	Result 1 Mg(mg/l)	Result 2 Mg (mg/l)	R	Relative R
PF2,2700-3000 mm	35.8	42.8	7.0	0.18
PT1,0-300mm	27.2	26.8	0.4	0.01
T1(Dam water)	353.0	380.0	27.0	0.07
PT1,300-600mm	159.6	157.2	2.4	0.02
		Mean:		0.07
		Std.dev:		0.06 (r.s.d)
		95% Conf. interval :		9 %

Table A7: SO_4^{2-} ion concentration of saturated paste extracts

Core position	Depth interval (mm)	$mmol_c$ /kg	Core position	Depth interval (mm)	$mmol_c$ /kg
Pivot Major	0-200	3.77	Pivot Major	0-300	0.17
(irrigated to field	200-420	5.76	(not irrigated)	300-600	0.14
capacity)	420-600	6.02	Core PM4	600-900	
Core PM2	600-900			900-1200	0.24
	900-1100	1.59		1200-1500	0.19
	1100-1300			1500-1800	
	1300-1500	0.67		1800-2100	0.00
	1500-1800			2100-2400	
	1800-2100	0.98		2400-2700	
	2100-2400			2700-3000	0.15
	2400-2700				
	2700-3000	0.62			
Pivot Four	0-300	0.34	Pivot Four	0-300	0.16
(irrigated to field	300-600	0.78	(not irrigated)	300-600	0.14
capacity)	600-900		Core PF4	600-900	
Core PF2	900-1200	1.02		900-1200	0.14
	1200-1500			1200-1500	
	1500-1800	2.74		1500-1800	0.02
	1800-2100			1800-2100	
	2100-2400	0.34		2100-2400	0.01
	2400-2700			2400-2700	
	2700-3000	0.42		2700-3000	0.01
	3000-3300	0.08		3000-3300	0.01
Pivot Tweefontein	0-300	2.32	Pivot Tweefontein	0-300	0.30
(irrigated to field capacity) Core PT1	300-600	3.60	(not irrigated) Core PT2	300-600	0.42

Duplicate analyses for estimation of analytical precision

Sample	Result 1 SO_4^{2-} (mg/l)	Result 2 SO_4^{2-} (mg/l)	R	Relative R
PF2,2700-3000 mm	62.6	58.8	3.5	0.06
PT1,0-300mm	565.5	561.0	4.5	0.01
T1(Dam water)	2122.9	2196.1	73.2	0.03
PT1,300-600mm	1010.9	967.0	43.9	0.04
		Mean:		0.04
		Std.dev:		0.03 (r.s.d)
		95% Conf. interval :		5 %

Table A8: Na^+ ion concentration of saturated paste extracts

Core position	Depth interval (mm)	$mmol_e$ /kg	Core position	Depth interval (mm)	$mmol_e$ /kg
Pivot Major	0-200	1.82	Pivot Major	0-300	0.07
(irrigated to field	200-420	3.55	(not irrigated)	300-600	0.24
capacity)	420-600	4.22	Core PM4	600-900	
Core PM2	600-900			900-1200	0.15
	900-1100	0.89		1200-1500	0.76
	1100-1300			1500-1800	
	1300-1500	0.58		1800-2100	0.12
	1500-1800			2100-2400	
	1800-2100	0.70		2400-2700	
	2100-2400			2700-3000	0.27
	2400-2700				
	2700-3000	0.62			
Pivot Four	0-300	0.18	Pivot Four	0-300	0.14
(irrigated to field	300-600	0.45	(not irrigated)	300-600	0.18
capacity)	600-900		Core PF4	600-900	
Core PF2	900-1200	0.94		900-1200	0.15
	1200-1500			1200-1500	
	1500-1800	0.23		1500-1800	0.15
	1800-2100			1800-2100	
	2100-2400	0.91		2100-2400	0.12
	2400-2700			2400-2700	
	2700-3000	1.16		2700-3000	0.12
	3000-3300	0.38		3000-3300	0.13
Pivot Tweefontein	0-300	0.24	Pivot Tweefontein	0-300	0.15
(irrigated to field capacity) Core PT1	300-600	0.27	(not irrigated) Core PT2	300-600	0.14

Duplicate analyses for estimation of analytical precision

Sample	Result 1 Na^+(mg/l)	Result 2 Na^+(mg/l)	R	Relative R
PF2,2700-3000 mm	84.8	80.0	4.8	0.06
PT1,0-300mm	28.0	29.0	1.0	0.03
T1(Dam water)	307.0	296.0	11.0	0.04
PT1,300-600mm	34.4	37.2	2.8	0.08
		Mean:		0.05
		Std.dev:		0.05(r.s.d.)
		95% Conf. interval :		6 %

Table A9: Cl^- ion concentration of saturated paste extracts

Core position	Depth interval (mm)	$mmol_c$ /kg	Core position	Depth interval (mm)	$mmol_c$ /kg
Pivot Major	0-200	1.3	Pivot Major	0-300	0.1
(irrigated to field	200-420	2.7	(not irrigated)	300-600	0.2
capacity)	420-600	3.3	Core PM4	600-900	
Core PM2	600-900			900-1200	0.1
	900-1100	0.7		1200-1500	0.6
	1100-1300			1500-1800	
	1300-1500	0.4		1800-2100	0.1
	1500-1800			2100-2400	
	1800-2100	0.5		2400-2700	
	2100-2400			2700-3000	0.3
	2400-2700				
	2700-3000	0.4			
Pivot Four	0-300	0.2	Pivot Four	0-300	0.8
(irrigated to field	300-600	0.3	(not irrigated)	300-600	0.2
capacity)	600-900		Core PF4	600-900	
Core PF2	900-1200	0.6		900-1200	0.1
	1200-1500			1200-1500	
	1500-1800	0.1		1500-1800	0.1
	1800-2100			1800-2100	
	2100-2400	1.2		2100-2400	0.1
	2400-2700			2400-2700	
	2700-3000	1.4		2700-3000	0.0
	3000-3300	1.3		3000-3300	0.1
Pivot Tweefontein	0-300	0.1	Pivot Tweefontein	0-300	0.1
(irrigated to field capacity) Core PT1	300-600	0.1	(not irrigated) Core PT2	300-600	0.1

Duplicate analyses for estimation of analytical precision

Sample	Result 1 Cl^-(mg/l)	Result 2 Cl^-(mg/l)	R	Relative R
PF2,2700-3000 mm	151.2	145.2	5.9	0.04
PT1,0-300mm	24.9	23.9	1.0	0.04
T1(Dam water)	288.2	302.3	17.1	0.06
PT1,300-600mm	13.9	18.3	4.4	0.27
		Mean:		0.10
		Std.dev:		0.09 (r.s.d)
		95% Conf. interval :		13 %

Table A10: NO_3^- ion concentration of saturated paste extracts

Core position	Depth interval (mm)	$mmol_c$ /kg	Core position	Depth interval (mm)	$mmol_c$ /kg
Pivot Major	0-200	0.1	Pivot Major	0-300	0.6
(irrigated to field	200-420	0.2	(not irrigated)	300-600	0.1
capacity)	420-600	1.0	Core PM4	600-900	
Core PM2	600-900			900-1200	0.9
	900-1100	0.3		1200-1500	0.0
	1100-1300			1500-1800	
	1300-1500	0.2		1800-2100	0.2
	1500-1800			2100-2400	
	1800-2100	0.2		2400-2700	
	2100-2400			2700-3000	0.0
	2400-2700				
	2700-3000	0.2			
Pivot Four	0-300	0.1	Pivot Four	0-300	0.7
(irrigated to field	300-600	0.1	(not irrigated)	300-600	0.2
capacity)	600-900		Core PF4	600-900	
Core PF2	900-1200	0.2		900-1200	0.4
	1200-1500			1200-1500	
	1500-1800	0.1		1500-1800	0.1
	1800-2100			1800-2100	
	2100-2400	0.5		2100-2400	0.0
	2400-2700			2400-2700	
	2700-3000	0.6		2700-3000	0.0
	3000-3300	0.1		3000-3300	0.1
Pivot Tweefontein	0-300	0.1	Pivot Tweefontein	0-300	0.1
(irrigated to field capacity) Core PT1	300-600	0.1	(not irrigated) Core PT2	300-600	0.1

Duplicate analyses for estimation of analytical precision

Sample	Result 1 NO_3^-(mg/l)	Result 2 NO_3^-(mg/l)	R	Relative R
PF2,2700-3000 mm	109.4	104.9	4.6	0.04
PT1,0-300mm	33.9	30.9	3.0	0.09
T1(Dam water)	12.7	8.8	3.9	0.36
PT1,300-600mm	49.6	46.9	2.7	0.06
		Mean:		0.14
		Std.dev:		0.12(r.s.d.)
		95% Conf. interval :		17 %

Table A11: K^+ ion concentration of saturated paste extracts

Core position	Depth interval (mm)	$mmol_c$ /kg	Core position	Depth interval (mm)	$mmol_c$ /kg
Pivot Major	0-200	0.1	Pivot Major	0-300	0.1
(irrigated to field	200-420	0.0	(not irrigated)	300-600	0.0
capacity)	420-600	0.3	Core PM4	600-900	
Core PM2	600-900			900-1200	0.1
	900-1100	0.1		1200-1500	0.0
	1100-1300			1500-1800	
	1300-1500	0.1		1800-2100	0.0
	1500-1800			2100-2400	
	1800-2100	0.1		2400-2700	
	2100-2400			2700-3000	0.0
	2400-2700				
	2700-3000	0.1			
Pivot Four	0-300	0.1	Pivot Four	0-300	0.3
(irrigated to field	300-600	0.0	(not irrigated)	300-600	0.0
capacity)	600-900		Core PF4	600-900	
Core PF2	900-1200	0.0		900-1200	0.0
	1200-1500			1200-1500	
	1500-1800	0.0		1500-1800	0.0
	1800-2100			1800-2100	
	2100-2400	0.0		2100-2400	0.0
	2400-2700			2400-2700	
	2700-3000	0.0		2700-3000	0.0
	3000-3300	0.0		3000-3300	0.0
Pivot Tweefontein	0-300	0.1	Pivot Tweefontein	0-300	0.0
(irrigated to field capacity) Core PT1	300-600	0.1	(not irrigated) Core PT2	300-600	0.0

Duplicate analyses for estimation of analytical precision

Sample	Result 1 K^+(mg/l)	Result 2 K^+(mg/l)	R	Relative R
PF2,2700-3000 mm	3.8	3.2	0.6	0.17
PT1,0-300mm	22.6	22.4	0.2	0.01
T1(Dam water)	34.0	22.0	12.0	0.43
PT1,300-600mm	12.4	12.4	0.0	0.00
		Mean:		0.15
		Std.dev:		0.13
		95% Conf. interval :		19 %

Table A12: NH_4^+ concentration of saturated paste extracts

Core position	Depth interval (mm)	$mmol_c/kg$	Core position	Depth interval (mm)	$mmol_c/kg$
Pivot Major	0-200	0.00	Pivot Major	0-300	0.09
(irrigated to field	200-420	0.44	(not irrigated)	300-600	0.01
capacity)	420-600	0.00	Core PM4	600-900	
Core PM2	600-900			900-1200	0.08
	900-1100	0.00		1200-1500	0.00
	1100-1300			1500-1800	
	1300-1500	0.04		1800-2100	0.06
	1500-1800			2100-2400	
	1800-2100	0.06		2400-2700	
	2100-2400			2700-3000	0.00
	2400-2700				
	2700-3000	0.04			
Pivot Four	0-300	0.02	Pivot Four	0-300	0.02
(irrigated to field	300-600	0.00	(not irrigated)	300-600	0.00
capacity)	600-900		Core PF4	600-900	
Core PF2	900-1200	0.00		900-1200	0.00
	1200-1500			1200-1500	
	1500-1800	0.03		1500-1800	0.00
	1800-2100			1800-2100	
	2100-2400	0.09		2100-2400	0.00
	2400-2700			2400-2700	
	2700-3000	0.00		2700-3000	0.00
	3000-3300	0.00		3000-3300	0.00
Pivot Tweefontein	0-300	0.00	Pivot Tweefontein	0-300	0.00
(irrigated to field	300-600	0.00	(not irrigated)	300-600	0.00
capacity)			Core PT2		
Core PT1					

Table A13: Alkalinity of saturated paste extracts

Core position	Depth interval (mm)	$mmol_c/kg$	Core position	Depth interval (mm)	$mmol_c/kg$
Pivot Major	0-200	0.2	Pivot Major	0-300	0.1
(irrigated to field	200-420	0.0	(not irrigated)	300-600	
capacity)	420-600	0.0	Core PM4	600-900	
Core PM2	600-900			900-1200	
	900-1100			1200-1500	0.1
	1100-1300			1500-1800	
	1300-1500	0.1		1800-2100	
	1500-1800			2100-2400	
	1800-2100			2400-2700	
	2100-2400			2700-3000	0.1
	2400-2700				
	2700-3000	0.1			
Pivot Four	0-300	0.1	Pivot Four	0-300	0.0
(irrigated to field	300-600	0.0	(not irrigated)	300-600	
capacity)	600-900		Core PF4	600-900	
Core PF2	900-1200			900-1200	
	1200-1500			1200-1500	
	1500-1800	0.1		1500-1800	0.1
	1800-2100			1800-2100	
	2100-2400			2100-2400	
	2400-2700			2400-2700	
	2700-3000	0.1		2700-3000	0.0
	3000-3300			3000-3300	
Pivot Tweefontein	0-300	0.0	Pivot Tweefontein	0-300	
(irrigated to field	300-600	0.0	(not irrigated)	300-600	0.0
capacity)			Core PT2		
Core PT1					

Duplicate analyses for estimation of analytical precision

Sample	Result 1 (mmol/l)	Result 2 (mmol/l)	R	Relative R
PM2, 400-600 mm	0.077	0.082	0.005	0.06
PT1, 0-300 mm	0.112	0.176	0.064	0.40
PF2, 2700-3000 mm	0.138	0.178	0.040	0.25
		Mean:		0.25
		Std.dev:		0.22
		95% Conf. interval :		32 %

Table A14: Soluble organic carbon in saturated paste extracts

Core position	Depth interval (mm)	mg/kg	Core position	Depth interval (mm)	mg/kg
Pivot Major	0-200	26.3	Pivot Major	0-300	11.6
(irrigated to field	200-420	19.0	(not irrigated)	300-600	
capacity)	420-600	15.0	Core PM4	600-900	
Core PM2	600-900			900-1200	
	900-1100			1200-1500	5.1
	1100-1300			1500-1800	
	1300-1500	6.6		1800-2100	
	1500-1800			2100-2400	
	1800-2100			2400-2700	
	2100-2400			2700-3000	5.5
	2400-2700	7.0			
	2700-3000				
Pivot Four	0-300	12.3	Pivot Four	0-300	8.6
(irrigated to field	300-600	13.0	(not irrigated)	300-600	
capacity)	600-900		Core PF4	600-900	
Core PF2	900-1200			900-1200	
	1200-1500			1200-1500	
	1500-1800	7.7		1500-1800	4.6
	1800-2100			1800-2100	
	2100-2400			2100-2400	
	2400-2700			2400-2700	
	2700-3000	4.6		2700-3000	4.0
	3000-3300			3000-3300	
Pivot Tweefontein	0-300	5.1	Pivot Tweefontein	0-300	
(irrigated to field	300-600	6.2	(not irrigated)	300-600	5.2
capacity)			Core PT2		
Core PT1					

Duplicate analyses for estimation of analytical precision

Sample	Result 1 mg/l	Result 2 mg/l	R	Relative R
PM2, 400-600 mm	72.0	72.0	0	0.0
PT1, 0-300 mm	22.8	29.6	6.6	0.25
PF2, 2700-3000 mm	13.8	14.4	0.6	0.04
		Mean:	2.4	0.10
		Std.dev:	2.1	0.09
		95% Conf. interval :		12 %

Table A15: Gypsum saturation indices of saturated paste extracts

Core position	Depth interval (mm)	
Pivot Major (irrigated to field capacity) Core PM2	0-200	-0.5
	200-420	-0.2
	420-600	-0.2
	600-900	
	900-1100	-1.1
	1100-1300	-1.8
	1300-1500	
	1500-1800	-1.8
	1800-2100	
	2100-2400	
	2400-2700	-2.0
	2700-3000	
Pivot Four (irrigated to field capacity) Core PF2	0-300	-2.0
	300-600	-1.4
	600-900	
	900-1200	-1.3
	1200-1500	
	1500-1800	-0.9
	1800-2100	
	2100-2400	-1.8
	2400-2700	
	2700-3000	-1.8
	3000-3300	-2.9
Pivot Tweefontein (irrigated to field capacity) Core PT1	0-300	-0.6
	300-600	-0.4

Table A16: Sulphate in increasingly dilute soil extracts

Sample: PM2, 200-400 mm
Soil:Water ratio

$mmol_c/kg$ soil	1:1	1:2	1:5	1:10	1:20
SO_4^{2-}	6.5	7.0	8.1	9.0	9.0

Sample: PM2, 400-600 mm
Soil:Water ratio

$mmol_c/kg$ soil	1:1	1:2	1:5	1:10	1:20
Ca^{2+}	6.4	6.6	7.8	7.4	9.8
Mg^{2+}	2.9	3.0	3.5	3.4	4.2
SO_4^{2-}	**6.5**	**7.2**	**8.3**	**9.4**	**9.4**
Na^{+}	1.3	1.2	1.3	1.5	1.6
K^{+}	0.5	0.6	0.8	0.9	#
Cl^{-}	0.9	0.9	1.1	1.1	1.2
NO_3^{-}	1.3	1.3	1.2	1.2	1.2
Gypsum saturation index	**-1**	**-1.4**	**-1.92**	**-2.4**	**-2.8**

- result missing

Table A17: Total organic carbon

Core position	Depth interval (mm)	Organic carbon (weight %)	Core position	Depth interval (mm)	Organic carbon (weight %)
Pivot Major	0-200	0.83	Pivot Major	0-300	0.65
(irrigated to field	200-420	0.25	(not irrigated)	300-600	0.33
capacity)	420-600	0.48	Core PM4	600-900	
Core PM2	600-900			900-1200	0.34
	900-1100	0.26		1200-1500	0.21
	1100-1300			1500-1800	
	1300-1500	0.09		1800-2100	0.08
	1500-1800			2100-2400	
	1800-2100	0.10		2400-2700	
	2100-2400			2700-3000	0.09
	2400-2700				
	2700-3000	0.12			
Pivot Four	0-300	0.50	Pivot Four	0-300	0.47
(irrigated to field	300-600	0.20	(not irrigated)	300-600	0.26
capacity)	600-900		Core PF4	600-900	
Core PF2	900-1200	0.12		900-1200	0.10
	1200-1500			1200-1500	
	1500-1800	0.10		1500-1800	0.10
	1800-2100			1800-2100	
	2100-2400	0.09		2100-2400	0.03
	2400-2700			2400-2700	
	2700-3000	0.00		2700-3000	0.03
	3000-3300	0.05		3000-3300	0.04
Pivot Tweefontein	0-300	0.32	Pivot Tweefontein	0-300	0.18
(irrigated to field	300-600	0.26	(not irrigated)	300-600	0.10
capacity)			Core PT2		
Core PT1					

Duplicate analyses for estimation of analytical precision

Sample	Result 1 (% C)	Result 2 (% C)	R	Relative R
PM2, 1800-2100mm	0.10	0.09	0.01	
PF2,0-300mm	0.50	0.46	0.04	
PF4,300-600mm	0.26	0.19	0.07	
PF4,900-1200mm	0.10	0.11	0.01	
		Mean:	0.03	
		Std.dev:	0.03	
		95% Conf. interval :	4 %	

Table A18: 0.1M Ammonium acetate extractable Ca^{2+}

Core position	Depth interval (mm)	$mmol_c/kg$	Core position	Depth interval (mm)	$mmol_c/kg$
Pivot Major	0-200	31.3	Pivot Major	0-300	11.6
(irrigated to field	200-420	9.6	(not irrigated)	300-600	5.7
capacity)	420-600	15.4	Core PM4	600-900	
Core PM2	600-900			900-1200	5.3
	900-1100	10.8		1200-1500	3.5
	1100-1300			1500-1800	
	1300-1500	8.8		1800-2100	5.0
	1500-1800			2100-2400	
	1800-2100	10.4		2400-2700	
	2100-2400			2700-3000	7.2
	2400-2700				
	2700-3000	8.1			
Pivot Four	0-300	12.0	Pivot Four	0-300	10.9
(irrigated to field	300-600	8.9	(not irrigated)	300-600	15.9
capacity)	600-900		Core PF4	600-900	
Core PF2	900-1200	6.5		900-1200	
	1200-1500			1200-1500	
	1500-1800	13.6		1500-1800	3.9
	1800-2100			1800-2100	
	2100-2400	8.7		2100-2400	2.9
	2400-2700			2400-2700	
	2700-3000	7.5		2700-3000	4.2
	3000-3300	9.1		3000-3300	5.0
Pivot Tweefontein	0-300	20.7	Pivot Tweefontein	0-300	6.8
(irrigated to field	300-600	13.2	(not irrigated)	300-600	7.7
capacity)			Core PT2		
Core PT1					

Duplicate analyses for estimation of analytical precision

Sample	Result 1 ($mmol_c/kg$)	Result 2 ($mmol_c/kg$)	R	Relative R
PM2 400-600 mm	16.77	14.32	2.44	0.16
PM2 1300-1500 mm	8.78	8.83	0.05	0.005
PM4 1800-2100 mm	4.99	5.09	0.10	0.02
PM4 300-600 mm	5.74	7.63	1.89	0.28
PF4 2100-2400 mm	2.58	3.19	0.61	0.21
		Mean:	1.02	0.14
		Std.dev:	0.90	0.12
		95% Conf. interval :	1.28	17 %

Table A19: 0.1M Ammonium acetate extractable Mg^{2+}

Core position	Depth interval (mm)	$mmol_c/kg$	Core position	Depth interval (mm)	$mmol_c/kg$
Pivot Major	0-200	1.3	Pivot Major	0-300	2.2
(irrigated to field	200-420	3.5	(not irrigated)	300-600	11.1
capacity)	420-600	3.8	Core PM4	600-900	
Core PM2	600-900			900-1200	4.7
	900-1100	7.4		1200-1500	5.9
	1100-1300			1500-1800	
	1300-1500	11.5		1800-2100	6.3
	1500-1800			2100-2400	
	1800-2100	17.1		2400-2700	
	2100-2400			2700-3000	6.4
	2400-2700				
	2700-3000	10.9			
Pivot Four	0-300	5.6	Pivot Four	0-300	4.4
(irrigated to field	300-600	4.1	(not irrigated)	300-600	4.6
capacity)	600-900		Core PF4	600-900	
Core PF2	900-1200	5.5		900-1200	
	1200-1500			1200-1500	
	1500-1800	6.3		1500-1800	2.0
	1800-2100			1800-2100	
	2100-2400	6.0		2100-2400	2.5
	2400-2700			2400-2700	
	2700-3000	9.3		2700-3000	6.0
	3000-3300	11.1		3000-3300	6.6
Pivot Tweefontein	0-300	2.2	Pivot Tweefontein	0-300	2.4
(irrigated to field	300-600	8.3	(not irrigated)	300-600	2.7
capacity)			Core PT2		
Core PT1					

Duplicate analyses for estimation of analytical precision

Sample	Result 1 ($mmol_c/kg$)	Result 2 ($mmol_c/kg$)	R	Relative R
PM2 400-600 mm	3.70	3.85	0.15	0.04
PM2 1300-1500 mm	11.67	11.35	0.31	0.03
PM4 1800-2100 mm	6.26	6.40	0.14	0.02
PF4 2100-2400 mm	2.59	2.43	0.16	0.06
		Mean:	0.19	0.04
		Std.dev:	0.17	0.03
		95% Conf. interval :	0.24	5 %

Table A20: 0.1M Ammonium acetate extractable Na^+

Core position	Depth interval (mm)	$mmol_c/kg$	Core position	Depth interval (mm)	$mmol_c/kg$
Pivot Major	0-200	1	Pivot Major	0-300	2
(irrigated to field	200-420	2	(not irrigated)	300-600	2
capacity)	420-600	3	Core PM4	600-900	
Core PM2	600-900			900-1200	2
	900-1100	2		1200-1500	2
	1100-1300			1500-1800	
	1300-1500	2		1800-2100	3
	1500-1800			2100-2400	
	1800-2100	3		2400-2700	
	2100-2400			2700-3000	2
	2400-2700				
	2700-3000	3			
Pivot Four	0-300	2	Pivot Four	0-300	3
(irrigated to field	300-600	3	(not irrigated)	300-600	2
capacity)	600-900		Core PF4	600-900	
Core PF2	900-1200	2		900-1200	
	1200-1500			1200-1500	
	1500-1800	3		1500-1800	2
	1800-2100			1800-2100	
	2100-2400	3		2100-2400	3
	2400-2700			2400-2700	
	2700-3000	3		2700-3000	2
	3000-3300	3		3000-3300	2
Pivot Tweefontein	0-300	2	Pivot Tweefontein	0-300	3
(irrigated to field	300-600	2	(not irrigated)	300-600	2
capacity)			Core PT2		
Core PT1					

Duplicate analyses for estimation of analytical precision

Sample	Result 1 ($mmol_c/kg$)	Result 2 ($mmol_c/kg$)	R	Relative R
PM2 400-600 mm	3.22	1.99	1.28	0.49
PM2 1300-1500 mm	2.24	2.77	0.53	0.21
PM4 1800-2100 mm	3.03	2.84	0.18	0.06
PM4 300-600 mm	1.97	2.93	0.96	0.39
PF4 2100-2400 mm	2.97	2.97	0.00	0.00
		Mean:	0.59	0.23
		Std.dev:	0.52	0.20
		95% Conf. interval :	0.74	28 %

Table A21: 0.1M Ammonium acetate extractable K^+

Core position	Depth interval (mm)	$mmol_c/kg$	Core position	Depth interval (mm)	$mmol_c/kg$
Pivot Major	0-200	2.5	Pivot Major	0-300	2.5
(irrigated to field	200-420	2.8	(not irrigated)	300-600	1.5
capacity)	420-600	3.3	Core PM4	600-900	
Core PM2	600-900			900-1200	1.1
	900-1100	2.6		1200-1500	2.3
	1100-1300			1500-1800	
	1300-1500	2.3		1800-2100	1.0
	1500-1800			2100-2400	
	1800-2100	3.0		2400-2700	
	2100-2400			2700-3000	1.3
	2400-2700				
	2700-3000	3.4			
Pivot Four	0-300	2.1	Pivot Four	0-300	1.3
(irrigated to field	300-600	0.8	(not irrigated)	300-600	1.0
capacity)	600-900		Core PF4	600-900	
Core PF2	900-1200	0.7		900-1200	
	1200-1500			1200-1500	
	1500-1800	0.7		1500-1800	0.7
	1800-2100			1800-2100	
	2100-2400	0.7		2100-2400	0.8
	2400-2700			2400-2700	
	2700-3000	1.0		2700-3000	0.9
	3000-3300	1.2		3000-3300	0.9
Pivot Tweefontein	0-300	2.1	Pivot Tweefontein	0-300	1.0
(irrigated to field	300-600	1.0	(not irrigated)	300-600	1.1
capacity)			Core PT2		
Core PT1					

Duplicate analyses for estimation of analytical precision

Sample	Result 1 ($mmol_c/kg$)	Result 2 ($mmol_c/kg$)	R	Relative R
PM2 400-600 mm	2.97	3.54	0.58	0.18
PM2 1300-1500 mm	2.90	1.76	1.14	0.49
PM4 1800-2100 mm	0.96	1.01	0.05	0.05
PM4 300-600 mm	1.53	1.38	0.15	0.11
PF4 2100-2400 mm	0.82	0.80	0.02	0.02
		Mean:	0.39	0.17
		Std.dev:	0.34	0.15
		95% Conf. interval :	0.48	21 %

Table A22: 1M KCl extractable acidity

Core position	Depth interval (mm)	$mmol_c/kg$	Core position	Depth interval (mm)	$mmol_c/kg$
Pivot Major	0-200	0	Pivot Major	0-300	5
(irrigated to field	200-420	5	(not irrigated)	300-600	8
capacity)	420-600	2	Core PM4	600-900	
Core PM2	600-900			900-1200	6
	900-1100	0		1200-1500	3
	1100-1300			1500-1800	
	1300-1500	1		1800-2100	3
	1500-1800			2100-2400	
	1800-2100	1		2400-2700	
	2100-2400			2700-3000	1
	2400-2700				
	2700-3000	2			
Pivot Four	0-300	1	Pivot Four	0-300	3
(irrigated to field	300-600	2	(not irrigated)	300-600	0
capacity)	600-900		Core PF4	600-900	
Core PF2	900-1200	5		900-1200	2
	1200-1500			1200-1500	
	1500-1800	1		1500-1800	5
	1800-2100			1800-2100	
	2100-2400	3		2100-2400	11
	2400-2700			2400-2700	
	2700-3000	1		2700-3000	7
	3000-3300	5		3000-3300	6
Pivot Tweefontein	0-300	0	Pivot Tweefontein	0-300	3
(irrigated to field capacity) Core PT1	300-600	3	(not irrigated) Core PT2	300-600	0

Duplicate analyses for estimation of analytical precision

Sample	Result 1 (ml base added)	Result 2 (ml base added)	R	Relative R
PT1 0-300 mm	0.26	0.18	0.08	0.22
PF2 0-300 mm	0.25	0.33	0.08	0.37
PT2 300-600 mm	0.32	0.24	0.08	0.29
PF2 1500-1800 mm	0.29	0.15	0.14	0.23
		Mean:	0.09	0.28
		Std.dev:	0.08	0.25
		95% Conf. interval :	0.11 ml = 1.13 $mmol_c/kg$	35%

Table A23: $Ca(HPO_4)$ extractable SO_4^{2-}

Core position	Depth interval (mm)	$mmol_c/kg$	Core position	Depth interval (mm)	$mmol_c/kg$
Pivot Major	0-200	6	Pivot Major	0-300	bdl
(irrigated to field	200-420	10	(not irrigated)	300-600	2
capacity)	420-600	12	Core PM4	600-900	
Core PM2	600-900			900-1200	7
	900-1100	9		1200-1500	7
	1100-1300			1500-1800	
	1300-1500	6		1800-2100	bdl
	1500-1800			2100-2400	
	1800-2100	7		2400-2700	
	2100-2400			2700-3000	bdl
	2400-2700				
	2700-3000	6			
Pivot Four	0-300	3	Pivot Four	0-300	bdl
(irrigated to field	300-600	6	(not irrigated)	300-600	bdl
capacity)	600-900		Core PF4	600-900	
Core PF2	900-1200	11		900-1200	7
	1200-1500			1200-1500	
	1500-1800	16		1500-1800	3
	1800-2100			1800-2100	
	2100-2400	7		2100-2400	3
	2400-2700			2400-2700	
	2700-3000	bdl		2700-3000	3
	3000-3300	3		3000-3300	bdl
Pivot Tweefontein	0-300	11	Pivot Tweefontein	0-300	7
(irrigated to field	300-600	15	(not irrigated)	300-600	6
capacity)			Core PT2		
Core PT1					

Duplicate analyses for estimation of analytical precision

Sample	Result 1 $mmol_c/kg$	Result 2 $mmol_c/kg$	R	Relative R
PT1 0-300 mm	9.22	11.13	1.91	0.19
PT1 300-600 mm	14.86	15.32	0.46	0.03
PT2 300-600 mm	6.71	4.67	2.04	0.36
		Mean:	1.47	0.19
		Std.dev:	1.30	0.17
		95% Conf. interval :	1.84	24 %

Table A24: Grain-size analysis of irrigated soil samples

Core position	Depth interval (mm)	Sand (weight %)	Silt (weight %)	Clay (weight %)
Pivot Major	0-200	68.7	13.7	17.6
(irrigated to field	200-420	68.6	12.8	18.6
capacity)	420-600	68.6	12.0	19.4
Core PM2	600-900			
	900-1100	57.8	17.1	25.1
	1100-1300			
	1300-1500	52.1	18.6	29.3
	1500-1800			
	1800-2100	44.1	23.5	32.4
	2100-2400			
	2400-2700			
	2700-3000	52.1	19.5	28.4
Pivot Four	0-300	70.7	11.5	17.8
(irrigated to field	300-600	69.9	11.2	18.9
capacity)	600-900			
Core PF2	900-1200	62.1	14.5	23.4
	1200-1500			
	1500-1800	57.9	15.7	26.4
	1800-2100			
	2100-2400	56.6	16.3	27.2
	2400-2700			
	2700-3000			
	3000-3300	49.9	18.1	32.0

Table A25: Effective cation exchange capacity

Core position	Depth interval (mm)	$mmol_c/kg$	Core position	Depth interval (mm)	$mmol_c/kg$
Pivot Major	0-200	37	Pivot Major	0-300	23
(irrigated to field	200-420	23	(not irrigated)	300-600	28
capacity)	420-600	27	Core PM4	600-900	
Core PM2	600-900			900-1200	19
	900-1100	23		1200-1500	17
	1100-1300			1500-1800	
	1300-1500	27		1800-2100	18
	1500-1800			2100-2400	
	1800-2100	34		2400-2700	
	2100-2400			2700-3000	18
	2400-2700				
	2700-3000	27			
Pivot Four	0-300	23	Pivot Four	0-300	23
(irrigated to field	300-600	19	(not irrigated)	300-600	24
capacity)	600-900		Core PF4	600-900	
Core PF2	900-1200	20		900-1200	
	1200-1500			1200-1500	
	1500-1800	25		1500-1800	14
	1800-2100			1800-2100	
	2100-2400	21		2100-2400	20
	2400-2700			2400-2700	
	2700-3000	22		2700-3000	21
	3000-3300	29		3000-3300	20
Pivot Tweefontein	0-300	27	Pivot Tweefontein	0-300	15
(irrigated to field	300-600	27	(not irrigated)	300-600	14
capacity)			Core PT2		
Core PT1					

Estimation of analytical precision: The confidence limits at 95% for the ECEC values were derived by summing the confidence limits of every component – i.e. exchangaeble Ca, Mg, Na, K & acidity, and range between 3 $mmol_c/kg$ for the lowest ECEC's and 7 $mmol_c/kg$ for the highest.

Table A26: ΔpH ($pH_{KCl} - pH_{saturated\ paste}$)

Core position	Depth interval (mm)	ΔSoil pH	Core position	Depth interval (mm)	ΔSoil pH
Pivot Major	0-200	-0.7	Pivot Major	0-300	-0.8
(irrigated to field	200-420	-0.6	(not irrigated)	300-600	-0.8
capacity)	420-600	-0.5	Core PM4	600-900	
Core PM2	600-900			900-1200	-0.7
	900-1100	-0.9		1200-1500	-0.6
	1100-1300			1500-1800	
	1300-1500	-0.9		1800-2100	-1.3
	1500-1800			2100-2400	
	1800-2100	-0.9		2400-2700	
	2100-2400			2700-3000	-0.9
	2400-2700				-0.9
	2700-3000	-0.9			-1.0
Pivot Four	0-300	-0.8	Pivot Four	0-300	-0.9
(irrigated to field	300-600	-0.9	(not irrigated)	300-600	-1.0
capacity)	600-900		Core PF4	600-900	
Core PF2	900-1200	-0.7		900-1200	-1.0
	1200-1500			1200-1500	
	1500-1800	-0.8		1500-1800	-1.2
	1800-2100			1800-2100	
	2100-2400	-0.7		2100-2400	-1.5
	2400-2700			2400-2700	
	2700-3000	-1.4		2700-3000	-1.6
	3000-3300	-0.9		3000-3300	-1.3
Pivot Tweefontein	0-300	-0.1	Pivot Tweefontein	0-300	-0.7
(rrigated to field	300-600	-1.1	(not irrigated)	300-600	-0.8
capacity)			Core PT2		
Core PT1					

Appendix B – Solute mass balance data and calculations

The irrigation water quantity and quality data are presented in Tables B1, B2 and B3

Example of calculation of salt input

The total quantity of an ion applied to 1 m^2 of the soil during irrigation was calculated by multiplying the volume of irrigation water and the concentration of the ion in the irrigation water. For example, the quantity of Ca^{2+} applied to pivot Major in January 1998 was

19.8 mm x 26.0 $mmol_c/l$ which is equivalent to:
19.8 l/m^2 x 26.0 $mmol_c/l$ = 515 $mmol_c/m^2$

Once the quantity for each month is known, the total is simply the sum of the quantities of all the months during which irrigation took place.

Table B1: Quantities of irrigation water applied and irrigation water quality for pivot Major

Pivot Major		$mmol_c/l$						
Date	Irrigation (mm)	Ca	SO_4	Mg	Na	Cl	K	Alkalinity
Jan-98	19.8	26	40	16	1.6	0.5	0.3	1.7
Feb-98	55.2	26	40	16	1.6	0.5	0.3	1.7
Mar-98	6.5	18	28	11	1.1	0.4	0.2	1.7
Jul-98	59.5	24	35	14	1	0.5	0.3	1.8
Aug-98	118.9	18	30	12	0.9	0.4	0.2	1.7
Sep-98	101.9	26	40	16	1.2	0.6	0.3	1.7
Oct-98	48.8	26	40	16	1.2	0.6	0.3	1.7
Jan-99	41.1	26	40	16	1.6	0.6	0.3	1.7
Feb-99	89.9	27	42	17	1.7	0.6	0.3	1.7
Mar-99	113.4	30	45	18	1.8	0.6	0.3	1.6
Apr-99	19.1	27	43	17	1.5	0.6	0.3	1.7
Jul-99	48.8	25	37	14	1.25	0.45	0.3	1.7
Aug-99	42.6	27	42	17	1.7	0.6	0.3	1.7
Sep-99	64.4	28	43	17	1.7	0.6	0.3	1.7
Oct-99	67.1	30	45	18	1.8	0.6	0.3	0.6
Nov-99	61.6	24	37	15	1.3	0.55	0.2	1.5
Dec-99	37.3	26	35	15	1.3	0.55	0.2	1.3
Jan-00	3.6	25	38	15	1.4	0.5	0.3	1.2

Table B2: Quantities of irrigation water applied and irrigation water quality for pivot Tweefontein

Pivot Tweefontein		$mmol_c/l$						
Date	Irrigation (mm)	Ca	SO_4	Mg	Na	Cl	K	Alkalinity
Feb-98	60.9	15	27	12	2.4	0.9	0.5	2
Mar-98	9.3	16	28	11	2.5	0.9	0.5	2
Jul-98	83	20	35	15	2.5	0.9	0.5	2
Aug-98	73.9	22	35	15	2.5	0.9	0.5	2
Sep-98	77.4	24	36	12	2.5	0.9	0.5	2
Oct-98	87.7	8	45	16	1.65	0.9	0.5	0
Nov-98	16.8	13	40	17	1.9	0.9	0.5	0
Jan-99	23.9	20	37	15	1.5	1	0.4	2
Feb-99	64.6	20	37	17	2.4	1	0.4	1.6
Mar-99	128.9	18	39	18	2.5	1	0.5	2
Apr-99	19.5	16	40	18	2.5	1	0.5	2
Jul-99	29	21	38	17	2.5	1.1	0.6	1.9
Aug-99	62.4	21	40	17	2.4	1	0.5	2
Sep-99	117.5	23	42	20	2.5	1	0.5	1.8
Oct-99	168.3	25	40	21	2.5	1.2	0.4	1.8
Nov-99	80.9	22	45	20	2.7	1.2	0.4	1.4
Dec-99	2.7	22	38	20	2.4	1.2	0.4	1.7
Mar-00	10.5	18	40	20	2.7	1.1	0.4	1.4

Table B3: Quantities of irrigation water applied and irrigation water quality for pivot Four

Pivot Four		$mmol_c/l$						
Date	Irrigation (mm)	Ca	SO_4	Mg	Na	Cl	K	Alkalinity
Jul-99	40.3	21	38	17	2.5	1.1	0.6	1.9
Aug-99	48.6	21	40	17	2.4	1	0.5	2
Sep-99	71.3	23	42	20	2.5	1	0.5	1.8
Oct-99	89.9	25	40	21	2.5	1.2	0.4	1.8
Nov-99	44.8	22	45	20	2.7	1.2	0.4	1.4
Jan-00	3.6	24	38	15	1.5	0.5	0.4	1.2
Feb-00	3.8	15	36	21	2.6	1.2	0.4	1.2
Mar-00	1.1	18	40	20	2.7	1.1	0.4	1.4

Example of calculation of solute retained in soils

The total quantity of an ion retained in a soil profile is calculated by multiplying the extractable concentration of the ion and the soil's dry bulk density.

For example, the total quantity of Ca^{2+} retained in a slice of soil 1 m^2 in surface area, between the depths of 0 mm and 200 mm, is calculated as follows, assuming a soil bulk density of 1500 kg/m^3:

31.34 $mmol_c/kg$ x 1500 kg/m^3 x 0.2 m = 9.4 mol_c/m^2

This calculation is repeated for each depth interval in the profile. The sum of the quantities of Ca^{2+} retained in each slice is the total quantity of Ca^{2+} retained in the profile.

Table B4: Calculation of total quantity of Ca^{2+} retained in the irrigated soil from pivot Major

Depth (mm)	Ca^{2+} ($mmol_c/kg$)	Ca^{2+} (mol_c/m^2)
0-200	31.34	9.4
200-400	9.63	2.9
400-600	15.54	4.7
600-900	13.17	5.9
900-1100	10.80	3.2
1100-1300	9.81	2.9
1300-1500	8.81	2.6
1500-1800	9.60	4.3
1800-2100	10.38	4.7
2100-2400	9.63	4.3
2400-2700	8.88	4.0
2700-3000	8.13	3.7
	Total	**52.7**

Appendix C: Thermodynamic data used in PHREEQC modeling and example input and output files

The following list is a selection from the WATEQ4F database of thermodynamic data which is used by the PHREEQC program (Parkhurst & Appelo, 1999). Only the solid phases and aqueous species relevant to the particular solution compositions considered in this study are included. The following notation is used:

log K – the natural logarithm of the equilibrium constant
ΔH – the entropy change for the reaction (here in kilocalories per mole)
-analytical – co-efficients used by PHREEQC to calculate the temperature dependence of K
-gamma – co-effecients a_0 and b for the WATEQ Debye-Hückel equation (refer to Chapter 2, Methods)

Note: For some species only the log K value is available.

1) Solid phases

Anhydrite
$CaSO_4 = Ca^{2+} + SO_4^{2-}$
log K -4.36
ΔH -1.71 kcal
-analytical 197.52 0.0 -8669.8 -69.835 0.0

Aragonite
$CaCO_3 = Ca^{2+} + CO_3^{2-}$
log K -8.336
ΔH -2.589 kcal
-analytical -171.9773 -0.077993 2903.293 71.595 0.0

Brucite
$Mg(OH)2 + 2H^+ = Mg^{2+} + 2H_2O$
log K 16.84
ΔH -27.1 kcal

Calcite
$CaCO_3 = Ca^{2+} + CO_3^{2-}$
log K -8.48
ΔH -2.297 kcal
-analytical -171.9065 -0.077993 2839.319 71.595 0.0

Dolomite
$CaMg(CO_3)2 = Ca^{2+} + Mg^{2+} + 2CO_3^{2-}$
log K -17.09
ΔH -9.436 kcal

Epsomite
$MgSO_4{:}7H_2O = Mg^{2+} + SO_4^{2-} + 7H_2O$
log K -2.140
ΔH 2.820 kcal

Gypsum
$CaSO_4:2H_2O = Ca^{2+} + SO_4^{2-} + 2H_2O$
log K -4.58
ΔH -0.109 kcal
-analytical 68.2401 0.0 -3221.51 5.0627 0.0

Halite
$NaCl = Na^+ + Cl^-$
log K 1.582
ΔH 0.918 kcal

Huntite
$CaMg3(CO_3)4 = 3Mg^{2+} + Ca^{2+} + 4CO_3^{2-}$
log K -29.968
ΔH -25.760 kcal

Hydromagnesite
$Mg5(CO_3)4(OH)2:4H_2O + 2H^+ = 5Mg^{2+} + 4CO_3^{2-} + 6H_2O$
log K -8.762
ΔH -52.244 kcal

Magnesite
$MgCO_3 = Mg^{2+} + CO_3^{2-}$
log K -8.029
ΔH -6.169 kcal

Mirabilite
$Na2SO_4:10H_2O = 2Na^+ + SO_4^{2-} + 10H_2O$
log K -1.114
ΔH 18.987 kcal

Portlandite
$Ca(OH)2 + 2H^+ = Ca^{2+} + 2H_2O$
log K 22.8
ΔH -31.0 kcal

Rhodochrosite
$MnCO_3 = MN_2^+ + CO_3^{2-}$
log K -11.13
ΔH -1.43 kcal

Sulfur
$S + 2e^- = S^{2-}$
log K -15.026
ΔH 7.9 kcal

Thenardite
$Na2SO_4 = 2Na^+ + SO_4^{2-}$
log K -0.179
ΔH -0.572 kcal

2) Aqueous species

$NH_4^+ = NH_3 + H^+$
log K -9.252
ΔH 12.48 kcal

$NH_4^+ + SO_4^{2-} = NH_4SO_4$
log K 1.11

$Ca^{2+} + SO_4^{2-} = CaSO_4$
log K 2.3
ΔH 1.65 kcal

$Ca^{2+} + HSO_4^- = CaHSO_4$
log K 1.08

$Ca^{2+} + H_2O = CaOH^+ + H^+$
log K -12.78

$Ca^{2+} + HCO_3^- = CaHCO_3$
log K 1.106
ΔH 2.69 kcal
-analytical 1209.12 0.31294 -34765.05 -478.7820.0

$Ca^{2+} + CO_3^{2-} = CaCO_3$
log K 3.224
ΔH 3.545 kcal
-analytical -1228.732 -0.299444 35512.75 485.818 0.0

$CO_3^{2-} + 10\ H^+ + 8\ e^- = CH_4 + 3\ H_2O$
log K 41.071
ΔH -61.039 kcal

$HCO_3^- + H^+ = H_2CO_3$
log K 6.351
ΔH -2.247 kcal
-analytical 356.3094 0.06091960 -1834.37 -126.8339 1684915.0

$CO_3^{2-} + 2\ H^+ = CO_2 + H_2O$
log K 16.681
ΔH -5.738 kcal
-analytical 464.1965 0.09344813 6986.16 -165.75951 2248628.9

$H^+ + CO_3^{2-} = HCO_3^-$
log K 10.329
ΔH -3.561 kcal
-analytical 107.8871 0.03252849 -5151.79 -38.92561 563713.9
-gamma 5.4 0.0

$0.5H_2O = 0.25O_2 + H^+ + e^-$
log K $^{2-}$0.780
ΔH 34.157000 kcal

$2H_2O = O_2 + 4H^+ + 4e^-$
log K -86.08
ΔH 134.79 kcal

$2 H^+ + 2 e^- = H_2$
log K -3.15
ΔH -1.759

CO_2 (g) + $H_2O = H_2CO_3$
-1.468 -4.776 108.38650 0.01985076 -6919.530 -40.45154 -669365.0

$0.5H_2O = 0.25O_2$(aq) + $H^+ + e^-$
log K -20.780
ΔH 33.457 kcal

$H_2O = OH^- + H^+$
log K -14.0
ΔH 13.362 kcal
-analytical -283.971-0.05069842 13323.0 102.24447 -1119669.0

$K^+ + SO_4^{2-} = KSO_4^-$
log K 0.85
ΔH 2.25 kcal

$Mg^{2+} + H_2O = MgOH^+ + H^+$
log K -11.44
ΔH 15.952 kcal

$Mg^{2+} + CO_3^{2-} = MgCO_3$
log K 2.98
ΔH 2.713 kcal
-analytical 0.9910 0.00667

$Mg^{2+} + HCO_3^- = MgHCO_3$
log K 1.07
ΔH 0.79 kcal
-analytical -59.215 0.0 2537.455 20.92298 0.0

$Mg^{2+} + SO_4^{2-} = MgSO_4$
log K 2.37
ΔH 4.55 kcal

$Na^+ + CO_3^{2-} = NaCO_3^-$
log K 1.27
ΔH 8.91 kcal

$Na^+ + HCO_3^- = NaHCO_3$
log K -0.25

$Na^+ + SO_4^{2-} = NaSO_4$
log K 0.7
ΔH 1.12 kcal

$2\ NO_3^- + 12\ H^+ + 10\ e^- = N_2 + 6\ H_2O$
log K 207.080
ΔH -312.130 kcal

$NO_3^- + 10H^+ + 8e^- = NH_4^+ + 3H_2O$
log K 119.077
ΔH -187.055 kcal

$NO_3^- + 2H^+ + 2e^- = NO_2^- + H_2O$
log K 28.57
ΔH -43.76 kcal

$H^+ + SO_4^{2-} = HSO_4^-$
log K 1.988
ΔH 3.85 kcal
-analytical -56.889 0.006473 2307.9 19.8858 0.0

$SO_4^{2-} + 10H^+ + 8e^- = H_2S + 4H_2O$
log K 40.644
ΔH -65.44 kcal

$H_2S = HS^- + H^+$
log K -6.994
ΔH 5.3 kcal

$HS^- = S^{2-} + H^+$
log K -12.918
ΔH 12.1 kcal

Example input file for PHREEQC modeling

The example given here is for the saturated paste extract composition from sample PM2, 0-200 mm. The output file follows, below.

```
TITLE Pivot Major - saturated paste extract calculation
SOLUTION 1  pm2 0-200
pH    5.69
temp   20.0
pe      4
units ppm
Na 127.2
K 15.6
Mg 28
Ca 317.6
Cl 138.72
N(5) 15.72 as NO3
S(6) 550.88 as SO4
Alkalinity 40.93 as HCO3
END
```

Example output file

```
SOLUTION_MASTER_SPECIES
        SOLUTION_SPECIES
        PHASES
        EXCHANGE_MASTER_SPECIES
        EXCHANGE_SPECIES
        SURFACE_MASTER_SPECIES
        SURFACE_SPECIES
        RATES
        END
------------------------------------
Reading input data for simulation 1.
------------------------------------

        TITLE Pivot Major - saturated paste extract calculation
        SOLUTION 1  PM2 0-200
             pH     5.69
             temp   20.0
                  pe                4
        units ppm
        Na 127.2
        K 15.6
        Mg 28
        Ca 317.6
        Cl 138.72
        N(5) 15.72 as NO3
        S(6) 550.88 as SO4
        Alkalinity 40.93 as HCO3
        END
-----
TITLE
-----

 Pivot Major - saturated paste extract calculation

-------------------------------------------
Beginning of initial solution calculations.
-------------------------------------------

Initial solution 1. pm2 0-200

-----------------------------Solution composition------------------------------

        Elements          Molality     Moles

        Alkalinity        6.716e-04  6.716e-04
        Ca                7.934e-03  7.934e-03
        Cl                3.918e-03  3.918e-03
        K                 3.994e-04  3.994e-04
        Mg                1.153e-03  1.153e-03
        N(5)              2.538e-04  2.538e-04
        Na                5.540e-03  5.540e-03
        S(6)              5.742e-03  5.742e-03

----------------------------Description of solution----------------------------
                                pH  =  5.690
                                pe  =  4.000
                        Activity of water  =  1.000
                          Ionic strength  =  2.816e-02
```

Mass of water (kg) = 1.000e+00
Total carbon (mol/kg) = 3.376e-03
Total CO2 (mol/kg) = 3.376e-03
Temperature (deg C) = 20.000
Electrical balance (eq) = 7.787e-03
Percent error, 100*(Cat-|An|)/(Cat+|An|) = 23.21
Iterations = 8
Total H = 1.110131e+02
Total O = 5.553737e+01

----------Distribution of species----------

	Species	Molality	Log Activity	Log Molality	Log Activity	Gamma
	H+	2.327e-06	2.042e-06	-5.633	-5.690	-0.057
	OH-	3.915e-09	3.324e-09	-8.407	-8.478	-0.071
	H2O	5.551e+01	9.995e-01	-0.000	-0.000	0.000
C(4)	3.376e-03					
	CO2	2.702e-03	2.719e-03	-2.568	-2.566	0.003
	HCO3-	6.423e-04	5.526e-04	-3.192	-3.258	-0.065
	CaHCO3+	2.664e-05	2.292e-05	-4.574	-4.640	-0.065
	MgHCO3+	3.807e-06	3.253e-06	-5.419	-5.488	-0.068
	NaHCO3	1.449e-06	1.458e-06	-5.839	-5.836	0.003
	CaCO3	6.146e-08	6.186e-08	-7.211	-7.209	0.003
	CO3-2	2.081e-08	1.140e-08	-7.682	-7.943	-0.261
	MgCO3	5.135e-09	5.168e-09	-8.289	-8.287	0.003
	NaCO3-	9.020e-10	7.707e-10	-9.045	-9.113	-0.068
Ca	7.934e-03					
	Ca+2	6.459e-03	3.539e-03	-2.190	-2.451	-0.261
	CaSO4	1.448e-03	1.457e-03	-2.839	-2.836	0.003
	CaHCO3+	2.664e-05	2.292e-05	-4.574	-4.640	-0.065
	CaCO3	6.146e-08	6.186e-08	-7.211	-7.209	0.003
	CaOH+	3.365e-10	2.875e-10	-9.473	-9.541	-0.068
Cl	3.918e-03					
	Cl-	3.918e-03	3.329e-03	-2.407	-2.478	-0.071
H(0)	5.936e-23					
	H2	2.968e-23	2.987e-23	-22.528	-22.525	0.003
K	3.994e-04					
	K+	3.938e-04	3.347e-04	-3.405	-3.475	-0.071
	KSO4-	5.625e-06	4.806e-06	-5.250	-5.318	-0.068
	KOH	5.644e-13	5.681e-13	-12.248	-12.246	0.003
Mg	1.153e-03					
	Mg+2	9.224e-04	5.131e-04	-3.035	-3.290	-0.255
	MgSO4	2.269e-04	2.284e-04	-3.644	-3.641	0.003
	MgHCO3+	3.807e-06	3.253e-06	-5.419	-5.488	-0.068
	MgCO3	5.135e-09	5.168e-09	-8.289	-8.287	0.003
	MgOH+	6.744e-10	5.762e-10	-9.171	-9.239	-0.068
N(5)	2.538e-04					
	NO3-	2.538e-04	2.147e-04	-3.595	-3.668	-0.073
Na	5.540e-03					
	Na+	5.481e-03	4.693e-03	-2.261	-2.329	-0.067
	NaSO4-	5.769e-05	4.929e-05	-4.239	-4.307	-0.068
	NaHCO3	1.449e-06	1.458e-06	-5.839	-5.836	0.003
	NaCO3-	9.020e-10	7.707e-10	-9.045	-9.113	-0.068
	NaOH	1.508e-11	1.518e-11	-10.822	-10.819	0.003
O(0)	0.000e+00					
	O2	0.000e+00	0.000e+00	-49.008	-49.006	0.003
S(6)	5.742e-03					
	SO4-2	4.003e-03	2.164e-03	-2.398	-2.665	-0.267

CaSO4	1.448e-03	1.457e-03	-2.839	-2.836	0.003
MgSO4	2.269e-04	2.284e-04	-3.644	-3.641	0.003
NaSO4-	5.769e-05	4.929e-05	-4.239	-4.307	-0.068
KSO4-	5.625e-06	4.806e-06	-5.250	-5.318	-0.068
HSO4-	4.519e-07	3.861e-07	-6.345	-6.413	-0.068

----------Saturation indices----------

Phase	SI	log IAP	log KT	
Anhydrite	-0.77	-5.12	-4.34	CaSO4
Aragonite	-2.09	-10.39	-8.31	CaCO3
Calcite	-1.94	-10.39	-8.45	CaCO3
CO2(g)	-1.16	-19.32	-18.16	CO2
Dolomite	-4.66	-21.63	-16.97	CaMg(CO3)2
Gypsum	-0.54	-5.12	-4.58	CaSO4:2H2O
H2(g)	-19.40	-19.38	0.02	H2
O2(g)	-46.07	38.76	84.83	O2

End of simulation.

Appendix D: X-ray diffractograms of clay fractions of soil samples from cores PM2 and PF2

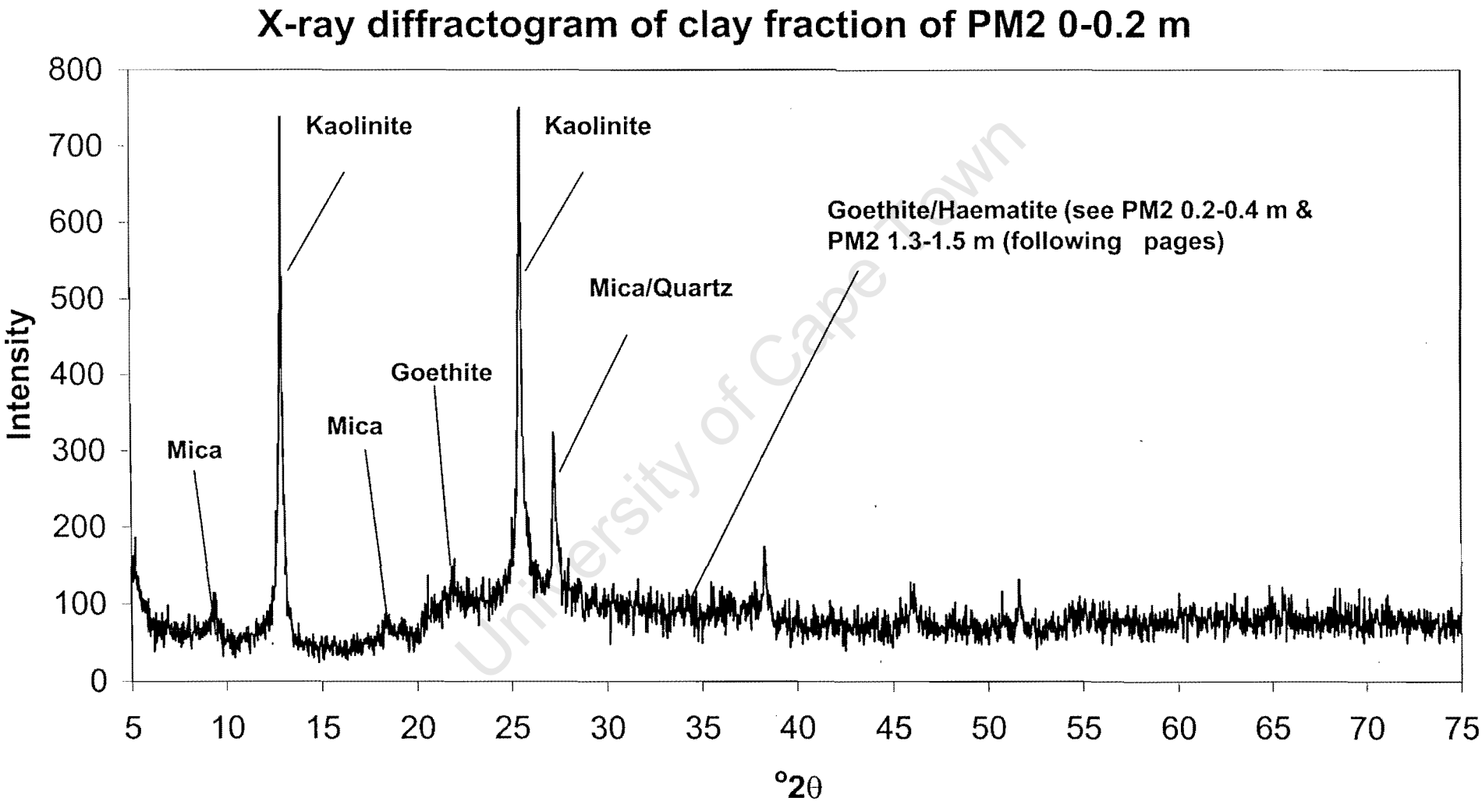

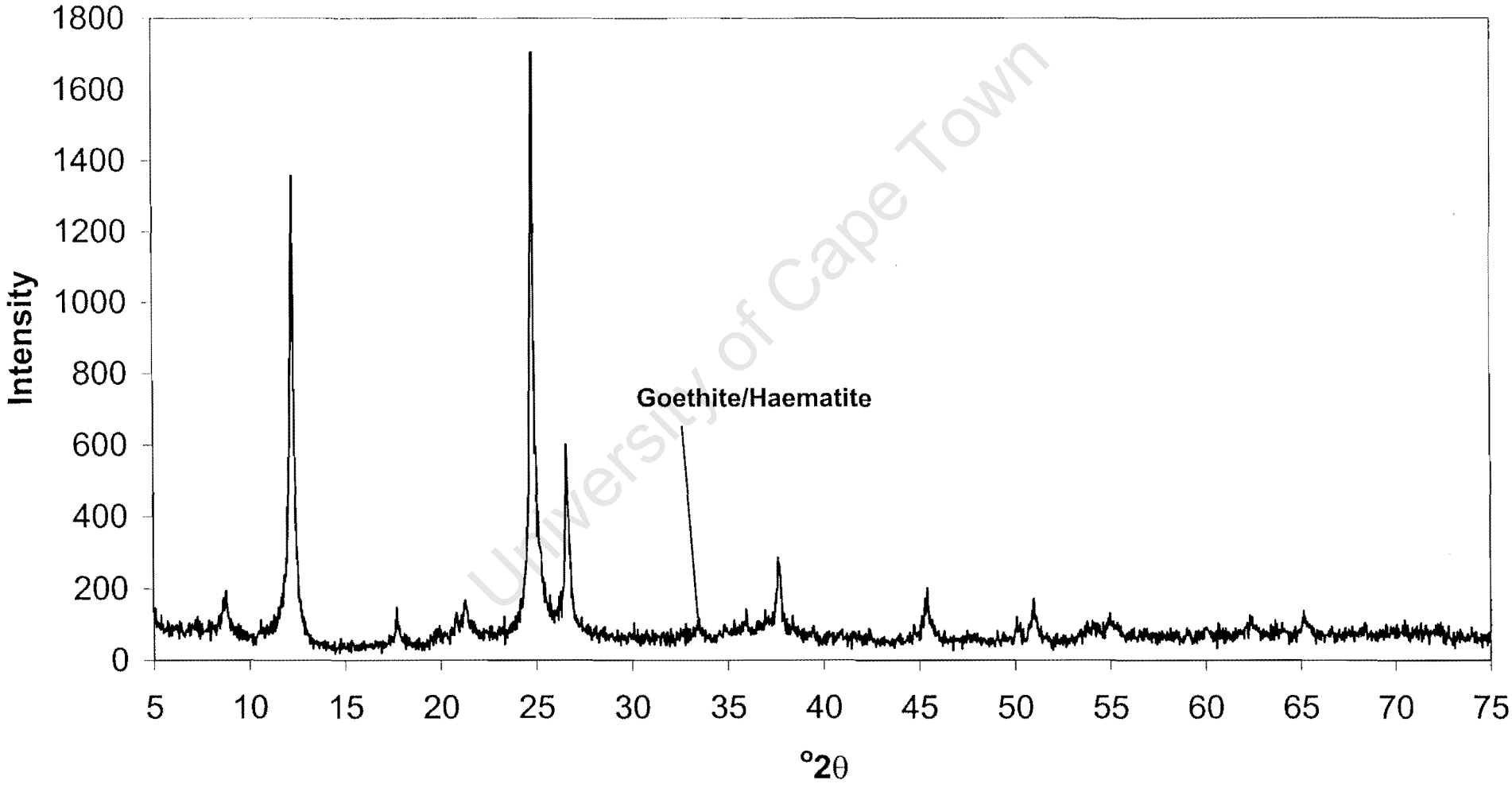

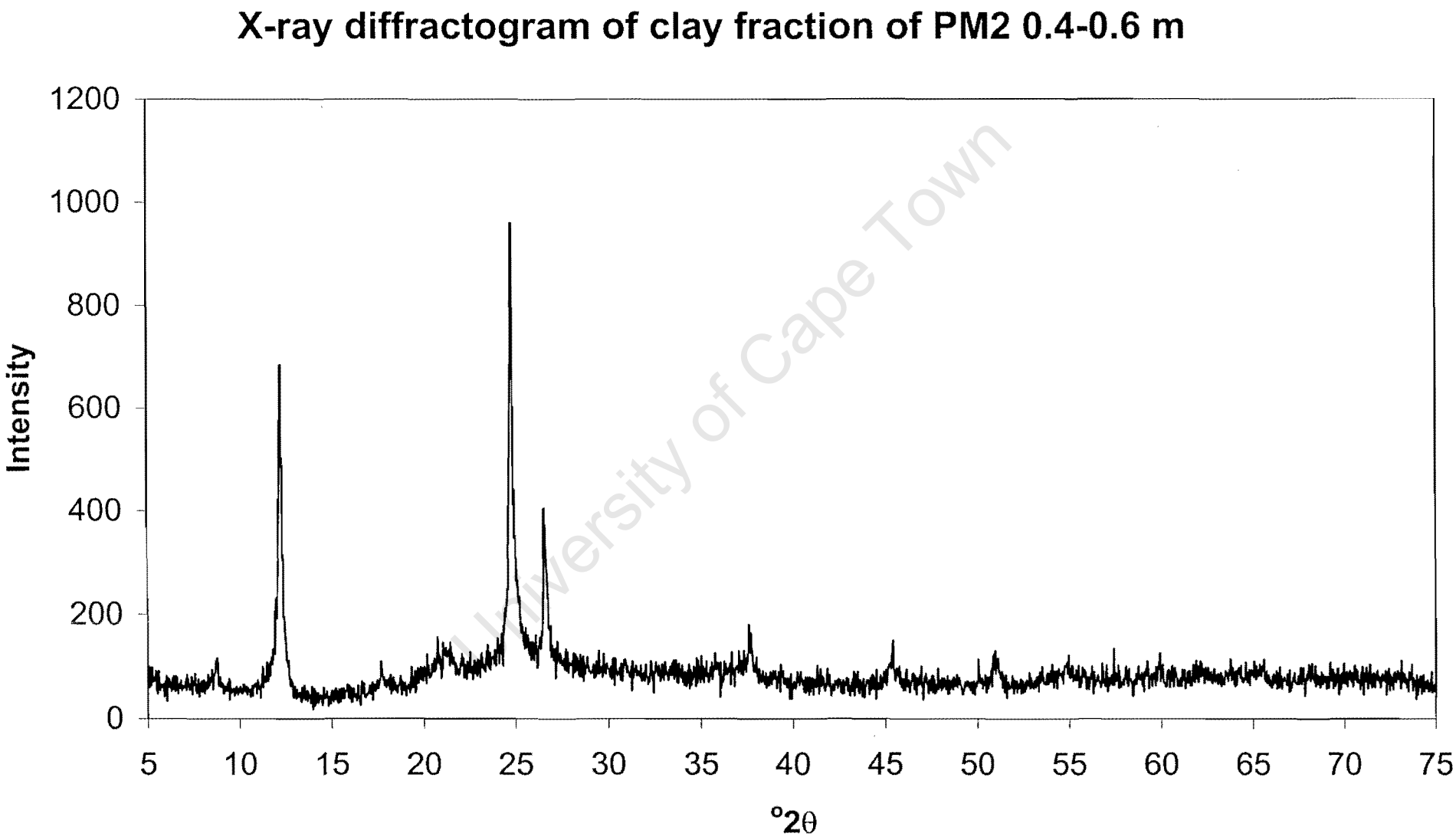

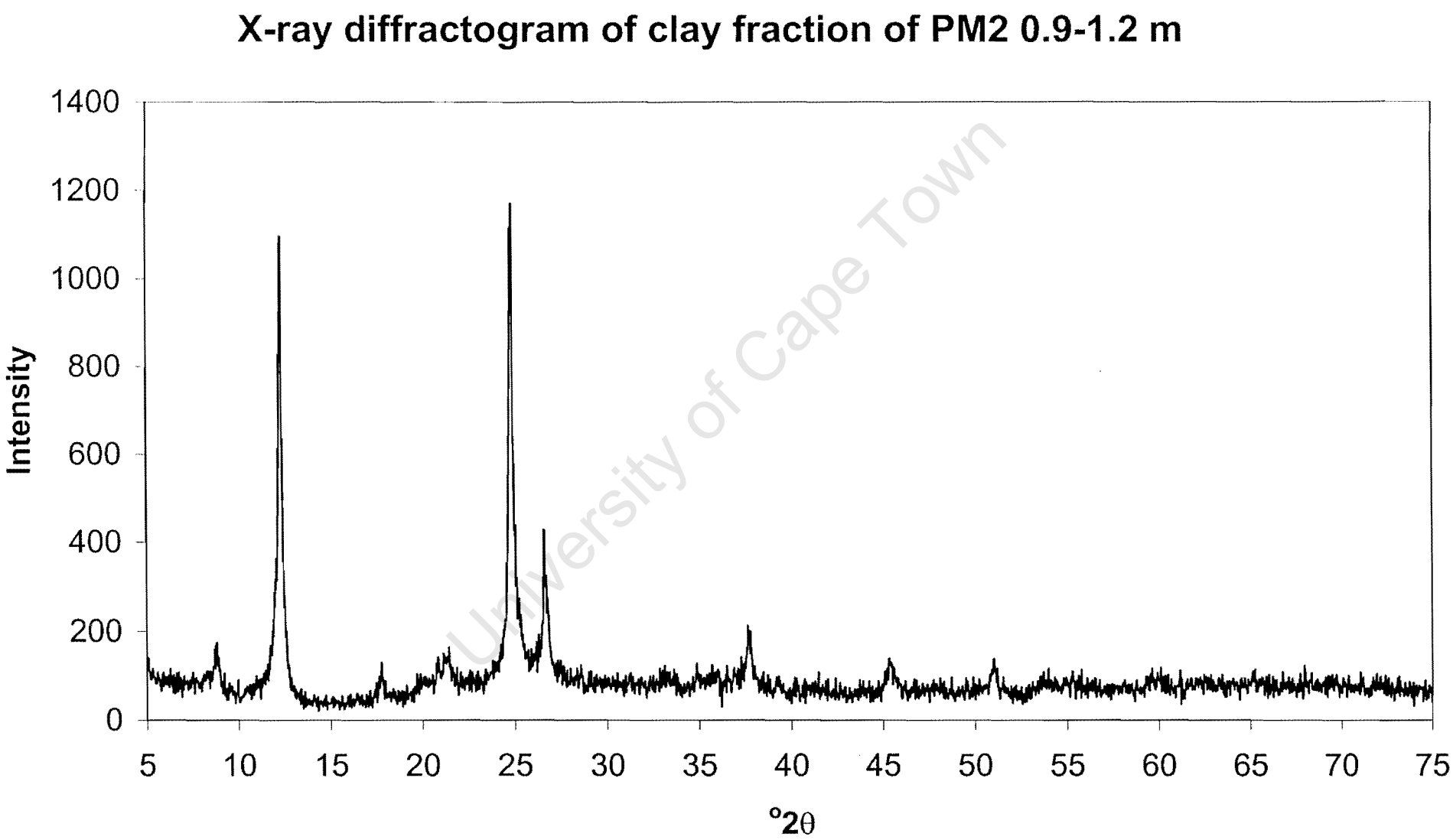

X-ray diffractogram of clay fraction of PM2 1.3-1.5 m

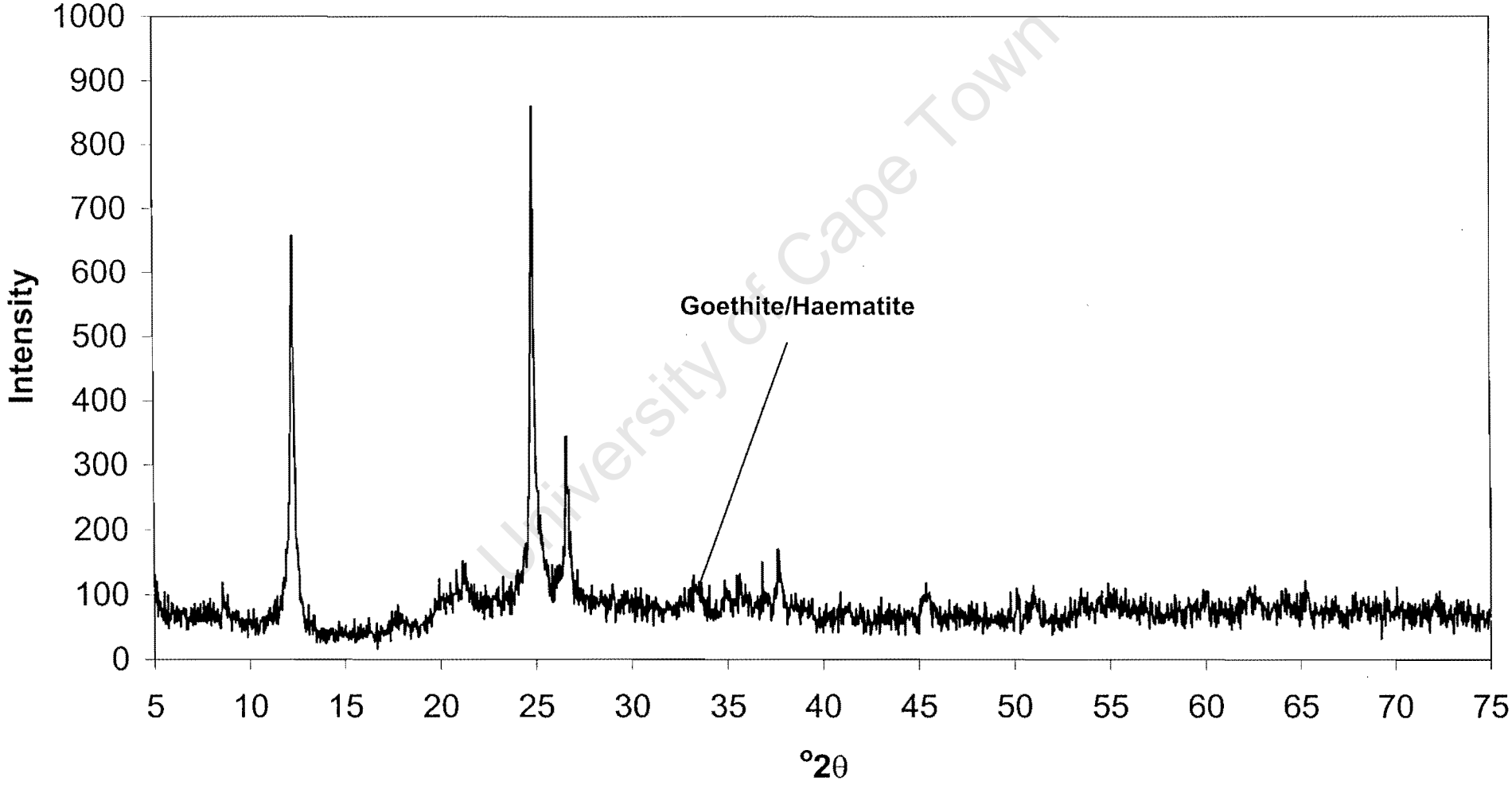

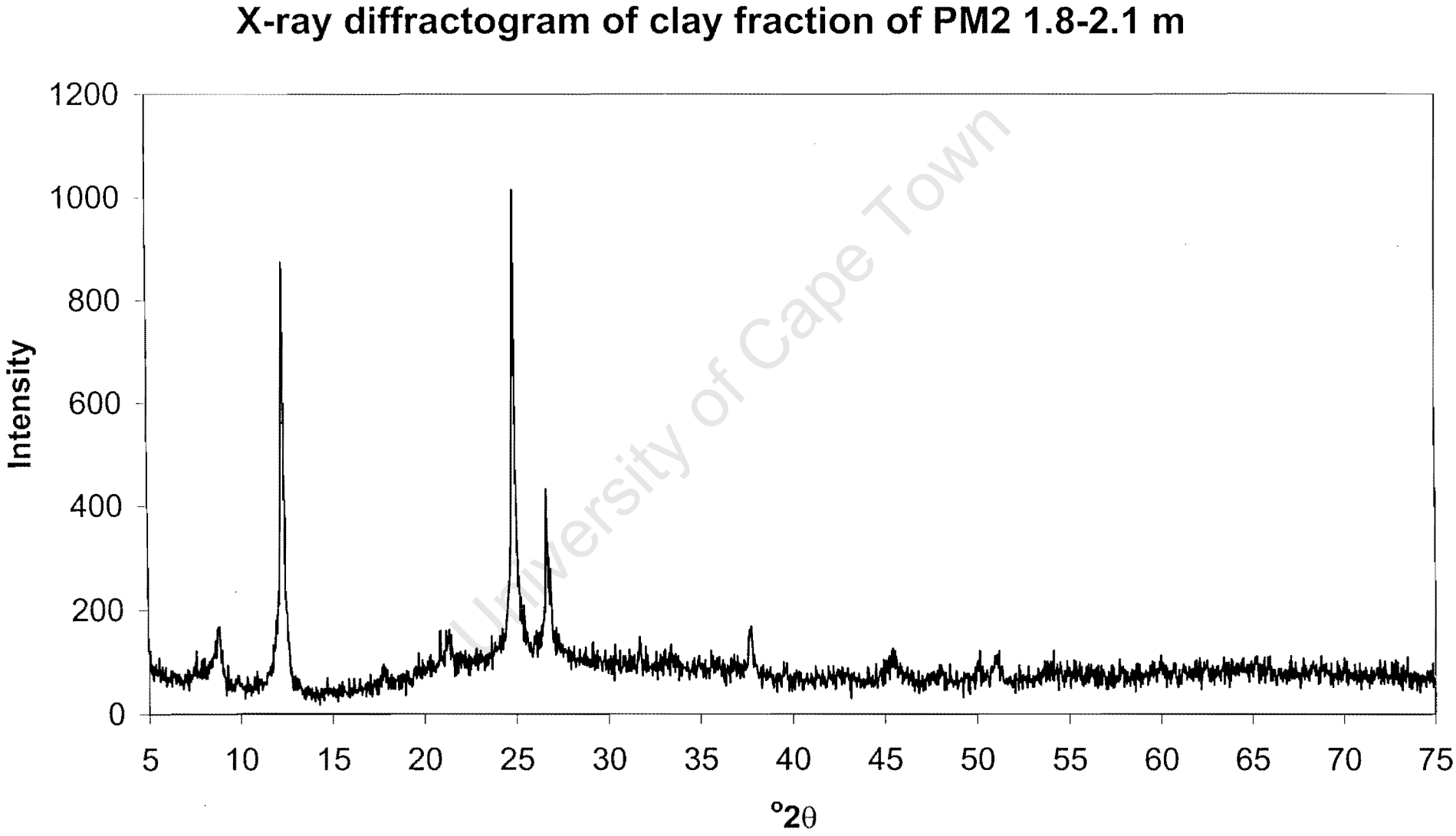

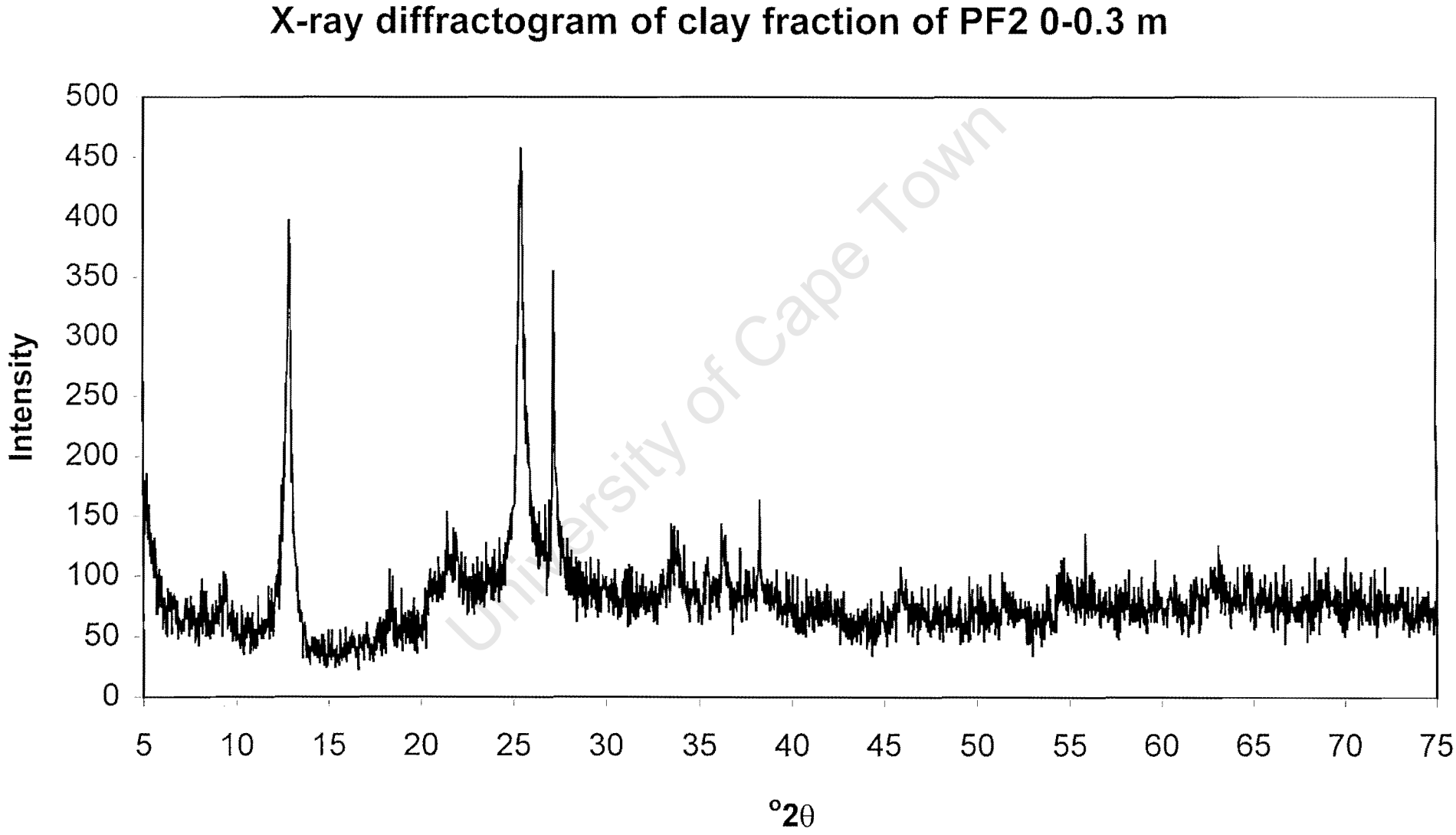

X-ray diffractogram of clay fraction of PF2 0.3-0.6 m